

# Handling Qualities Criteria for Training Effectiveness Assessment of the BS115 Aircraft

B. van Lierop

Technische Universiteit Delft





# HANDLING QUALITIES CRITERIA FOR TRAINING EFFECTIVENESS ASSESSMENT OF THE BS115 AIRCRAFT

by

**B. van Lierop**

in partial fulfillment of the requirements for the degree of

**Master of Science**  
in Aerospace Engineering

at the Delft University of Technology,  
to be defended publicly on Wednesday August 23, 2017 at 9:30 AM.

Supervisor:	Ir. J. A. Melkert	TU Delft
Thesis committee:	Dr. Ir. M. F. M. Hoogreef	TU Delft
	Ir. T. J. Mulder	TU Delft

An electronic version of this thesis is available at <http://repository.tudelft.nl/>.  
Thesis Registration Number: 147#17#MT#FPP



# PREFACE

*"Man's flight through life is sustained by the power of his knowledge"*

Austin Dusty Miller

I am proud to present this master thesis, which marks the end of my time as an aerospace engineering student at Delft University of Technology. It would not have been possible to complete this thesis without the support of all the people around me, for which I would like to express my gratitude.

First of all I would like to thank Blackshape SpA, and in particular Giuseppe Verde, for providing me with the opportunity to do my thesis work at this wonderful company. Secondly I would like to thank my supervisor Joris Melkert for his guidance, support, and feedback throughout this project. I would also like to thank Maurice Hoogreef and Hans Mulder for being a part of my thesis committee.

Special thanks to Paolo Mezzanotte for his never-ending enthusiasm and support throughout both my master thesis and internship. I have thoroughly enjoyed our conversations and discussions over the past years. I would also like to thank Balázs Fehér, Agostino De Giuseppe and all other colleagues from Blackshape for their involvement, enthusiasm and inspiring conversations.

Finally I would like to thank my family and friends, for all the support and love they have given me over the years.

*B. van Lierop  
Delft, August 2017*



# SUMMARY

With the introduction of the BS115, successor of the Blackshape Prime, a new opportunity for military training is presented. In this thesis the training effectiveness of the BS115 was investigated to identify how the training potential could be increased.

During the investigation of the available training effectiveness evaluation methods in literature it was found that the effect of handling qualities on the training effectiveness is one of the most important criteria. However, none of the available methods covered this topic to a satisfactory extend. As a result, the objective of this thesis has been to find what handling qualities should be improved to maximize the training effectiveness of the BS115 with respect to developing flying skills.

The first task towards this objective was to establish proper evaluation criteria. Based on the aircraft characteristics and United States Air Force training program the BS115 was identified to be suitable for the introductory and primary phases of training. The evaluation criteria were then determined based on the stability and control requirements from the military standard, as well as by using some typical training missions.

To test the criteria established, data from a series of CS-VLA certification test flights for the BS115 was available. Additionally, stability and control derivatives of the aircraft, established using DATCOM, were used to compute the aircraft characteristics that could not be determined from the flight test data. The method was validated using the Cessna Citation as a reference. It was found that derivatives could be obtained quickly, but accuracy was limited.

Based on the training effectiveness evaluation performed on the BS115, stability characteristics were found to be adequate. Additionally, roll response and roll performance met the requirements posed. Both longitudinal control and aileron control forces were found to be too low to achieve satisfactory handling qualities. Finally, the training tasks showed that the avionics system needs some improvement for optimum ground reference manoeuvring and that steep turn performance is reduced in turbulent air.

To perform a complete training effectiveness evaluation, it is important to cover the entire spectrum of pilot skills and not only handling qualities. Therefore it is recommended for future research to integrate the method presented here into a complete training effectiveness evaluation method.



# CONTENTS

<b>Summary</b>	<b>v</b>
<b>List of Figures</b>	<b>xi</b>
<b>List of Tables</b>	<b>xiii</b>
<b>Nomenclature</b>	<b>xvi</b>
List of Abbreviations . . . . .	xvi
List of Symbols . . . . .	xvi
<b>1 Introduction</b>	<b>1</b>
1.1 Motivation . . . . .	1
1.2 Literature Review . . . . .	2
1.2.1 Training Effectiveness: The Bazzocchi Method . . . . .	2
1.2.2 Effectiveness of Military Training Aircraft . . . . .	4
1.2.3 Multi-Criteria Decision Making Processes and Fuzzy Logic . . . . .	4
1.3 Objective and Research Question . . . . .	5
1.4 Range and Scope . . . . .	6
1.5 Project Outline . . . . .	7
<b>2 Training Effectiveness Evaluation Criteria</b>	<b>9</b>
2.1 Training Program . . . . .	9
2.1.1 Joint Specialized Undergraduate Pilot Training . . . . .	9
2.1.2 Next Generation Fighter Pilot Training . . . . .	11
2.1.3 Training Role of the BS115 . . . . .	12
2.2 Military Standard Criteria . . . . .	12
2.2.1 MIL-F-8785C . . . . .	13
2.2.2 Longitudinal Handling Qualities Criteria . . . . .	13
2.2.3 Lateral-Directional Handling Qualities Criteria . . . . .	14
2.2.4 Maximum Roll Control Force . . . . .	15
2.3 Closed-loop Handling Quality Criteria . . . . .	15
2.3.1 Cooper-Harper Rating . . . . .	15
2.3.2 BS115 Training Missions . . . . .	15
2.4 Conclusion . . . . .	17
<b>3 Flight Testing</b>	<b>19</b>
3.1 Flight Test Instrumentation . . . . .	19
3.2 Flight Test Procedure . . . . .	21
3.2.1 Configuration Requirements . . . . .	21
3.2.2 Longitudinal Stability With Respect to Speed . . . . .	22
3.2.3 Phugoid Stability . . . . .	22
3.2.4 Short-period Oscillation . . . . .	23
3.2.5 Pitch Manoeuvring Force . . . . .	24
3.2.6 Dutch Roll . . . . .	24
3.2.7 Roll Mode . . . . .	24

<b>4</b>	<b>BS115 DATCOM Model</b>	<b>27</b>
4.1	BS115 DATCOM Input . . . . .	27
4.1.1	Flight Conditions . . . . .	27
4.1.2	Reference Points . . . . .	27
4.1.3	Fuselage . . . . .	28
4.1.4	Wing . . . . .	28
4.1.5	Empennage . . . . .	28
4.1.6	Power Plant . . . . .	28
4.2	Code Verification . . . . .	28
4.3	Calculation Verification . . . . .	30
4.3.1	Longitudinal Stability Derivatives Verification . . . . .	31
4.3.2	Lateral-Directional Stability Derivatives Verification . . . . .	33
4.4	Model Validation . . . . .	34
4.4.1	Longitudinal Stability Derivatives Validation . . . . .	34
4.4.2	Lateral-Directional Stability Derivatives Validation . . . . .	35
4.5	BS115 Stability Derivatives . . . . .	35
<b>5</b>	<b>BS115 Handling Quality Evaluation</b>	<b>37</b>
5.1	Longitudinal Stability With Respect to Speed . . . . .	38
5.1.1	Longitudinal Stability at Test Point 1 . . . . .	39
5.1.2	Longitudinal Stability at Test Point 2 . . . . .	40
5.1.3	Longitudinal Stability - Summary . . . . .	41
5.2	Phugoid Motion . . . . .	42
5.2.1	Phugoid Motion at Test Point 1 . . . . .	43
5.2.2	Phugoid Motion at Test Point 2 . . . . .	44
5.2.3	Phugoid Motion - Summary of Results . . . . .	44
5.3	Short Period . . . . .	45
5.3.1	Short Period Motion at Test Point 1 . . . . .	46
5.3.2	Short Period Motion at Test point 2 . . . . .	46
5.4	BS115 Longitudinal Control Characteristics . . . . .	47
5.4.1	Control Forces at Test Point 3 . . . . .	47
5.4.2	Control Forces at Test Point 2 . . . . .	49
5.4.3	Control Forces - Summary of Results . . . . .	50
5.5	BS115 Dutch Roll Characteristics . . . . .	51
5.5.1	Dutch Roll at Test Point 2 . . . . .	51
5.5.2	Dutch Roll Motion - Summary of Results . . . . .	52
5.5.3	Dutch Roll Evaluation Criteria . . . . .	53
5.6	BS115 Roll Mode . . . . .	54
5.6.1	Roll-mode Time Constant . . . . .	54
5.6.2	Roll Performance . . . . .	55
5.6.3	Roll Control Force . . . . .	57
5.7	Spiral Mode . . . . .	59
5.8	BS115 Pilot Feedback . . . . .	61
5.9	Discussion of Results . . . . .	64
<b>6</b>	<b>Conclusions</b>	<b>67</b>
<b>7</b>	<b>Recommendations</b>	<b>69</b>
<b>A</b>	<b>BS115 Aircraft Data</b>	<b>71</b>
A.1	BS115 3-View . . . . .	71
A.2	General Characteristics . . . . .	72
A.3	Wing Characteristics . . . . .	73
A.4	Empennage Characteristics . . . . .	73

<b>B</b>	<b>BS115 Weight and Balance</b>	<b>75</b>
<b>C</b>	<b>Dynon Flight Test Logging Parameters</b>	<b>79</b>
<b>D</b>	<b>DATCOM Files</b>	<b>81</b>
<b>E</b>	<b>Characteristics of Reference Aircraft</b>	<b>83</b>
E.1	BS115 Model . . . . .	83
E.2	Cessna 172 Skyhawk . . . . .	83
E.2.1	Longitudinal Stability and Control Derivatives . . . . .	83
E.2.2	Lateral-Directional Stability and Control Derivatives . . . . .	83
E.2.3	Hinge Moment Coefficients . . . . .	84
E.3	Diamond DA-20. . . . .	84
E.4	Stability Characteristics . . . . .	84
E.4.1	Longitudinal Stability Characteristics . . . . .	84
E.4.2	Lateral-Directional Stability Characteristics . . . . .	85
E.5	Control Forces in Manoeuvring Flight. . . . .	86
<b>F</b>	<b>Flight Test Results - Additional Plots</b>	<b>87</b>
F1	Phugoid Oscillation . . . . .	87
F1.1	Test Point 1 Additional Results . . . . .	87
F1.2	Test Point 2 Additional Results . . . . .	89
F2	Longitudinal Control Forces . . . . .	90
F3	Dutch Roll . . . . .	91
F3.1	Test Point 1 Additional Results . . . . .	91
F3.2	Test Point 2 Additional Results . . . . .	92
F4	Roll Mode . . . . .	93
F4.1	Test Point 1 Additional Results . . . . .	93
F4.2	Test Point 3 Additional Results . . . . .	96
	<b>Bibliography</b>	<b>99</b>



# LIST OF FIGURES

1.1	Blackshape - Prime and BS115 aircraft	1
1.2	Relationship between skill and time [1, p.29]	2
1.3	The Aermacchi MB-326 Aircraft [2]	3
1.4	The Cessna T-37 Aircraft [3]	3
1.5	Training Effectiveness Comparison - Aircraft Used	4
1.6	Elements that influence handling qualities [4, p.3]	6
1.7	Definitions of handling and flying qualities [5, p.3]	7
1.8	Focus area of thesis project [4]	7
2.1	The DA-20 [6]	10
2.2	The T-6B [7]	10
2.3	The Northrop T-38C Talon [8]	11
2.4	Next Generation Aircraft Fighters	12
2.5	Cooper-Harper Rating Scale [4, p.12]	16
3.1	BS115 - FTI System	19
3.2	BS115 Instrument Panel	20
3.3	Ground station layout	21
3.4	BS115 CG Envelope	22
3.5	Phugoid time history example [9, p.8.37]	23
3.6	Elevator doublet input	23
3.7	Example of stick force per g plot [10]	24
3.8	Roll rate response for an aileron step input [9, p.8.42]	25
4.1	Top View of the BS115 DATCOM Model	29
4.2	Side View of the BS115 DATCOM Model	29
4.3	Front View of the BS115 DATCOM Model	29
4.4	Lift coefficient as a function of the angle of attack for different DATCOM model configurations	30
4.5	Lift coefficient as a function of the angle of attack before and after downwash correction	31
4.6	Cessna 172 'Skyhawk'	34
5.1	BS115 CG Envelope - repeated	37
5.2	Longitudinal Stability wrt Speed (detailed) - 85 kts - Test point 1	38
5.3	Longitudinal Stability wrt Speed - 85 kts - Test point 1	39
5.4	Longitudinal Stability wrt Speed - Cruise - Test point 1	39
5.5	Longitudinal Stability wrt Speed - Manoeuvres - Test point 1	40
5.6	Longitudinal Stability wrt Speed - Cruise - Test point 2	40
5.7	Longitudinal Stability wrt Speed - Manoeuvres - Test point 2	41
5.8	Transient Peak Ratio - Definitions	42
5.9	Phugoid Oscillation - Test Point 1 - 120 kts	43
5.10	Phugoid Oscillation - Test Point 2 - 120 kts	44
5.11	Phugoid Confidence Interval (90%) - CG Aft	45
5.12	Short Period - Test Point 1 - 108 kts	46
5.13	Short Period - Test Point 1 - 108 kts	46
5.14	Short Period - Test Point 2 - 110 kts	47
5.15	Manoeuvring Control Forces - Test point 3 - 120 kts	48

5.16 Stick Force per G - Test Point 3 . . . . .	48
5.17 90% Confidence Interval - Test Point 3 . . . . .	49
5.18 Manoeuvring Control Forces - Test point 2 - 120 kts . . . . .	50
5.19 Stick force per g - Test point 2 - 120 kts . . . . .	50
5.20 Dutch Roll - Test Point 2 - 120 kts . . . . .	52
5.21 Lateral Stability Diagram [11, p.156] . . . . .	53
5.22 Roll Mode - Test Point 1 - 130 kts . . . . .	54
5.23 Roll Performance - Test Point 1 - 130 kts . . . . .	56
5.24 Roll Performance - Test Point 3 - Confidence Interval . . . . .	57
5.25 Aileron Control Forces - BS115 . . . . .	58
5.26 Aileron Control Forces - Reference Aircraft Comparison . . . . .	59
5.27 Eigenvalue location for the asymmetric motions - BS115 . . . . .	59
5.28 Normal Approach and Landing - Cooper Harper Evaluation . . . . .	61
5.29 S-turn ground reference Manoeuvre - Cooper Harper Evaluation . . . . .	62
5.30 Steep Turn Performance Manoeuvre - Cooper Harper Evaluation . . . . .	63
5.31 Recovery from Unusual Attitudes - Cooper Harper Evaluation . . . . .	64
A.1 BS115 - Front View . . . . .	71
A.2 BS115 - Side View . . . . .	71
A.3 BS115 - Top View . . . . .	72
B.1 BS115 reference point definition . . . . .	75
D.1 Digital DATCOM Input File for the BS115 . . . . .	81
D.2 Digital DATCOM Output File for the BS115 . . . . .	82
E1 Phugoid Oscillation - Test Point 1 - 80 kts . . . . .	87
E2 Phugoid Oscillation - Test Point 1 - 85 kts . . . . .	88
E3 Phugoid Oscillation - Test Point 1 - 130 kts . . . . .	88
E4 Phugoid Oscillation - Test Point 2 - 85 kts . . . . .	89
E5 Phugoid Oscillation - Test Point 2 - 90 kts climb . . . . .	89
E6 Phugoid Oscillation - Test Point 2 - 140 kts . . . . .	90
E7 Manoeuvring Control Forces - Test Point 1 . . . . .	90
E8 Manoeuvring Control Forces - Test Point 3 - Other Speeds . . . . .	91
E9 Dutch Roll - Test Point 1 - 90 kts . . . . .	91
E10 Dutch Roll - Test Point 1 - 130 kts . . . . .	92
E11 Dutch Roll - Test Point 2 - 120 kts - run 2 . . . . .	92
E12 Dutch Roll - Test Point 2 - 140 kts . . . . .	93
E13 Roll Mode - Test Point 1 - 65 kts (Take-off) . . . . .	93
E14 Roll Mode - Test Point 1 - 70 kts (Landing) . . . . .	94
E15 Roll Mode - Test Point 1 - 90 kts . . . . .	94
E16 Roll Mode - Test Point 1 - 95 kts . . . . .	95
E17 Roll Mode - Test Point 1 - 120 kts . . . . .	95
E18 Roll Mode - Test Point 1 - 140 kts . . . . .	96
E19 Roll Mode - Test Point 3 - 70 kts (Take-off) . . . . .	96
E20 Roll Mode - Test Point 3 - 70 kts (Landing) . . . . .	97
E21 Roll Mode - Test Point 3 - 80 kts . . . . .	97
E22 Roll Mode - Test Point 3 - 100 kts . . . . .	98

# LIST OF TABLES

2.1	Comparison of Training Aircraft Characteristics	12
2.2	Control forces for centre stick controllers	14
2.3	Cooper-Harper Rating Equivalence With Flying Quality Level	15
2.4	Normal Approach and Landing Evaluation Criteria	17
2.5	S-turn Evaluation Criteria	17
2.6	Steep turn Evaluation Criteria	17
2.7	Unusual Attitude Recovery Evaluation Criteria	17
4.1	Output Parameters for the BS115 DATCOM Model	28
4.2	DATCOM Comparison for Different Aircraft	31
4.3	Conversion of DATCOM Results	32
4.4	Results with equal definition	33
4.5	Lateral Derivative Sign Comparison	33
4.6	Lateral Derivative Comparison - Reference Aircraft	33
4.7	Cessna 172 - Longitudinal Stability Derivatives Comparison	34
4.8	Cessna 172 - Lateral Directional Stability Derivatives Comparison	35
4.9	BS115 Longitudinal Stability Derivatives	35
4.10	BS115 Lateral-Directional Stability Derivatives	36
5.1	Longitudinal stability with respect to speed - Test Point 1 Summary	41
5.2	Longitudinal stability with respect to speed - Test Point 2 Summary	42
5.3	Phugoid Motion - Test point 2 - Complete Results	44
5.4	Damping Coefficient Comparison for Various Aircraft	45
5.5	Short Period Damping Coefficients for Various Aircraft	47
5.6	Stick Force per g - Summary	50
5.7	Stick Force per g - Comparison with Reference Aircraft	51
5.8	Dutch Roll Motion - Complete Results	52
5.9	Dutch Roll Criteria - Flight Test Comparison	53
5.10	Dutch Roll Criteria - Model Comparison	54
5.11	Roll Mode Time Constant - Test Point 1 Summary	55
5.12	Roll Mode Time Constant - Test Point 3 Summary	55
5.13	Roll Performance - Test Point 1 Summary	56
5.14	Roll Performance - Test Point 3 Summary	57
5.15	Aileron Control Surface Comparison	59
5.16	Spiral Mode - Comparison with Reference Aircraft	60
A.1	BS115 General Characteristics	72
A.2	BS115 Wing Characteristics	73
A.3	BS115 Horizontal Tail Characteristics	73
A.4	BS115 Elevator Characteristics	73
B.1	Weight Breakdown for Test Point 1	76
B.2	Weight Breakdown for Test Point 2	76
B.3	Weight Breakdown for Test Point 3	76
B.4	Weight Breakdown for Empty Weight	77
E.1	Longitudinal Stability and Control Derivatives - Cessna 172	83

---

E.2	Lateral-directional Stability and Control Derivatives - Cessna 172	84
E.3	DA-20 Longitudinal Stability Derivatives	84
E.4	DA-20 Lateral-Directional Stability Derivatives	84

# NOMENCLATURE

## List of Abbreviations

CAS	Calibrated Air Speed
CG	Centre of Gravity
CHR	Cooper-Harper Rating
CLHQ	Closed Loop Handling Qualities
CRM	Crew Resource Management
DATCOM	Data Compendium
EASA	European Aviation Safety Agency
EDM	Electronic Data Management
ESDU	Engineering Sciences Data Unit
FAA	Federal Aviation Administration
FTI	Flight Test Instrumentation
IFS	Initial Flight Screening
IFT	Introductory Flight Training
JPPT	Joint Primary Pilot Training
JSUPT	Joint Specialized Undergraduate Pilot Training
MAC	Mean Aerodynamic Chord
MCDM	Multi-Criteria Decision Making
MTOW	Maximum Take-off Weight
PPL	Private Pilot License
SUPT	Specialized Undergraduate Pilot Training
USAF	United States Air Force
VFR	Visual Flight Rules
VSI	Vertical Speed Indicator

## List of Symbols

$\alpha$	Angle of attack
$\bar{a}$	Aileron mean aerodynamic chord
$\bar{c}$	Mean aerodynamic chord
$\beta$	Angle of sideslip
$\delta_a$	Aileron deflection angle
$\delta_e$	Elevator deflection angle
$\delta_r$	Rudder deflection angle
$\epsilon$	Downwash
$\epsilon_0$	Downwash at zero angle of attack
$\Lambda$	Sweep angle
$\omega_d$	Damped frequency
$\omega_n$	Natural frequency
$\omega_{nd}$	Dutch roll natural frequency
$\Phi$	Bank angle
$\phi$	Roll angle
$\tau_r$	Roll-mode time constant
$\xi$	Heading angle
$\zeta_d$	Dutch roll damping ratio
$\zeta_p$	Phugoid damping ratio

$\zeta_{sp}$	Short-period damping ratio
$A$	Aspect ratio
$C_A$	Aerodynamic force coefficient
$C_D$	Drag coefficient
$C_L$	Lift coefficient
$C_m$	Aerodynamic Moment coefficient
$C_N$	Normal force coefficient
$C_p$	Power coefficient
$C_{h_0}$	Hinge moment breakout force component
$C_{h_a}$	Aileron hinge moment coefficient
$C_{h_\alpha}$	Hinge moment derivative with respect to angle of attack
$C_{h_\delta}$	Hinge moment derivative with respect to control surface deflection
$C_{l_p}$	Derivative of rolling moment with respect to angular velocity in the X-axis
$C_{Lq}$	Derivative of lift coefficient with respect to pitching velocity
$C_{l_r}$	Derivative of rolling moment with respect to angular velocity in the Z-axis
$C_{L\alpha}$	Derivative of lift coefficient with respect to angle of attack
$C_{l_\beta}$	Derivative of rolling moment with respect to angle of sideslip
$C_{L\dot{\alpha}}$	Derivative of lift coefficient with respect to angle of attack rate
$C_{m_q}$	Derivative of moment coefficient with respect to pitching velocity
$C_{m_\alpha}$	Derivative of moment coefficient with respect to angle of attack
$C_{m\dot{\alpha}}$	Derivative of moment coefficient with respect to angle of attack rate
$C_{n_p}$	Derivative of normal force coefficient with respect to angular velocity in the X-axis
$C_{n_r}$	Derivative of normal force coefficient with respect to angular velocity in the Z-axis
$C_{n_\beta}$	Derivative of normal force coefficient with respect to angle of sideslip
$C_{Y_p}$	Derivative of lateral force coefficient with respect to angular velocity in the X-axis
$C_{Y_\beta}$	Derivative of lateral force coefficient with respect to angle of sideslip
$F$	Task frequency matrix
$F_a$	Aileron force
$F_s$	Stick force
$J$	advance ratio
$l_h$	Horizontal tail length
$n$	load factor
$n_L$	limit load factor
$p$	Angular velocity in the X-axis
$q$	Pitching velocity
$R$	Requirement matrix
$r$	Angular velocity in the Z-axis
$S$	Single criterion score matrix
$S$	Wing surface area
$S_a$	Aileron surface area
$S_h$	Horizontal tail surface area
$T$	Period
$T$	Sensitivity matrix
$T_{EV}$	Training effectiveness value
$V$	Velocity
$V_h$	Velocity at the horizontal tail
$W$	Weighting matrix
$X$	Actual value matrix
$x_w$	x-coordinate of the a.c. of the wing with fuselage and nacelles
$x_{cg}$	x-position of the centre of gravity

# 1

## INTRODUCTION

### 1.1. MOTIVATION

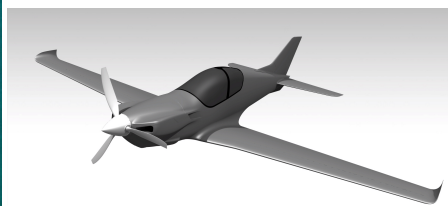
During a six month internship period I have spent at Blackshape I have been involved in the design of a new aircraft. I was asked to continue my work after my internship ended, and for this reason I decided to perform my thesis at Blackshape as well. Blackshape SpA is an Italian aircraft manufacturer located in the southern part of Italy, specialized in high-performance composite aircraft for both leisure and training. The company was founded in 2009 after acquiring the plans of the "Millenium Master" aircraft. This two-seater aircraft was further developed by Blackshape and eventually became known as the Blackshape Prime, which received the Flieger Magazine Award for best airplane in the world (ultra-light category) in 2013.

The Blackshape Prime (Figure 1.1a) is an ultra-light general aviation aircraft, featuring a full carbon fibre airframe. Its design enables it to operate off an aircraft carrier and therefore the Prime offers an opportunity for military aviation training. As a result, the Italian Navy is currently working with Blackshape to develop a program using the Prime to train its pilots on carrier-borne operations [12]. One of the important aspects considered by the company in this regard is the training effectiveness, which is defined as "the efficiency and capability of military training aircraft" [13].

Presently the company is working on the successor of the Prime, which is called the BS115 (Figure 1.1b). This aircraft features a new wing design and an increase in power, allowing the maximum take-off weight (MTOW) to increase to 750 kg. As mentioned in the previous paragraph, training effectiveness is one of the important research topics at the company. Due to its increased performance the BS115 might offer new training opportunities as compared to the Blackshape Prime, which is why the assessment of training effectiveness has become a topic of even greater importance. By analysing the training effectiveness of the BS115 and identifying shortcomings in this perspective, the training potential of the aircraft can be increased. Moreover, the obtained results could lead to a better understanding of the evaluation of training effectiveness for a modern training aircraft. This has been the main focus of my thesis work.



(a) The Blackshape Prime



(b) The BS115

Figure 1.1: Blackshape - Prime and BS115 aircraft

## 1.2. LITERATURE REVIEW

The first and one of the most important considerations on the topic of training effectiveness in literature is made by Ermanno Bazzocchi, the general manager of Aeronautica Macchi (now Alenia Aermacchi) back in 1978. In his lecture he describes how the fundamental concepts for the development of a second-generation jet trainer are defined, and how this effectively boils down to a cost-effectiveness optimization [1, p.1]. His work is examined in subsection 1.2.1. Subsections 1.2.2 and 1.2.3 cover other methods used to examine training effectiveness.

### 1.2.1. TRAINING EFFECTIVENESS: THE BAZZOCCHI METHOD

To determine training effectiveness, Bazzocchi uses an adapted operational analysis method, originally developed by the Aerospace Technical Department of the Italian Ministry of Defense [1, p.9]. In the operational analysis method, skill acquisition is assumed to follow the qualitative curve of Figure 1.2. Initially the skill acquisition takes place at a slow rate, due to adaptation problems to the new learning situation. This phase is followed by a period of time with a steady teaching rate. Finally, the student can no longer gain any additional skills in the learning situation and saturation takes place. The gradient of the linear part of the curve is called the teaching rate.

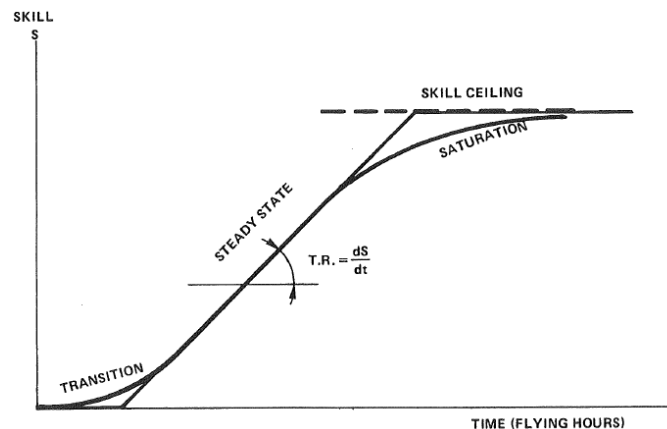


Figure 1.2: Relationship between skill and time [1, p.29]

Using the linear part of the skill curve in Figure 1.2, the operational analysis method allows to compute the training effectiveness as the ratio of the teaching rate of the aircraft, compared to that of a reference aircraft. It is assumed that this teaching rate can be correlated to a number of quantifiable aircraft characteristics like the maximum speed, take-off rapidity (inverse of the take-off time) and maximum rate of climb [1, p.34].

The training program is then divided into typical missions, related to the pilot skills to be acquired. For all typical missions, the relative importance of each aircraft characteristic described above is rated by expert pilots and given a score between zero (not important) and three (essential). This weighting coefficient is then multiplied by the aircraft characteristic, normalized with respect to the reference aircraft. In the case of Bazzocchi this is the MB-326, which is shown in Figure 1.3. Addition of all these scores for a given mission is assumed to be the teaching effectiveness of that aircraft for that type of mission.



Figure 1.3: The Aermacchi MB-326 Aircraft [2]

Next, the hours flown in each mission are determined using statistical data. Multiplication with the aforementioned teaching effectiveness results in the equivalent time in the reference aircraft to obtain the same skill level. Finally, the total teaching effectiveness is obtained by the ratio of the sum of the equivalent training times to the actual training time.

The final topic treated by Bazzocchi is the cost-effectiveness of each aircraft. By determining the cost per syllabus hour, which equals an hour within the training program, the teaching cost-effectiveness can be computed as the ratio between teaching effectiveness and the relative cost of the syllabus hour. The teaching cost-effectiveness therefore is a measure of skill increase per unit cost related to a reference aircraft.

The principles of the operational analysis method have been applied by Pilatus [14] to evaluate 18 training aircraft, using the T-37 aircraft and the USAF training syllabus as baseline. The T-37 is shown in Figure 1.4. In addition, a more recent paper applies the method to optimize a fighter trainer aircraft with a double-delta wing [15]. Using a first prototype as the reference aircraft, the wing planform was altered in an optimization algorithm with the training effectiveness as objective function.



Figure 1.4: The Cessna T-37 Aircraft [3]

### 1.2.2. EFFECTIVENESS OF MILITARY TRAINING AIRCRAFT

Based on the earlier work of Bazzocchi, Min *et al.* [13] have developed a software program that is able to analyse and evaluate the effectiveness of military trainers. The evaluation is done using two steps: single criterion scoring and comprehensive scoring. The mathematical formulation of single criterion scoring is:

$$S = f(R, T, X) \quad (1.1)$$

In equation 1.1,  $R$  represents the requirement matrix with the desired criteria values,  $T$  the sensitivity matrix with the upper and lower bounds, while  $X$  contains the actual values. Through the scoring function  $f$ ,  $S$  is calculated, which is the single criterion score matrix.

The mathematical formula for comprehensive scoring is as follows:

$$T_{EV} = (S \times W) \times F \quad (1.2)$$

Where  $T_{EV}$  is the training effectiveness value, and  $F$  is the task frequency in a certain training phase. The weighting matrix  $W$  represents the relative importance of each criteria in different training tasks and is determined by expert evaluation.

This program is used to compare the training effectiveness of three different aircraft: the HAWK, the MB-339 and the FT-6 (Figures 1.5a to 1.5c). With similar evaluation criteria used as in the Bazzocchi method, the MB-339 is found to have the highest teaching effectiveness of the three.



Figure 1.5: Training Effectiveness Comparison - Aircraft Used

### 1.2.3. MULTI-CRITERIA DECISION MAKING PROCESSES AND FUZZY LOGIC

A slightly different approach to the evaluation of military training aircraft is offered by Sánchez-Lozano *et al.* [16]. In their paper, several alternatives for a training aircraft for the Spanish air force are considered. It is suggested to use Multi-Criteria Decision Making (MCDM) processes to cope with the large amount of evaluation criteria involved in assessing trainer effectiveness. Moreover, due to the different nature of these criteria (both qualitative and quantitative) the MCDM method should be combined with fuzzy logic. In this study, the TOPSIS method [17] is used to select the preference order of the several aircraft alternatives under investigation.

The principle of the evaluation method is still similar to the operational analysis method of subsection 1.2.1, although it is used in a different manner. First of all a set of evaluation criteria is established, after which weighting values are assigned for each criterion. For the assessment criteria that cannot be defined in a quantitative way, a linguistic variable is introduced to allow evaluation using fuzzy logic. In this way, all criteria can be quantified. The weighing factors are determined based on expert opinions. The fuzzy TOPSIS method that is used provides a ranking of the alternative options, based on the relative proximity to the ideal solution. After defuzzification, where the fuzzy numbers are transformed into crisp values, a ranking with real numbers is obtained that is in line with the results expected by the experts.

### 1.3. OBJECTIVE AND RESEARCH QUESTION

As seen in the previous section, the method to evaluate the training effectiveness of an aircraft generally contains the same steps:

1. Establish a set of evaluation criteria for the trainer aircraft
2. Assign a weighting value to each of the criteria to reflect its importance
3. Obtain the characteristics of each aircraft to be evaluated
4. Compute the training effectiveness value for each aircraft based on its characteristics and the weighting value
5. Compare the results to determine the best available option

One aspect that is not taken into consideration to a sufficient extent in the available methods is the effect of handling qualities on training effectiveness. Even though this is identified by Sánchez-Lozano *et al.* [16, p.62] as one of the most important criteria, the topic is not covered extensively. Sánchez-Lozano *et al.* [16] assign only a single score to the handling quality characteristics based on expert opinions, while the other methods devote even less attention to the topic.

To increase understanding about the influence of handling qualities, the objective of this master thesis project is to assess the effect of handling qualities on the training effectiveness of the BS115 aircraft using relevant evaluation criteria. Thereto a combination of theoretical computations and a series of flight tests is performed with the purpose of examining the aircraft's handling qualities in this perspective. The project's research question is as follows:

*Which handling qualities of the BS115 aircraft should be improved such that the training effectiveness of the aircraft is maximized for the development of flying skills?*

## 1.4. RANGE AND SCOPE

As stated in Section 1.3, this thesis project focuses on the influence of handling quality characteristics on training effectiveness. According to Cooper and Harper [4, p.2], handling qualities can be defined as "those qualities or characteristics of an aircraft that govern the ease and precision with which a pilot is able to perform the tasks required in support of an aircraft role". The factors that influence handling qualities are shown in Figure 1.6:

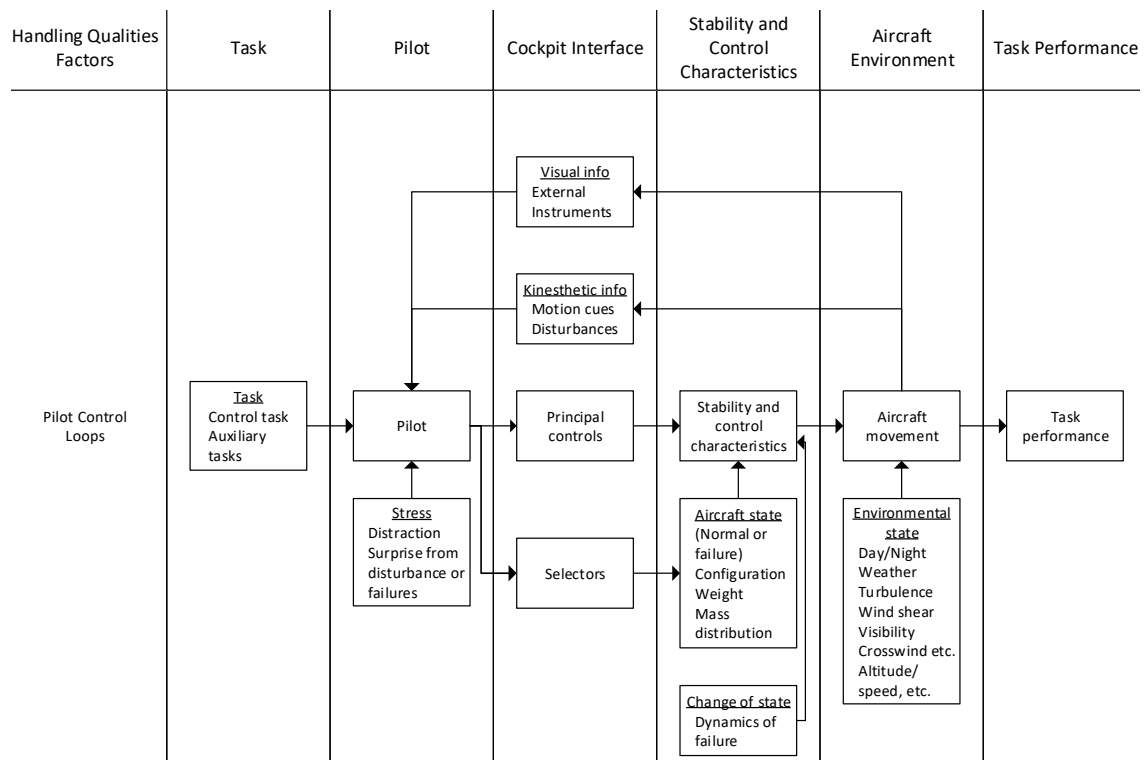


Figure 1.6: Elements that influence handling qualities [4, p.3]

In addition to handling qualities, a term often encountered in literature is flying qualities. Although Cooper and Harper make no distinction between the two, flying qualities are defined by Phillips as "the stability and control characteristics that have an important bearing on the safety of flight and on the pilot's impressions of the ease of flying an airplane in steady flight and in manoeuvre" [18]. This definition suggests a differentiation should be made between handling and flying qualities, which is supported by Cook [5]. Handling qualities are defined as "the pilot's qualitative description of the adequacy of the short-term dynamic response to controls in the execution of the flight task", and flying qualities as "a pilot's qualitative description of how well the airplane carries out the commanded task". This is visualized in Figure 1.7. This distinction between flying and handling qualities will also be used in this thesis.

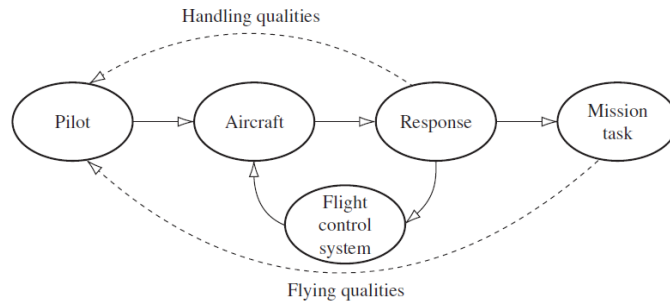


Figure 1.7: Definitions of handling and flying qualities [5, p.3]

It has been well established that the flying and handling qualities of an aircraft are intimately dependent on stability and control characteristics, including the flight control system [5, p.4]. Since stability and control characteristics are easily quantified, they can be used as a measure of handling qualities. Therefore this research project will mostly focus on these characteristics. The relevant handling quality elements are indicated in Figure 1.8. It has to be noted that only the aircraft normal state will be considered. The influence of any aircraft failure is beyond the scope of this thesis project.

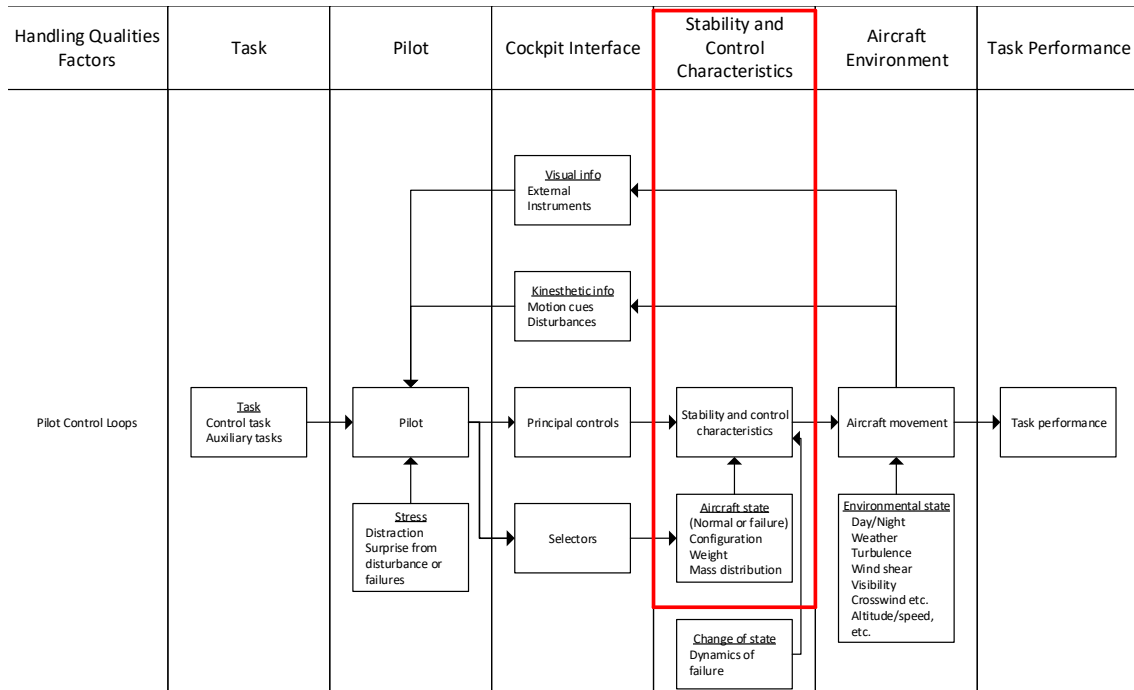


Figure 1.8: Focus area of thesis project [4]

### 1.5. PROJECT OUTLINE

The previous sections of this chapter have focused on explaining the research goals, scope, and motivation of this thesis project. Chapter 2 will in-depth discuss the training effectiveness evaluation criteria required for the evaluation of the BS115 handling qualities. Once these criteria have been defined, they have to be evaluated. To this purpose, several flight tests have been performed. Chapter 3 explains the flight test procedure followed to obtain the flight test data. In addition to the flight test data, a model representing the BS115 characteristics is constructed in Chapter 4. The results of the handling quality criteria evaluation is presented in Chapter 5. Chapter 6 summarizes the work and discusses the implications of the obtained results. Finally, recommendations for future work are given in Chapter 7.



# 2

## TRAINING EFFECTIVENESS EVALUATION CRITERIA

In the previous chapter, the general thesis layout and the project goals have been discussed. The next step is to examine how transfer of training in the aircraft can be assessed. As stated in Section 1.4, stability and control characteristics can be used as an indication of handling qualities. Therefore, these will serve as a basis for establishing assessment criteria. First of all, the relevant training profile is deduced in Section 2.1. The evaluation criteria are set up in Sections 2.2 to 2.4.

### 2.1. TRAINING PROGRAM

To understand what role the BS115 can play in the training of military pilots, a general comprehension about fighter pilot training programs is necessary. As seen in Section 1.2, the training missions and the time spent on each of them have a big influence on the final training effectiveness value. This should also be a major consideration in determining the handling quality evaluation criteria.

Although multiple pilot training programs exist, only the USAF program is discussed in this thesis. Not only is most literature devoted to this program, but it also serves as an example for training programs of other countries such as Italy [19].

#### 2.1.1. JOINT SPECIALIZED UNDERGRADUATE PILOT TRAINING

The USAF currently employs the Joint Specialized Undergraduate Pilot Training (JSUPT) program, originating from the 1990's. The first step in this program is the Introductory Flight Training (IFT), also known as Initial Flight Screening (IFS) [20]. During this phase, candidate pilots are screened, motivated and prepared for entry in the undergraduate pilot training program. Since this is the absolute beginning of flight training, skills learned in IFT are very similar to the skills required for obtaining a private pilot license (PPL) [21]. The program is therefore performed at civilian flight schools as well, and is typically executed in an aircraft like the Diamond Da-20 [22] (shown in Figure 2.1). JSUPT consists of three blocks [23]:

1. *Orientation*: In this part of the program, basic aircraft control is practised together with some basic manoeuvres. Examples are cockpit organisation, departure and arrival, trim use and clearing.
2. *Fundamental manoeuvres*: The next step builds further on basic aircraft control and includes some additional manoeuvres like traffic patterns, steep turns and ground reference manoeuvres.
3. *Navigation fundamentals*: In addition to the previously learned skills, situational awareness is built and students learn the basics of navigation.



Figure 2.1: The DA-20 [6]

After completion of the IFT, students move to the Joint Primary Pilot Training (JPPT). In this part of the program students learn several basic manoeuvres, patterns, and arrivals/departures [20] while flying the T-6B aircraft (Figure 2.2). During the primary training students should develop towards a specified skill level, in order to qualify for follow-on advanced jet training. The current curriculum for the primary pilot training on the T-6B consists of several distinct training stages, each covering a specific flight training regime [24]:

- Ground training
- Contact training
- Instrument training
- Navigation training
- Formation training



Figure 2.2: The T-6B [7]

The first part of the primary pilot training, the ground training, aims to familiarize the student with the aircraft systems and procedures. In this part of the training no flight sorties are made and learning takes place in a class environment.

During contact training, the student flies the aircraft together with an instructor. The aim is to teach the fundamental flight skills required to safely solo in the T-6B, as well as to successfully complete JPPT. This training phase consists of a variety of procedural tasks, basic flying skills and manoeuvres.

The next two stages, navigation training and formation training, focus mostly on teaching cockpit procedures. Instrument training is broken down into two parts: basic instruments and radio instruments. The basic instrument skills are taught completely in a simulator, while radio instrument skills are practised during actual flights as well. Navigation training covers the topics of VFR flying and low-level navigation and planning. It includes both day and night navigation. Similar to radio instrument skills practice, simulator training as well as flight training is used.

In the final stage of the JPPT, students develop formation flying skills. It serves as the last step in preparation for the advanced training phase and contains basic formations, formation procedures and three-dimensional manoeuvring skills.

In the advanced training program, the T-38C is flown (Figure 2.3). Four phases can be recognized; transition, instruments/navigation, formation and low-level navigation. In the transition phase, students can adapt to the different characteristics of the T-38C as compared to the T-6B and perform mostly similar tasks as in the JPPT. This is also the case for the instrument/navigation phase. In the formation phase, more complex manoeuvres are introduced as part of a two or four-ship aircraft formation. Finally, navigation and procedures for low-level flights down to 500 feet are taught.



Figure 2.3: The Northrop T-38C Talon [8]

### 2.1.2. NEXT GENERATION FIGHTER PILOT TRAINING

With the introduction of the Specialized Undergraduate Pilot Training (SUPT) program in the 90's, students were able to receive specialized training at an earlier stage, leading to better prepared pilots as compared with the previous training program. However, the next generation of fighter aircraft, like the F/A-22 and F-35, puts even higher demands on pilot capabilities. As a result several investigations were performed to identify the challenges for next generation training, leading to the following observations and recommendations [25, 26]:

- The "collection, synthesis and prioritization of information" in the cockpit will become increasingly difficult.
- Flying the aircraft should remain to be second nature for the pilot. Therefore teaching the fundamentals of flying should continue to be the focus of the SUPT program.
- A training shortfall is present in the development of fighter pilot skills and crew resource management skills. A possible solution to this problem is to shift part of the advanced training to an earlier stage and increase the number of solo sorties. Additionally, certain tasks can be shifted from aircraft sorties to training device sorties, which take part in a simulator.



Figure 2.4: Next Generation Aircraft Fighters

### 2.1.3. TRAINING ROLE OF THE BS115

As seen in the previous subsections, a different aircraft is used in various stages of the training program. While students build up their skill level, the aircraft used becomes more advanced. To determine in which part of the training program the BS115 can best be used, and hence identify the applicable handling quality requirements, a comparison of basic aircraft characteristics is made with the aforementioned DA-20, T-6B and T-38C.

	BS115	DA-20	T-6B	T-38C
Maximum take-off weight [kg]	750	800	3130	5485
Maximum Speed [kts]	180	164	270	706
Maximum rate of climb [ft/min]	1827	930	4500	33000
Service ceiling [ft]	15000	17600	35000	55000
Load factor limits [g]	+5.0/-2.5	+4.4/-2.2	+7/-3.5	+7.33/-3
Power loading [kg/kW]	6.3	12.0	3.8	3.3

Table 2.1: Comparison of Training Aircraft Characteristics

As seen in Table 2.1 the BS115 aircraft has characteristics most similar to the DA-20 used in introductory flight training. However, in subsection 2.1.2 it is also suggested to shift part of the training to earlier stages. Therefore the BS115 is assumed to play a role in both the introductory and primary phases of training. The primary phase of training will become even more relevant for the follow-on up-rated versions of the BS115 aircraft, that will be certified for aerobatics and have an even larger increase in engine power.

## 2.2. MILITARY STANDARD CRITERIA

As stated in Section 1.4, handling qualities are intimately dependent on stability and control characteristics. To determine what criteria should be applied in the training effectiveness evaluation of the BS115, first the available regulation documentation is consulted. This documentation can be split into two categories; non-military requirements posed by airworthiness authorities like the FAA and EASA, and the requirements for military aircraft issued by organizations like the US Department of Defense.

Certification requirements issued by airworthiness authorities have the purpose of specifying a minimum acceptable standard and are primarily concerned with safety [5, p.268]. However, this does not guarantee that an aircraft meeting the requirements is easy to fly or suitable for its designed mission. On the other hand, military requirements are constructed to assure both adequate mission performance and safety. As a result, they are specified in much more detail. This makes them highly suitable as a basis for evaluation criteria. The remainder of this section is therefore concerned with identifying the appropriate criteria using the military standard.

### 2.2.1. MIL-F-8785C

The latest military standard available is MIL-STD-1797A, which focuses mostly on handling and flying quality requirements applicable to highly augmented aircraft. Since the BS115 has no control augmentation, it suffices to follow the original handling quality requirements as stated in MIL-F-8785C and hence the latter is discussed here. To cope with the distinctive characteristics of various categories of aircraft, MIL-F-8785C has specified different requirements for each of the following aircraft classes:

- Class I: Small, light airplanes
- Class II: Medium weight, low-to-medium manoeuvrability airplanes
- Class III: Large, heavy, low-to-medium manoeuvrability airplanes
- Class IV: High-manoevrability airplanes

In addition, a distinction is made between different flight phases. Category A flight phases relate to rapid manoeuvring, precision tracking and precise flight-path control. Category B comprises gradual manoeuvres not requiring precision tracking, while terminal flight phases are collected in Category C [27, p.2]. To evaluate the aircraft performance, handling qualities are reviewed based on three levels of acceptability:

- Level 1: Handling qualities clearly adequate for the mission Flight Phase
- Level 2: Handling qualities adequate to accomplish the mission Flight Phase, but some increase in pilot workload or degradation in mission effectiveness, or both, exists
- Level 3: Handling qualities such that the airplane can be controlled safely, but pilot workload is excessive or mission effectiveness is inadequate, or both. Category A Flight Phases can be terminated safely, and Category B and C Flight Phases can be completed

With the training goals as identified in Section 2.1, the BS115 can be regarded as a Class I aircraft. The goal should be to achieve level 1 handling qualities in both Category B and C manoeuvres, since these mission phases are the most common in the initial stages of flight training.

Although the MIL-F-8785-C has a wide range of specifications on handling qualities, not all of them have to be considered for training effectiveness evaluation, as many criteria will already need to be met in a normal certification process. Therefore, only the criteria considered most critical are evaluated. A summary of these criteria is given in subsections 2.2.2 and 2.2.3.

### 2.2.2. LONGITUDINAL HANDLING QUALITIES CRITERIA

Handling quality criteria can be divided between longitudinal qualities and lateral-directional qualities. In this subsection, the longitudinal flying characteristics are examined. MIL-F-8785C has the following longitudinal flying characteristics considered important for training effectiveness evaluation [27, p.11]:

#### LONGITUDINAL STABILITY WITH RESPECT TO SPEED

To obtain level 1 handling qualities, there should be no tendency for airspeed to diverge aperiodically when the airplane is disturbed from trim with cockpit controls fixed and free.

#### PHUGOID STABILITY

The long-period oscillations which occur when the airplane seeks a stabilized airspeed following a disturbance shall meet the following requirements:

$$\zeta_p \text{ at least } 0.04$$

**SHORT-PERIOD RESPONSE**

The equivalent short-period damping ratio,  $\zeta_{sp}$ , shall be within the following limits to achieve level 1 handling qualities:

$$0.35 < \zeta_{sp} < 1.30 \text{ for category C flight phases}$$

$$0.30 < \zeta_{sp} < 2.00 \text{ for category B flight phases}$$

Since the category C flight phase requirements are most critical, these will be considered.

**PITCH MANOEUVRING FORCE GRADIENT LIMITS**

The maximum gradient of the stick force per g shall be within the limits of Table 2.2:

Level	Maximum gradient, $(Fs/n)_{max}$	Minimum gradient, $(Fs/n)_{min}$
1	$\frac{240}{n/\alpha}$ , but no more than 28.0 nor less than $\frac{56}{n_L-1}$	The higher of $\frac{21}{n_L-1}$ and 3.0
2	$\frac{360}{n/\alpha}$ , but no more than 28.0 nor less than $\frac{85}{n_L-1}$	The higher of $\frac{21}{n_L-1}$ and 3.0
3	56.0	The higher of $\frac{12}{n_L-1}$ and 2.0

Table 2.2: Control forces for centre stick controllers

**2.2.3. LATERAL-DIRECTIONAL HANDLING QUALITIES CRITERIA**

The lateral-directional handling qualities considered are as follows [27, p.22]:

**DUTCH ROLL**

The Dutch roll frequency,  $\omega_{nd}$ , and damping ratio,  $\zeta_d$ , of the lateral-directional oscillations following a yaw disturbance shall exceed the following values:

- $\zeta_d > 0.08$
- $\zeta_d \cdot \omega_{nd} > 0.15 \text{ Hz}$
- $\omega_{nd} > 1.0 \text{ Hz}$

**ROLL MODE**

The roll-mode time constant,  $\tau_r$ , shall be no greater than 1.0 s.

**SPIRAL STABILITY**

The combined effects of spiral stability, flight-control-system characteristics and rolling moment change with speed shall be such that following a disturbance in bank, the time for the bank angle to double shall be greater than 12 seconds.

**ROLL PERFORMANCE**

It shall be possible for the aircraft to achieve a 30° bank angle within 1.3 seconds. Additionally, a 60° bank angle should be reached within 1.7 seconds.

#### 2.2.4. MAXIMUM ROLL CONTROL FORCE

The stick force required to obtain the rolling performance shall be neither greater than 20 lbs, nor less than the breakout force plus 5 lbs for level 1 handling qualities. The breakout force equals the initial force required to move the control surface. Level 2 handling qualities are achieved when the required stick force is neither greater than 20 lbs, nor less than 2.5 lbs and level 3 handling qualities are achieved when the required stick force is neither greater than 20 lbs, nor smaller than 0 lbs.

### 2.3. CLOSED-LOOP HANDLING QUALITY CRITERIA

Up to this point, the criteria considered are related to the open-loop handling qualities of the aircraft. In open-loop handling quality evaluation, pilot inputs are made without the consideration of the aircraft response. However, the ultimate goal of any aircraft should be to have good closed loop handling qualities (CLHQ) for its mission [9]. Therefore this section establishes the criteria that will be used to evaluate the closed-loop performance of the BS115.

#### 2.3.1. COOPER-HARPER RATING

CLHQ testing qualitatively evaluates an aircraft in the performance of a certain mission and is heavily dependent on pilot opinion. Therefore specific tasks and performance criteria for the task need to be established. Because of this difference with the specific requirements posed in the previous section, an alternative approach is necessary. The most common closed-loop handling qualities assessment method is the Cooper Harper rating method (CHR) [4], which evaluates the aircraft's suitability for the intended mission by appointing a score based on the rating system of Figure 2.5.

For the purpose of assessing the training effectiveness criteria of the BS115, a modified version of the Cooper-Harper scale is used. The original Cooper-Harper rating scale aims to rate aircraft handling qualities, which relate to the open-loop aircraft response. However, to evaluate the closed-loop performance of the BS115, the aircraft mission performance has to be evaluated. As seen previously in Figure 1.7 of Section 1.4, thereto the performance of the mission task has to be evaluated. To accommodate this evaluation, the approach suggested by Casali and Wierwille [28, p.626] is followed.

The obtained task rating will be converted to a level of flying qualities, which is done to achieve consistency throughout the evaluation. Table 2.3 shows the equivalence between the two, which is in agreement with Cook [5, p.275].

Level of Flying Qualities	Level 1	Level 2	Level 3	Below Level 3
Cooper-Harper Rating	1 - 3	< 6	< 8	> 8

Table 2.3: Cooper-Harper Rating Equivalence With Flying Quality Level

#### 2.3.2. BS115 TRAINING MISSIONS

To accommodate the evaluation of closed loop handling qualities, several distinctive training tasks will be examined that are common in the training curriculum. For each of these tasks, requirements are posed in agreement with the curriculum performance standards [29, 30]. This results in the following training tasks:

- Normal approach and landing
- S-turn ground reference manoeuvre
- Steep turn performance manoeuvre
- Recovery from unusual attitudes

A summary of the performance evaluation criteria related to these training tasks is given in Tables 2.4 to 2.7.

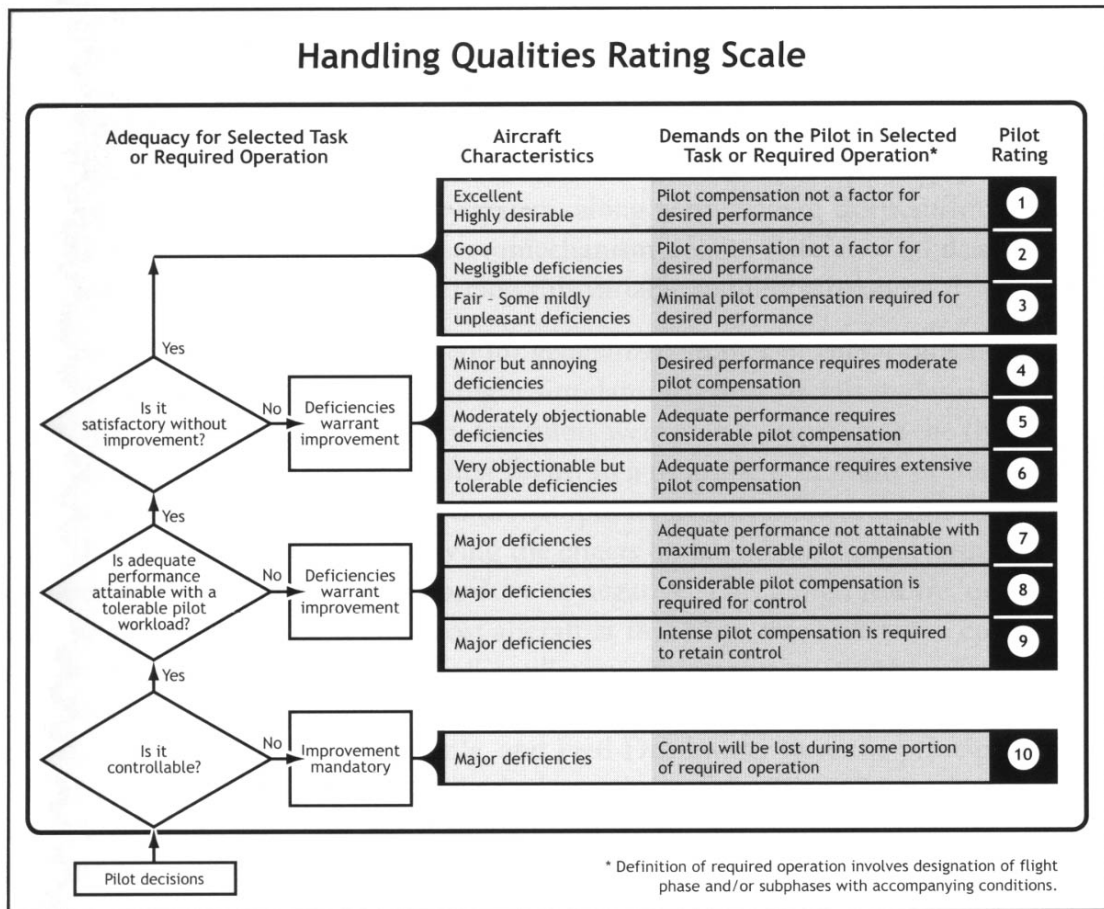


Figure 2.5: Cooper-Harper Rating Scale [4, p.12]

Rating 1-3	Rating 4-6	Rating 7-9
Approach speed +10/ -0 KIAS  Touch down within 1000 ft and ± 15 ft from centreline	Approach speed +20/ -0 KIAS  Touch down within 1000 ft and ± 15 ft from centreline	A safe approach and landing is possible

Table 2.4: Normal Approach and Landing Evaluation Criteria

Rating 1-3	Rating 4-6	Rating 7-9
Altitude within ± 100 ft Airspeed within ± 10 KIAS	Altitude within ± 150 ft Airspeed within ± 15 KIAS	Altitude within ± 250 ft Airspeed within ± 20 KIAS

Table 2.5: S-turn Evaluation Criteria

Rating 1-3	Rating 4-6	Rating 7-9
Bank angle within ± 10° Airspeed within ± 10 KIAS Roll-out heading within ± 15°	Bank angle within ± 15° Airspeed within ± 15 KIAS Roll-out heading within ± 20°	Bank angle within ± 20° Airspeed within ± 20 KIAS Roll-out heading within ± 30°

Table 2.6: Steep turn Evaluation Criteria

Rating 1-3	Rating 4-6	Rating 7-9
Recovery with minimum loss of altitude/speed	Recovery with marginal loss of altitude/speed	Recovery with acceptable loss of altitude/speed

Table 2.7: Unusual Attitude Recovery Evaluation Criteria

## 2.4. CONCLUSION

In the previous sections, the criteria for handling quality evaluation of the BS115 for the training of flying skills have been determined. Summarizing, the following steps will be taken:

- Firstly, the stability characteristics of the BS115 are examined both in longitudinal manoeuvring and lateral-directional manoeuvring.
- Secondly, the control forces will be checked for adequate performance.
- Finally, several typical training manoeuvres are examined using feedback from the test pilot.



# 3

## FLIGHT TESTING

With the training effectiveness evaluation criteria determined in Chapter 2, the next step in the evaluation procedure is to identify the relevant aircraft properties. To this purpose a series of CS-VLA certification test flights is available. However, it was stated in the introduction of Section 2.2 that certification flying requirements are less demanding than the military standards. As a result not all evaluation criteria determined in the previous chapter are covered in the flight test campaign and additional data is required. This is further discussed in Chapter 4. In this chapter, the test equipment and procedures used to obtain the flight test data are described. First of all, Section 3.1 describes the flight test instrumentation. With the test equipment defined, the test procedures are explained in Section 3.2.

### 3.1. FLIGHT TEST INSTRUMENTATION

The flight test instrumentation system for the BS115 aircraft consists of a customized configuration of the Dynon Skyview SV-D700, as displayed in Figure 3.1a.



(a) BS115 FTI Harness



(b) BS115 Air Data Boom

Figure 3.1: BS115 - FTI System

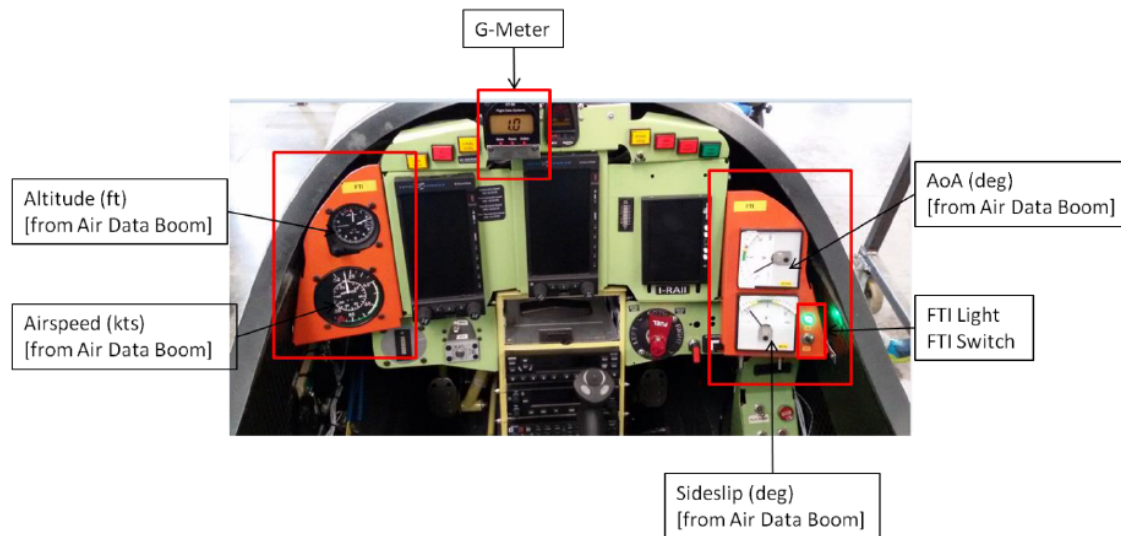


Figure 3.2: BS115 Instrument Panel

The FTI consists of the following components:

- FTI harness (3.1a) containing:
  - G-meter
  - Airspeed indicator
  - Altitude indicator
  - Angle of attack indicator
  - Sideslip indicator
- Mini air data boom (3.1b)
- FTI instrument panel (3.2)
- Linear transducers
- Strain gauges
- Potentiometers
- Antenna

In addition, a ground station is present equipped with the following instrumentation, as seen in Figure 3.3:

- Computer
- Speakers
- COM/NAV radio
- Radio module for data transmission
- Weather station
- Microphone and headsets



Figure 3.3: Ground station layout

The ground station decodes the received flight test data using software developed by Blackshape, in order to allow real-time flight monitoring. All data are stored in the FTI's internal memory with a 4 Hz data rate, while the ground station keeps a log file with a rate of 1 Hz, allowing to verify each recorded parameter by comparison of the two data sets. After the flight, all test data is downloaded from the FTI's internal memory, as well as from the EDM. A complete list of the recorded parameters is available in Appendix C.

## 3.2. FLIGHT TEST PROCEDURE

In order to obtain the flight test data required, several test flights have to be executed. These are described in this section. First of all the configuration requirements are discussed, after which the detailed flight test manoeuvres are given.

### 3.2.1. CONFIGURATION REQUIREMENTS

Due to the effect of the centre of gravity on the pitching moment, test flights are executed with a varying CG position. Two of the test points will be taken at the aircraft MTOW, while the final test point is taken at a forward CG position with a lower weight. In order to change the weight of the BS115, tabs of lead are either added or removed from the passenger seat. For the first test point a CG position of 23.6% MAC is selected. The second set of test flights is executed with a CG position of 31% MAC, which is the most aft CG position possible. Finally, the most forward CG position used is 17.3% MAC. The defined test flight points are visualized in the CG envelope of Figure 3.4. A detailed weight breakdown is provided in Appendix B.

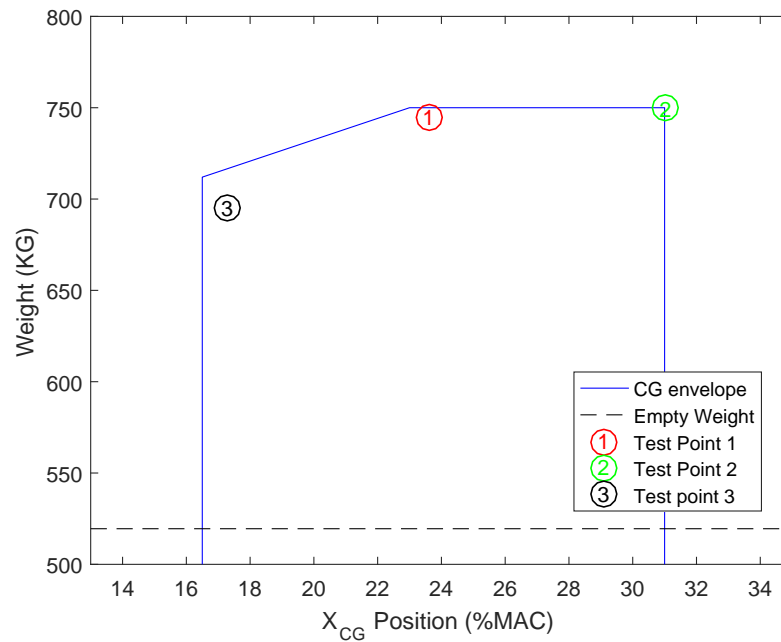


Figure 3.4: BS115 CG Envelope

### 3.2.2. LONGITUDINAL STABILITY WITH RESPECT TO SPEED

The first criteria to be tested is the overall longitudinal stability with respect to speed. The procedure followed is to initially trim the aircraft at the desired altitude and airspeed, after which a pull force is applied to reduce the airspeed. The pull force is then gradually relaxed to allow the airplane to slowly return toward trim speed and zero stick force; the speed at which the airplane stabilizes with zero stick force is observed. Starting again at the trim speed, a push force is applied to increase the airspeed. The control is then gradually relaxed in the same manner as previously described. This test method is called the Stabilized Long-Stat Stability Method, as covered in Roberts *et al.* [9, p.12.1].

To analyse the longitudinal stability the airspeed, stick force and elevator deflection time histories will be used. Points of interest are the speed at which the manoeuvre is initiated, the maximum deviation obtained and the final stabilized aircraft condition.

### 3.2.3. PHUGOID STABILITY

To test the phugoid stability of the BS115, the aircraft is stabilised and trimmed in the specified flight condition and configuration. The longitudinal control is then moved forward in order to increase the airspeed. Once an airspeed increment of 10% of the trim speed has been reached, the control is moved back to the trim position and released. The resulting oscillations in airspeed, rate of climb, altitude and pitch attitude are allowed as long as airspeed, load factor and other limitations are not exceeded.

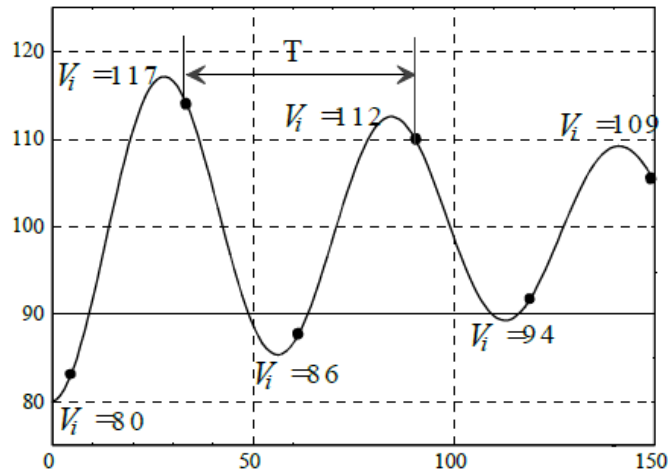


Figure 3.5: Phugoid time history example [9, p.8.37]

The frequency and damping characteristics of the phugoid motion are evaluated using the time histories of the significant parameters. For the phugoid, this can be the angle of attack, airspeed or pitch angle. In addition, the pitch rate can be retrieved by calculating the pitch angle derivative. An example response of the phugoid can be seen in Figure 3.5.

#### 3.2.4. SHORT-PERIOD OSCILLATION

Just as for the phugoid, the aircraft is stabilised and trimmed in the specified flight condition and configuration applicable to the test point. After a qualitative investigation of the longitudinal response by the pilot, a doublet input is applied to excite the aircraft motion as seen in Figure 3.6. The duration of the complete input application is chosen such that a good excitation of the short period mode is obtained.

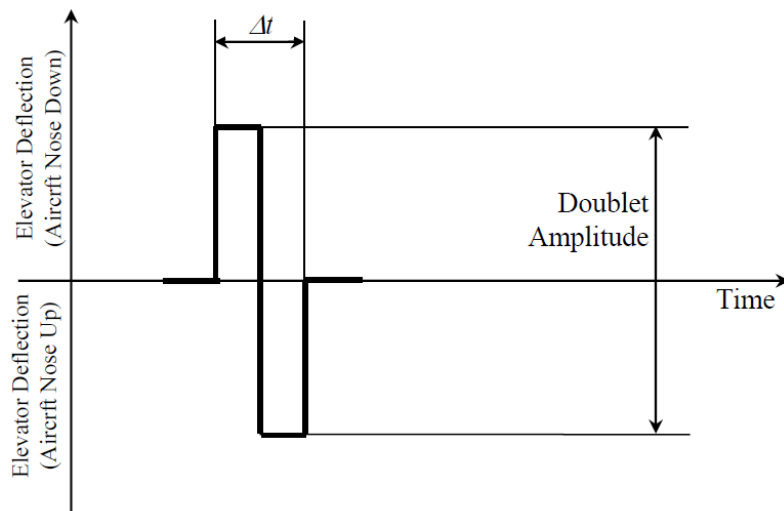


Figure 3.6: Elevator doublet input

The pilot applies the doublet starting with a forward motion of the stick, followed by an aft movement. When the pitch angle has returned to the trim value, the longitudinal control is brought back to its initial position. At this point, the control is restrained or released to obtain either the stick fixed or stick free response characteristics. To obtain the motion characteristics, the same steps are taken as for the phugoid motion.

### 3.2.5. PITCH MANOEUVRING FORCE

Starting from trimmed level flight at the test altitude and maintaining power setting and trim, the altitude is increased. During the descent back to the test altitude, a turn is performed to achieve the normal accelerations necessary for control force evaluation. In this way normal accelerations up to 3.5 g are evaluated. Additionally a pull-up manoeuvre is used to evaluate the stick force up to 5 g.

During the data analysis, variations of elevator and pitch trim deflections and longitudinal control force corresponding to the load factor variations will be evaluated. The resulting plot, similar to Figure 3.7, can be used to identify the maximum stick force gradient  $dF_s/dn_z$ .

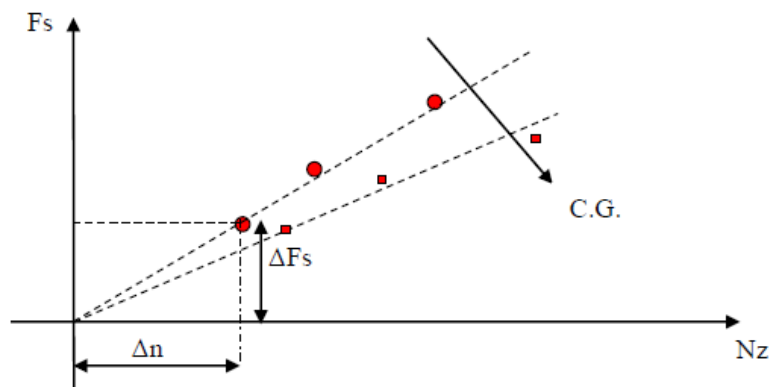


Figure 3.7: Example of stick force per g plot [10]

### 3.2.6. DUTCH ROLL

To excite the Dutch roll motion of the BS115, a lateral manoeuvre is performed. This lateral manoeuvre is executed by first stabilizing and trimming the aircraft in the previously specified flight condition and configuration, just as for the longitudinal manoeuvres discussed before. Then a rudder frequency sweep is performed to determine the Dutch roll natural frequency. The cyclic rudder push is continued until oscillations of sufficient magnitude are caused, after which the rudder pedals are brought back to the trim condition and restrained (stick fixed) or released (stick free).

Using the bank angle time history, the Dutch roll frequency and damping characteristics will be obtained in a similar way as for the short-period and phugoid modes.

### 3.2.7. ROLL MODE

As seen in Figure 3.8, the roll mode is examined using an aileron step input. First the aircraft is rolled towards a 30- or 60-degree bank angle and stabilized. Then a step lateral control input is applied, which is held until the roll rate stabilizes. When the roll rate has stabilized the controls are returned to the initial position and held fixed.

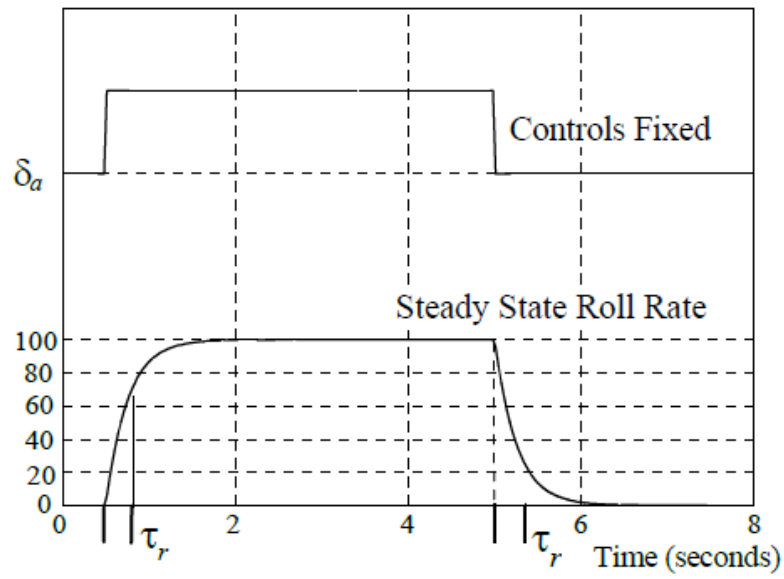


Figure 3.8: Roll rate response for an aileron step input [9, p.8.42]

After obtaining the roll rate, the roll mode time constant  $\tau_r$  can be determined from the time history of this parameter. It is defined as reaching 63% of the maximum steady-state value, as seen in Figure 3.8.



# 4

## BS115 DATCOM MODEL

In addition to the flight test data available, additional data is required to evaluate all training effectiveness criteria. To this purpose, a Digital DATCOM model of the BS115 is made. Digital Datcom is a computer program that is used to calculate static stability, high lift and control, and dynamic derivative characteristics using the USAF Stability and Control DATCOM methods [31]. These methods are a collection of best knowledge and judgement in the area of stability and control prediction methods, allowing the computation of a complete set of stability and control derivatives for given flight conditions. Since it provides a fast and efficient way of estimating these derivatives, it is suitable to compute the aircraft characteristics for the other evaluation criteria and additionally perform a check on the BS115 flight test results. In this chapter the DATCOM model and its verification and validation is described. Section 4.1 explains the various inputs required for the DATCOM analysis. The verification procedure of the Digital DATCOM model is described in Sections 4.2 and 4.3. Model validation and the final values for the BS115 stability derivatives are given in Sections 4.4 and 4.5 respectively.

Verification is done using a two-step procedure, using both code verification (Section 4.2) and calculation verification (Section 4.3). Code verification ensures that the model is working correctly, output is generated and that no programming errors are made. To check if the numerical model contains any errors, the obtained DATCOM results are compared with analytical approximations of the stability derivatives. Additionally, a check is made by generating DATCOM models of several comparable aircraft and comparing their results to the ones obtained from the BS115 model. This procedure is called the calculation verification. The results used for verification are the ones obtained from test point 2 conditions, of which the input file can be found in Appendix D. The results are given in Appendix D as well. Model validation is done by comparing the results of a DATCOM analysis to actual stability derivative values.

### 4.1. BS115 DATCOM INPUT

The digital DATCOM makes use of an input file, defining the characteristics of the aircraft under investigation. In this section the various aspects of the input file are described. The actual input file can be found in Appendix D.

#### 4.1.1. FLIGHT CONDITIONS

Defining a run case for digital DATCOM requires the set-up of related flight conditions, which are three-fold. First of all the flight speed(s) should be given, which is done by providing the Mach number. Secondly, the altitude should be provided and finally the sequence of angles of attack is required.

#### 4.1.2. REFERENCE POINTS

DATCOM requires all surface and body locations to be specified from a reference point. The origin of this reference location lies at the fuselage nose, in the same plane as the general reference location used

by Blackshape (Appendix B) and in the symmetry plane of the aircraft. The x-coordinate representing the CG position is determined in accordance with test point 2, as stated before. To obtain the model data for the other two test points, this x-coordinate is the only parameter that needs to be adapted.

#### 4.1.3. FUSELAGE

The fuselage of the BS115 is modelled in DATCOM by defining cross-sectional properties at various locations along the length. In this case the cross-sectional area, upper z-coordinate and lower z-coordinate are determined for twelve sections using the CAD model of the aircraft.

#### 4.1.4. WING

The wing planform is modelled according to the layout and dimensions presented in Appendix A. As can be seen, the BS115 wing planform contains a kink at a distance of 1.36 m from the centreline of the fuselage and is therefore effectively divided into two sections.

In order to determine the properties of these sections, some assumptions are made. As seen in the same Appendix, the BS115 wing consists of three different airfoils at the root, kink, and tip. Since the variation between these airfoils is linear, the average airfoil for each section can be determined. The lift and moment characteristics of these sections are determined using XFOIL.

#### 4.1.5. EMPENNAGE

Both the horizontal and vertical tail surfaces have a symmetrical NACA-63A010 airfoil applied. All other properties are taken from Appendix A.

#### 4.1.6. POWER PLANT

The constant speed, variable pitch propeller implemented on the BS115 is modelled with the geometrical characteristics listed in Appendix A. To determine the blade angle at 75% of the propeller radius, the propeller data charts provided by the manufacturer are used. First of all, the advance ratio  $J$  and power coefficient  $C_p$  are calculated. Together with the previously determined Mach number for the run case, an interpolation can be made.

## 4.2. CODE VERIFICATION

To examine whether or not the input file functions correctly, several checks are made. First of all, the output file generated by DATCOM is compared with the expected output parameters as defined in the Digital DATCOM manual [32]. The output parameters generated for the test point are shown in Table 4.1:

Force and Moment Coefficients	$C_D, C_L, C_m, C_N, C_A$
Static Stability Derivatives	$C_{L\alpha}, C_{m\alpha}, C_{Y\beta}, C_{n\beta}, C_{l\beta}$
Dynamic Stability Derivatives	$C_{Lq}, C_{mq}, C_{L\dot{\alpha}}, C_{m\dot{\alpha}}, C_{lp}, C_{Yp}, C_{np}, C_{nr}, C_{lr}$

Table 4.1: Output Parameters for the BS115 DATCOM Model

Secondly, the BS115 configuration is plotted using the *drawDATCOMaircraft* function in MATLAB, which visualizes the model components defined in the DATCOM input file. The resulting configuration plots are given in Figures 4.1 to 4.3. Unfortunately the function only takes the inboard panel sweep angle to draw the wing and is therefore incapable of addressing the wing kink. As a result, the leading edge sweep angle displayed in the plots is the average leading edge sweep angle over the wing span. This has no consequences for the DATCOM calculations, but is merely a limitation of the plotting tool used.

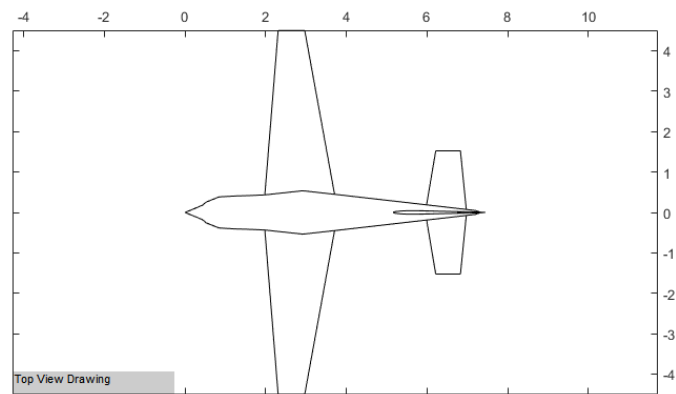


Figure 4.1: Top View of the BS115 DATCOM Model

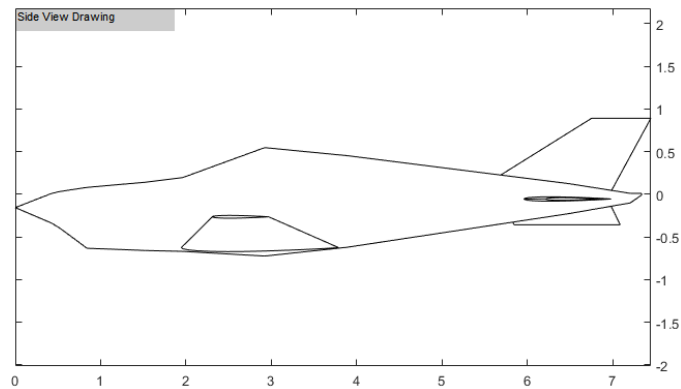


Figure 4.2: Side View of the BS115 DATCOM Model

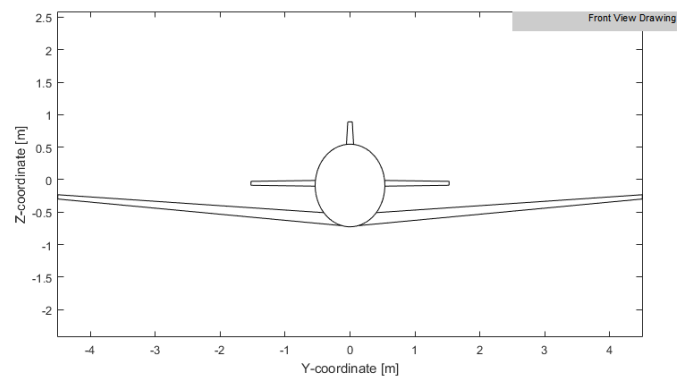


Figure 4.3: Front View of the BS115 DATCOM Model

Since the actual computed output parameters (as can be seen in Appendix D) match the expected output parameters given in Table 4.1 and the DATCOM model represents the actual aircraft as seen in Figures 4.1 to 4.3, the code seems to be working properly.

### 4.3. CALCULATION VERIFICATION

The first step in the calculation verification procedure is to visually check the obtained results and see if any problems occur. For this purpose, Figure 4.4 is created. In this figure the angle of attack referred to is that of the complete aircraft.

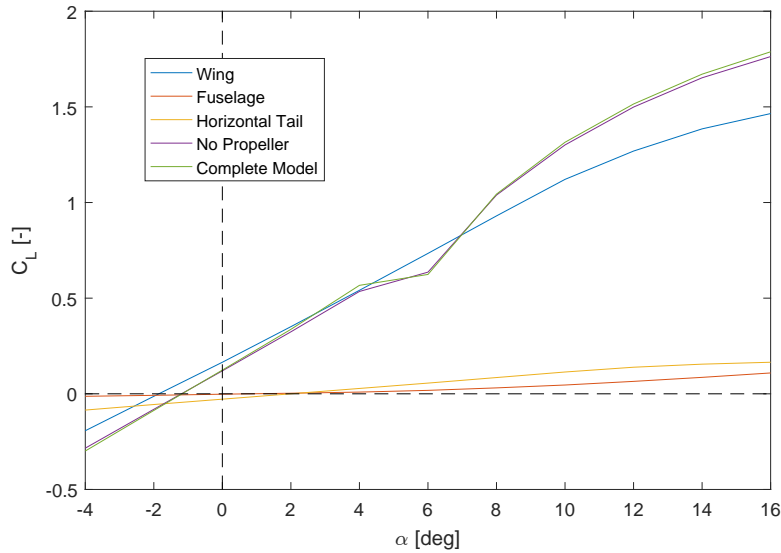


Figure 4.4: Lift coefficient as a function of the angle of attack for different DATCOM model configurations

Figure 4.4 shows that an irregularity occurs in the results as soon as all aircraft components are combined. After analysis of the output file, it is found that these miscalculations originate from ill-calculated downwash properties. To correct the model, a linear downwash model obtained from experimental data of the BS115 is used [33]. The model assumes the following relationship:

$$\epsilon = \epsilon_0 + \frac{d\epsilon}{d\alpha} \quad (4.1)$$

With  $\epsilon_0 = -0.25$  and  $d\epsilon/d\alpha = 0.3$  [33].

The resulting lift curve slope is plotted together with the lift curve slope before the correction in Figure 4.5.

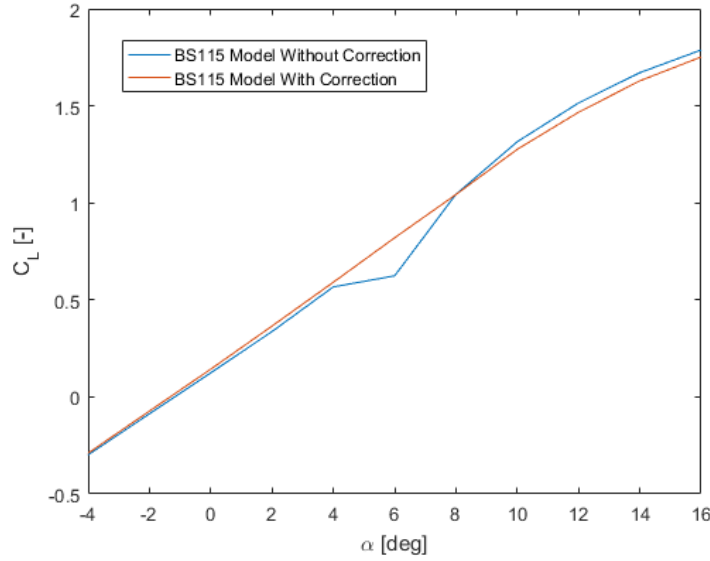


Figure 4.5: Lift coefficient as a function of the angle of attack before and after downwash correction

#### 4.3.1. LONGITUDINAL STABILITY DERIVATIVES VERIFICATION

To verify the longitudinal stability results, the first step is to run a DATCOM analysis for several comparable aircraft and see if the outcomes match. As seen in Table 4.2, the BS115 analysis and the reference aircraft computations show comparable results, except for  $C_{L_\alpha}$ . The BS115 seems to have a very high lift curve slope when compared to the other reference aircraft. Analysis shows that the lift curve slope value is increased significantly as soon as the fuselage is added into the DATCOM input file, which is not the case for the other two aircraft considered. In this case it seems the interference effects between the wing and fuselage are overestimated. Without fuselage, a lift curve slope of 0.0829 [1/deg] is found for the BS115. This value is also close to the lift curve slope value of solely the wing found using AVL [34].

	<b>BS115</b>	<b>Cessna 172</b>	<b>Diamond DA-20</b>
$C_{L_\alpha}$ [1/deg]	0.01085	0.0877	0.0842
$C_{m_\alpha}$ [1/deg]	-0.0168	-0.0184	-0.0223
$C_{L_q}$ [1/deg]	0.0611	0.0605	0.060
$C_{m_q}$ [1/deg]	-0.123	-0.124	-0.116
$C_{L_{\dot{\alpha}}}$ [1/deg]	0.0126	0.0187	0.0141
$C_{m_{\dot{\alpha}}}$ [1/deg]	-0.0372	-0.0556	-0.0516

Table 4.2: DATCOM Comparison for Different Aircraft

To correct the value for the lift curve slope to a more realistic value,  $C_{L_\alpha}$  is adapted by using the result without fuselage, and add the fuselage contribution to the lift curve slope separately. This results in a value for  $C_{L_\alpha}$  of 0.0857, which is also closer to the other reference aircraft.

Secondly, a comparison is made with analytical approximations of the stability derivatives. The aircraft characteristics necessary to use these equations are given in Appendix A, while the flight conditions are assumed to be equal to the second test flight point. The first derivative to be checked is the lift curve slope  $C_{L_\alpha}$ . An analytical approximation for this derivative is derived from the theoretical maximum lift curve slope value for a rectangular flat plate wing of infinite span and in incompressible flow, as given in Equation 4.2:

$$C_{L_{\alpha\infty}} = 2\pi \cos \Lambda_{le} \quad (4.2)$$

With  $\Lambda_{le}$  the leading edge sweep of the equivalent wing planform. The lift curve slope is further reduced due to the finite span of an actual wing, which is expressed by:

$$C_{L\alpha} = \frac{C_{L\alpha\infty}}{\left(1 + \frac{C_{L\alpha\infty}}{\pi A}\right)} \quad (4.3)$$

When the horizontal tail contribution is also considered, the equation changes as follows:

$$C_{L\alpha} = C_{L\alpha_w} + \left(1 - \frac{d\epsilon}{d\alpha}\right) \left(\frac{V_h}{V}\right)^2 \frac{S_h}{S} C_{L\alpha_{ht}} \quad (4.4)$$

The contribution of the fuselage is not taken into account in the above expression for the lift curve slope, since its influence is expected to be small.

The remaining longitudinal stability coefficients are evaluated using the approximation expressions given in Mulder *et al.* [11, p.187]. The moment curve slope can then be expressed as follows:

$$C_{m\alpha} = C_{N_{w\alpha}} \frac{x_{cg} - x_w}{\bar{c}} - C_{N_{h\alpha}} \left(1 - \frac{d\epsilon}{d\alpha}\right) \left(\frac{V_h}{V}\right)^2 \frac{S_h l_h}{S \bar{c}} \quad (4.5)$$

When considering small angles of attack,  $C_N$  is approximately equal to  $C_L$  which allows Equation 4.6 to be rewritten as:

$$C_{m\alpha} \approx C_{L_{w\alpha}} \frac{x_{cg} - x_w}{\bar{c}} - C_{L_{h\alpha}} \left(1 - \frac{d\epsilon}{d\alpha}\right) \left(\frac{V_h}{V}\right)^2 \frac{S_h l_h}{S \bar{c}} \quad (4.6)$$

This approximation is also made for the  $C_{L_q}$ ,  $C_{m_q}$ ,  $C_{L_{\dot{\alpha}}}$  and  $C_{m_{\dot{\alpha}}}$  derivatives:

$$C_{L_q} = 2 \left(C_{L_q}\right)_h = 2 C_{L_{h\alpha}} \left(\frac{V_h}{V}\right)^2 \frac{S_h l_h}{S \bar{c}} \quad (4.7)$$

$$C_{m_q} = -(1.1 \text{ to } 1.2) \left(C_{m_q}\right)_h = -(1.1 \text{ to } 1.2) C_{L_{h\alpha}} \left(\frac{V_h}{V}\right)^2 \frac{S_h l_h^2}{S \bar{c}^2} \quad (4.8)$$

$$C_{L_{\dot{\alpha}}} = C_{L_{h\alpha}} \left(\frac{V_h}{V}\right)^2 \frac{d\epsilon}{d\alpha} \frac{S_h l_h}{S \bar{c}} \quad (4.9)$$

$$C_{m_{\dot{\alpha}}} = -C_{L_{h\alpha}} \left(\frac{V_h}{V}\right)^2 \frac{d\epsilon}{d\alpha} \frac{S_h l_h^2}{S \bar{c}^2} \quad (4.10)$$

In order to compare the longitudinal stability derivatives with the approximations, the DATCOM results have to be modified to match the analytical expressions. Due to the fact that Equations 4.6 to 4.10 relate the stability derivatives to  $\frac{q\bar{c}}{V}$  and  $\frac{\dot{\alpha}\bar{c}}{V}$  respectively, while the Digital DATCOM relates them to  $\frac{q\bar{c}}{2V}$  and  $\frac{\dot{\alpha}\bar{c}}{2V}$  respectively, they cannot be compared directly. As a result, the DATCOM outcomes for these stability derivatives are divided by a factor of 2, to relate them to  $\frac{q\bar{c}}{V}$  and  $\frac{\dot{\alpha}\bar{c}}{V}$  as well. This is shown in Table 4.3.

	DATCOM Result	DATCOM Result Modified
$C_{L\alpha}$ [1/deg]	0.0857	0.0857
$C_{m\alpha}$ [1/deg]	-0.0168	-0.0168
$C_{L_q}$ [1/deg]	0.122	0.0611
$C_{m_q}$ [1/deg]	-0.246	-0.123
$C_{L_{\dot{\alpha}}}$ [1/deg]	0.0251	0.0126
$C_{m_{\dot{\alpha}}}$ [1/deg]	-0.0743	-0.0372

Table 4.3: Conversion of DATCOM Results

Using Equations 4.2 to 4.10 combined with the DATCOM output of Table 4.3, Table 4.4 is generated:

	Analytical	Modified DATCOM Result	Difference [%]
$C_{L\alpha}$ [1/deg]	0.0948	0.0857	-9.6
$C_{m\alpha}$ [1/deg]	-0.0337	-0.0168	-50.2
$C_{Lq}$ [1/deg]	0.0815	0.0611	-25.0
$C_{mq}$ [1/deg]	-0.146	-0.123	-15.8
$C_{L\dot{\alpha}}$ [1/deg]	0.0122	0.0126	+3.3
$C_{m\dot{\alpha}}$ [1/deg]	-0.0364	-0.0372	+2.2

Table 4.4: Results with equal definition

As can be seen, most results show a difference less than 25%. The largest difference occurs in the  $C_{m\alpha}$  derivative, which can be explained by the destabilizing effect of the fuselage. This contribution is not considered in the approximation expression, resulting in a significant difference. The differences in  $C_{Lq}$  and  $C_{mq}$  can be explained by taking a look at the approximation expressions, which only give a very rough estimate of the derivatives based on their most dominant contributions. As a result, some difference between DATCOM and the analytical expressions is expected.

#### 4.3.2. LATERAL-DIRECTIONAL STABILITY DERIVATIVES VERIFICATION

As stated by [5, p.384], it is much more difficult to estimate the lateral-directional stability derivatives using analytical methods. This is due to the aerodynamic interferences between all aircraft components, making it difficult to identify the dominant contributions to the stability derivatives. Therefore, a different approach is needed. First of all a sign check is made, which is done in Table 4.5. Secondly the BS115 results are compared with a DATCOM analysis of the reference aircraft, similar to Table 4.2. This is done in Table 4.6.

	Expected Sign	BS115 DATCOM Result
$C_{l\beta}$ [1/deg]	-	-0.000537
$C_{Y\beta}$ [1/deg]	-	-0.00825
$C_{n\beta}$ [1/deg]	+	0.000438
$C_{l_p}$ [1/deg]	-	-0.00840
$C_{Y_p}$ [1/deg]	-	-0.00230
$C_{n_p}$ [1/deg]	-	-0.000485
$C_{l_r}$ [1/deg]	+	0.00118
$C_{n_r}$ [1/deg]	-	-0.00197

Table 4.5: Lateral Derivative Sign Comparison

	BS115	Cessna 172	Diamond DA-20
$C_{l\beta}$ [1/deg]	-0.000537	-0.00154	-0.00138
$C_{Y\beta}$ [1/deg]	-0.00825	-0.00425	-0.00354
$C_{n\beta}$ [1/deg]	0.000438	0.00051	-0.000505
$C_{l_p}$ [1/deg]	-0.00840	-0.00781	0.00928
$C_{Y_p}$ [1/deg]	-0.00230	-0.00070	-0.00091
$C_{n_p}$ [1/deg]	-0.000485	0.00015	0.00847
$C_{l_r}$ [1/deg]	0.00118	0.00036	0.00442
$C_{n_r}$ [1/deg]	-0.00197	-0.0010	-0.00105

Table 4.6: Lateral Derivative Comparison - Reference Aircraft

As can be seen in Table 4.5, the results of the BS115 analysis show the expected sign for the lateral-directional stability derivatives. Table 4.6 shows that there exists some variation between the different aircraft in the lateral-directional stability derivatives. The relatively large tail volume coefficient of the BS115 when compared to the other aircraft results in larger values for  $C_{Y\beta}$  and  $C_{l_p}$ , as well as a more positive value for  $C_{n\beta}$ . Other factors that cause differences between the lateral-directional stability derivatives are the relative positions of the wing and tail with respect to the reference point, as well as the wing dihedral for  $C_{l\beta}$ .

#### 4.4. MODEL VALIDATION

To make sure the results from the DATCOM analysis are reliable, it is important to perform a validation using a reference aircraft. To this purpose an aircraft with known stability derivatives is evaluated using DATCOM, which is the Cessna 172 'Skyhawk' (Figure 4.6). Both the longitudinal and lateral-directional stability derivatives of this aircraft are evaluated in this section.



Figure 4.6: Cessna 172 'Skyhawk'

##### 4.4.1. LONGITUDINAL STABILITY DERIVATIVES VALIDATION

The longitudinal stability derivatives calculated using the analytical method of Section 4.3 as well as DATCOM are shown in Table 4.7 below:

	Actual	Analytical Approximation	DATCOM
$C_{L\alpha}$ [1/deg]	0.081	0.0942 (+16.5%)	0.088 (+8.5%)
$C_{m\alpha}$ [1/deg]	-0.016	-0.019 (+22.3%)	-0.018 (+18.3%)
$C_{Lq}$ [1/deg]	0.034	0.077 (+125%)	0.061 (+77.8%)
$C_{mq}$ [1/deg]	-0.108	-0.1205 (+11.4%)	-0.124 (+14.2%)
$C_{L\ddot{\alpha}}$ [1/deg]	0.015	0.0162 (+9.2%)	0.019 (+26.3%)
$C_{m\ddot{\alpha}}$ [1/deg]	-0.045	-0.046 (+2.3%)	-0.056 (+22.5%)

Table 4.7: Cessna 172 - Longitudinal Stability Derivatives Comparison

The first observation to be made is that the analytical approximation shows small errors (within 23%) for  $C_{L\alpha}$ ,  $C_{m\alpha}$  as well as for the derivatives with respect to acceleration,  $C_{L\ddot{\alpha}}$  and  $C_{m\ddot{\alpha}}$ . In addition,  $C_{mq}$  is within 10% error. The error is largest for the pitch rate derivative  $C_{Lq}$ . This might be due to the simplifications made in the formula, where a rough estimate is made by taking twice the value of the estimated horizontal tail contribution. When considering the DATCOM output, the lift curve slope is predicted with 8.5% error, while the stability derivative  $C_{m\alpha}$  shows an error of 18.3%. For the rate of angle of attack derivatives,  $C_{L\ddot{\alpha}}$  and  $C_{m\ddot{\alpha}}$ , the error is 26.3% and 22.5% respectively. The largest deviation occurs in the estimate of the pitch rate derivative  $C_{Lq}$ , as was the case for the analytical approximation. In this case the value is overestimated by 77.8 %.

#### 4.4.2. LATERAL-DIRECTIONAL STABILITY DERIVATIVES VALIDATION

The lateral-directional stability derivatives calculated by DATCOM are compared with actual values in Table 4.8:

	Actual	DATCOM	Error (%)
$C_{l_\beta}$ [1/deg]	-0.00161	-0.00154	-4.4
$C_{y_\beta}$ [1/deg]	-0.00686	-0.00425	-38.0
$C_{n_\beta}$ [1/deg]	0.00103	0.00051	-50.2
$C_{l_p}$ [1/deg]	-0.00845	-0.00781	-7.5
$C_{y_p}$ [1/deg]	-0.00131	-0.0007	-46.5
$C_{n_p}$ [1/deg]	-0.00049	0.00015	-130.9
$C_{l_r}$ [1/deg]	0.00139	0.00036	-74.2
$C_{n_r}$ [1/deg]	-0.00164	-0.0010	-38.9

Table 4.8: Cessna 172 - Lateral Directional Stability Derivatives Comparison

As can be seen, the overall error percentage is higher for the lateral-directional derivatives than for the longitudinal derivatives. It was stated before that it is much more difficult to estimate lateral-directional stability derivatives due to the aerodynamic interferences between all aircraft components, and therefore this difference makes sense. The highest error percentages are found for  $C_{n_p}$  and  $C_{l_r}$ , where  $C_{n_p}$  is even positive. An attempt to improve the estimation for  $C_{n_p}$  is made by recalculating the derivative using ESDU data items [35]. Using this method a value of -0.00029 is found, which is an improvement with respect to the initial DATCOM estimate. For  $C_{l_r}$  a similar procedure is followed using ESDU data item 85010 [36], resulting in a value of 0.00063 and thereby reducing the error to 55%.

#### 4.5. BS115 STABILITY DERIVATIVES

The BS115 DATCOM model has been verified and validated in Sections 4.2 to 4.4. Since the geometry and properties of the BS115 aircraft are known in more detail than the Cessna 172 used for validation, where some of the properties had to be estimated from drawings, it is expected that the error percentage for the BS115 stability derivatives is reduced in comparison with the Cessna.

Based on the comparison with the analytical approximations and the validation results, the longitudinal stability derivatives obtained from the BS115 DATCOM model will be used. The final values are given in Table 4.9. For the lateral-directional stability derivatives it was found that  $C_{n_p}$  and  $C_{l_r}$  showed an improved accuracy when calculated using the ESDU data items. Therefore this procedure is also applied to the BS115. All other lateral-directional derivatives are still obtained from DATCOM. The resulting final set of stability derivatives is given in Table 4.10.

	BS115 Derivatives
$C_{L_\alpha}$ [1/deg]	0.0857
$C_{m_\alpha}$ [1/deg]	-0.0168
$C_{L_q}$ [1/deg]	0.0611
$C_{m_q}$ [1/deg]	-0.123
$C_{L_{\dot{\alpha}}}$ [1/deg]	0.0126
$C_{m_{\dot{\alpha}}}$ [1/deg]	-0.0372

Table 4.9: BS115 Longitudinal Stability Derivatives

	<b>BS115 Derivatives</b>
$C_{l_\beta}$ [1/deg]	-0.000537
$C_{Y_\beta}$ [1/deg]	-0.00825
$C_{n_\beta}$ [1/deg]	0.000438
$C_{l_p}$ [1/deg]	-0.00840
$C_{Y_p}$ [1/deg]	-0.00230
$C_{n_p}$ [1/deg]	-0.000254
$C_{l_r}$ [1/deg]	0.000759
$C_{n_r}$ [1/deg]	-0.00197

Table 4.10: BS115 Lateral-Directional Stability Derivatives

# 5

## BS115 HANDLING QUALITY EVALUATION

Using the test set-up and procedures described in Chapter 3 together with the DATCOM results from Chapter 4, the BS115 handling qualities are evaluated. As stated in Section 2.4, three categories of criteria can be distinguished: longitudinal stability and control characteristics, lateral-directional stability and control characteristics, and pilot feedback. Sections 5.1 to 5.4 cover the longitudinal characteristics. Lateral-directional characteristics are discussed in Sections 5.5 to 5.7 and the pilot feedback is covered in Section 5.8. Finally a discussion on the obtained results is presented in Section 5.9.

For clarity, the three test points as defined in Chapter 3 are repeated here. Test point 1 is taken at a CG position of 23.6% MAC, test point 2 is at the most aft CG position of 31.0% MAC, and test point 3 is at the most forward CG position of 17.3% MAC. This is seen in Figure 5.1 as well.

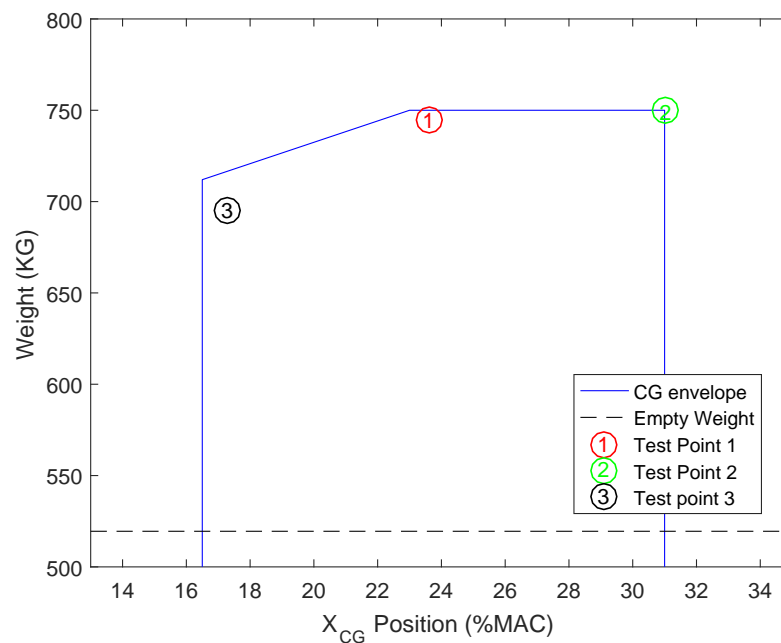


Figure 5.1: BS115 CG Envelope - repeated

## 5.1. LONGITUDINAL STABILITY WITH RESPECT TO SPEED

As stated in subsection 2.2.2, there shall be no tendency for airspeed to diverge aperiodically when the aircraft is disturbed from trim. To test this criteria, the Stabilized Long-Stat Stability Method will be used [9, p.12.1], as discussed in Chapter 3.

As an example, Figure 5.2 shows how this test is executed at a speed of 85 kts for test point 1. The results of the other tests are given in Tables 5.1 and 5.2. Airspeed, altitude, stick force and elevator deflection are plotted against time. After initialization, a pull force is exerted leading to a maximum stick force of 10.8 N at  $t = 985.3$  s. After reaching this maximum, controls are released and the return speed is observed. The same procedure is applied with a push force, leading to a maximum stick force of 5.69 N at  $t = 1097$  s.

To better present the data collected in the test flight manoeuvre, Figure 5.3 has been created. The black dot resembles the starting point of the manoeuvre, after which a pull or push force is applied on the stick. This causes a change in speed, shown by the arrow. After reaching maximum deviation, the aircraft is allowed to return towards trim condition. This is visualized by the dotted line.

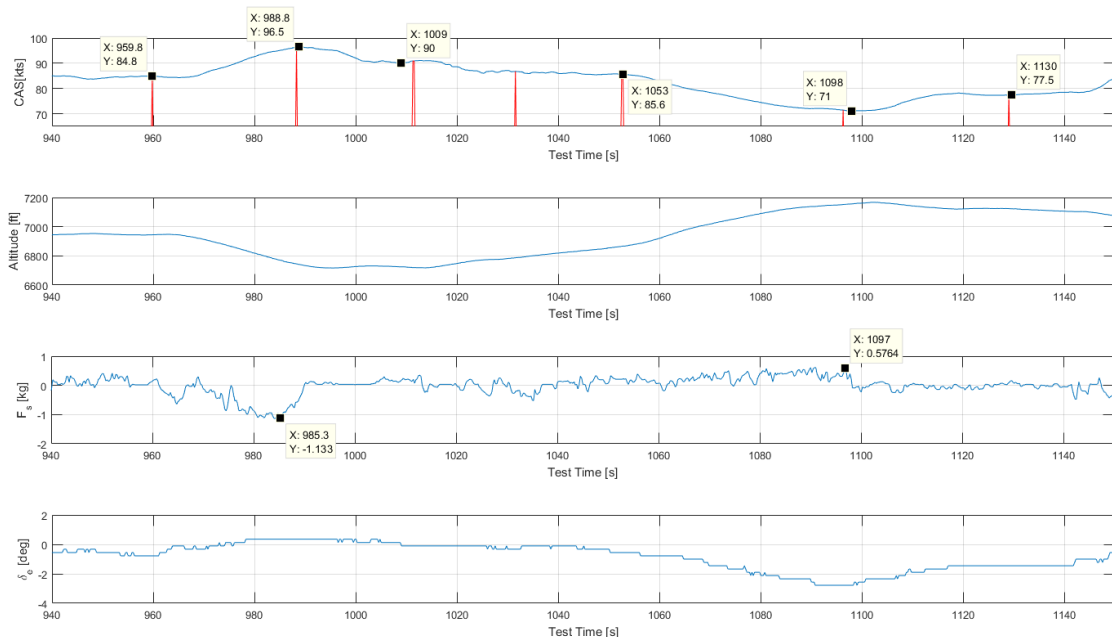


Figure 5.2: Longitudinal Stability wrt Speed (detailed) - 85 kts - Test point 1

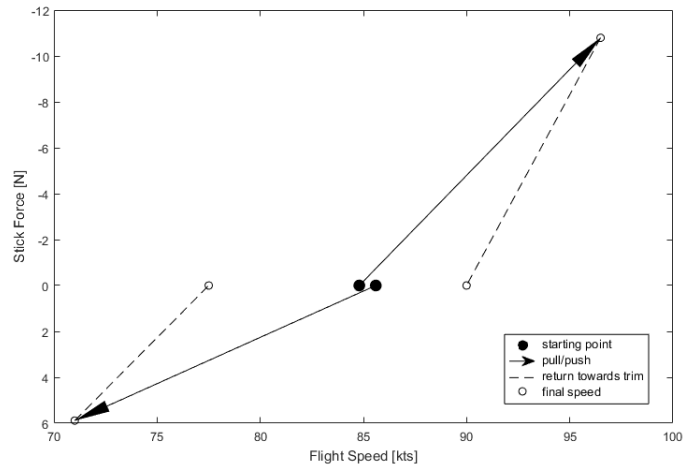


Figure 5.3: Longitudinal Stability wrt Speed - 85 kts - Test point 1

Figure 5.3 shows there is quite a large variation between the initial speed and the return speed ( $\Delta V = 5$  kts and  $\Delta V = 8.5$  kts for the push and pull respectively), indicating the aircraft was most likely not adequately trimmed.

### 5.1.1. LONGITUDINAL STABILITY AT TEST POINT 1

In a similar way as shown in Figures 5.2 and 5.3, the longitudinal stability is examined for other speeds. Results are shown in Figure 5.4 and 5.5.

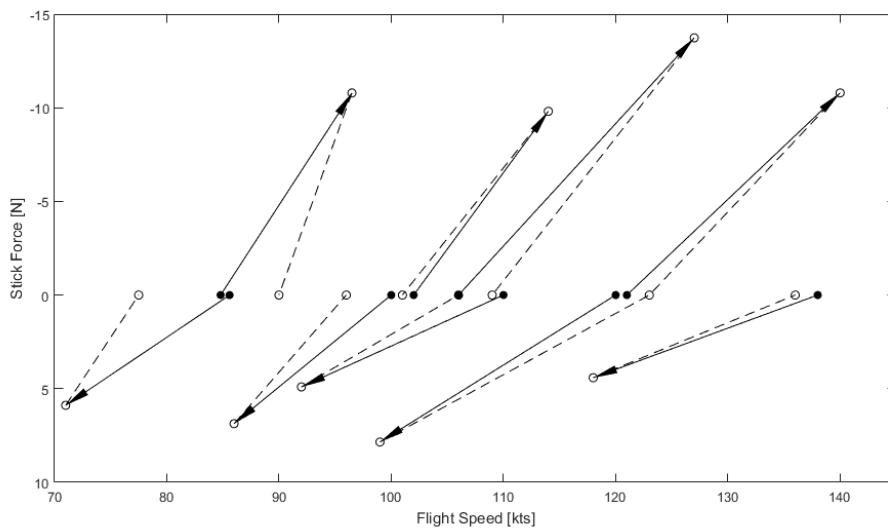


Figure 5.4: Longitudinal Stability wrt Speed - Cruise - Test point 1

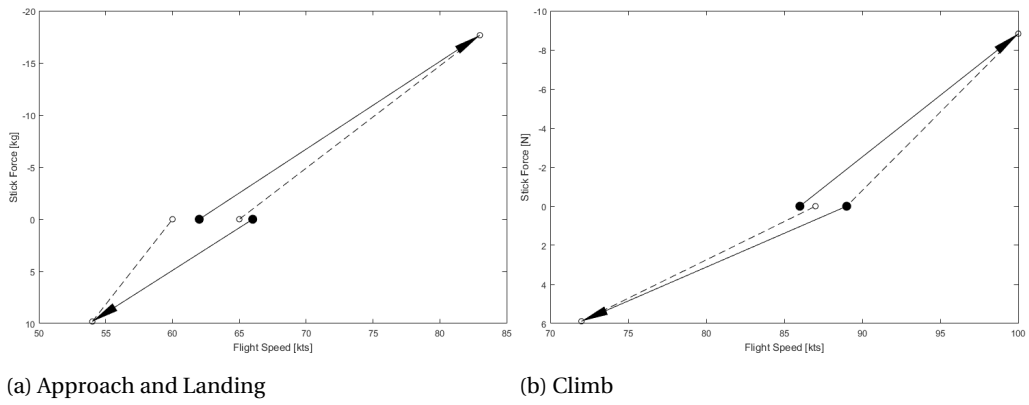


Figure 5.5: Longitudinal Stability wrt Speed - Manoeuvres - Test point 1

### 5.1.2. LONGITUDINAL STABILITY AT TEST POINT 2

The same procedure is applied for test point 2. Results are shown in Figures 5.6 and 5.7.

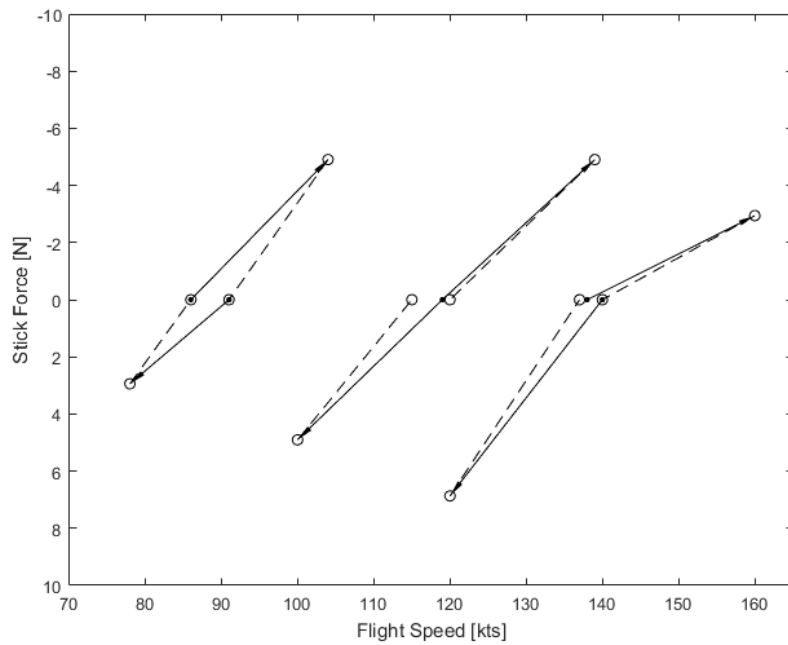


Figure 5.6: Longitudinal Stability wrt Speed - Cruise - Test point 2

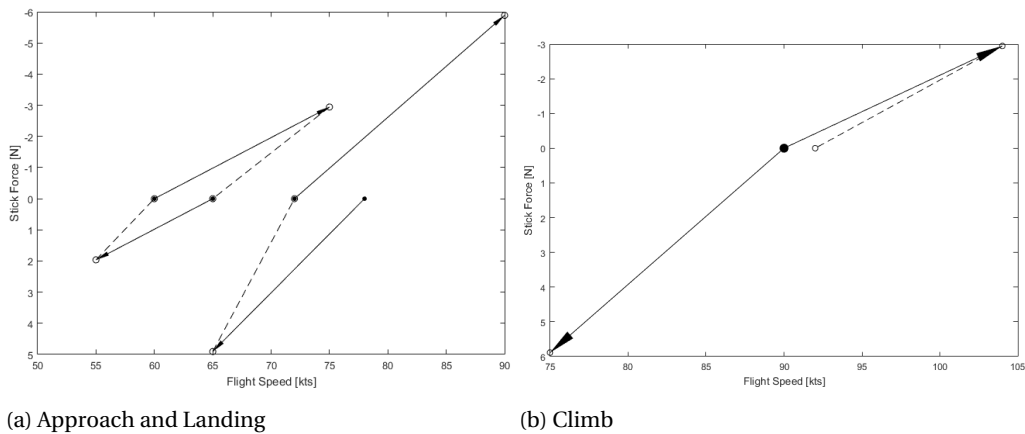


Figure 5.7: Longitudinal Stability wrt Speed - Manoeuvres - Test point 2

5.1.3. LONGITUDINAL STABILITY - SUMMARY

As seen in the previous subsections, the longitudinal stability with respect to speed has been evaluated for test point 1 and 2. To summarize, the trim speed, maximum deviation speed and return speed are given in Tables 5.1 and 5.2 for all test points. In all situations, the BS115 returns towards the initial conditions and hence no objectionable airspeed divergence is present. Therefore the first stability criteria has been met.

Cruise								
	V [kts]	$\Delta V$ [%]	V [kts]	$\Delta V$ [%]	V [kts]	$\Delta V$ [%]	V [kts]	$\Delta V$ [%]
Trim speed	85		102		106		121	
Return Speed	96.5	+6 %	114	-1 %	127	+3 %	140	+2 %
Trim speed	86		100		110		120	
Return Speed	71	-11 %	86	-4 %	92	-4 %	99	+3 %
	77.5		96		106		123	
	Cruise		Appr & land		Climb			
	V [kts]	$\Delta V$ [%]	V [kts]	$\Delta V$ [%]	V [kts]	$\Delta V$ [%]		
Trim speed	138		62		86			
Return Speed	118	-1 %	83	+5 %	100	+3 %		
Trim speed	136		65		89			
Return Speed	-	-	66	-9 %	72	-2 %		
			54		87			
			60					

Table 5.1: Longitudinal stability with respect to speed - Test Point 1 Summary

Cruise						
	V [kts]	$\Delta V$ [%]	V [kts]	$\Delta V$ [%]	V [kts]	$\Delta V$ [%]
Trim speed	86		119		138	
Return Speed	104	+6 %	139	+1 %	160	+1 %
Trim speed	91		120		140	
Return Speed	78	-5 %	100	-3 %	120	-2 %
Return Speed	86		115		137	
Approach & landing				Climb		
	V [kts]	$\Delta V$ [%]	V [kts]	$\Delta V$ [%]	V [kts]	$\Delta V$ [%]
Trim speed	60		72		90	
Return Speed	75	+8 %	90	+0 %	104	+2 %
Return Speed	65		72		92	
Trim speed	65		78		90	
Return Speed	55	-8 %	65	-8 %	75	+0 %
Return Speed	60		72		90	

Table 5.2: Longitudinal stability with respect to speed - Test Point 2 Summary

## 5.2. PHUGOID MOTION

The phugoid motion of the BS115 is evaluated at both test point 1 and test point 2, using the procedure described in section 3.2. The obtained results are discussed here. After analysis of the test flight data, it is found that the angle of attack vane has not captured the phugoid motion accurately and therefore  $\alpha$  measurements are not included in the results.

To evaluate phugoid characteristics, first of all the peak values have to be determined. This is done graphically and the results for both test points at a speed of 120 kts are in indicated in the plots of Figure 5.9 and 5.10. Using the time between two successive peaks, the phugoid period can be determined as follows (Using the definitions of Figure 5.8):

$$T_p = t_2 - t_1 \quad (5.1)$$

The next step is to determine the motions - damped frequency from the period:

$$\omega_d = \frac{2\pi}{T_p} \quad (5.2)$$

Since the phugoid is a relatively slow motion, the damping ratio can be determined using the transient peak ratio (TPR) method [37, p.212]. When the steady state system response is determined, Figure 5.8 can be used. Then the TPR can be found using equation 5.3. This is done for as many peaks as can be identified, after which an average is taken to account for the irregularity in flight testing.

$$TPR = \frac{\Delta x_1}{\Delta x_0} = \frac{\Delta x_2}{\Delta x_1} = \frac{\Delta x_3}{\Delta x_2} = \dots \quad (5.3)$$

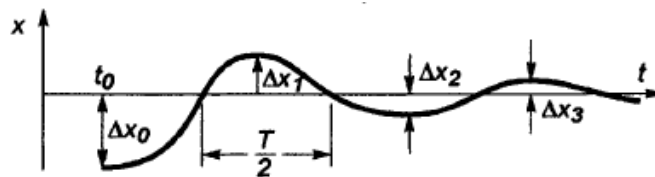


Figure 5.8: Transient Peak Ratio - Definitions

With the TPR determined, the damping ratio is found by using Vitsas Modified Transient Peak Ratio Method [38]:

$$\zeta_p = \frac{1}{\sqrt{1 + \left(\frac{\pi}{\log(TPR)}\right)^2}} \quad (5.4)$$

Finally, the natural frequency is obtained:

$$\omega_n = \frac{\omega_d}{1 - \zeta_p^2} \quad (5.5)$$

### 5.2.1. PHUGOID MOTION AT TEST POINT 1

For the first test point (CG at mid-range), results are shown in Figure 5.9 for a speed of 120 *kts*. Calibrated airspeed, altitude, pitch angle and pitch rate are plotted against time. The latter is not recorded directly during the test flight and is therefore derived from the pitch angle. The airspeed plot also shows the pilot markers used to indicate events in the test flight, which are helpful for identifying the motion characteristics.

Since the motion is best visible in the third plot, the pitch angle has been used to determine the motion characteristics. The steady state system response is found to be at  $-1.02^\circ$ . Using the method described previously, the following results are obtained:

- $T_p = 19.3$  [s]
- $\omega_d = 0.273$  [rad/s]
- $TPR = 0.54$  [-]
- $\zeta_p = 0.195$  [-]
- $\omega_n = 0.284$  [rad/s]

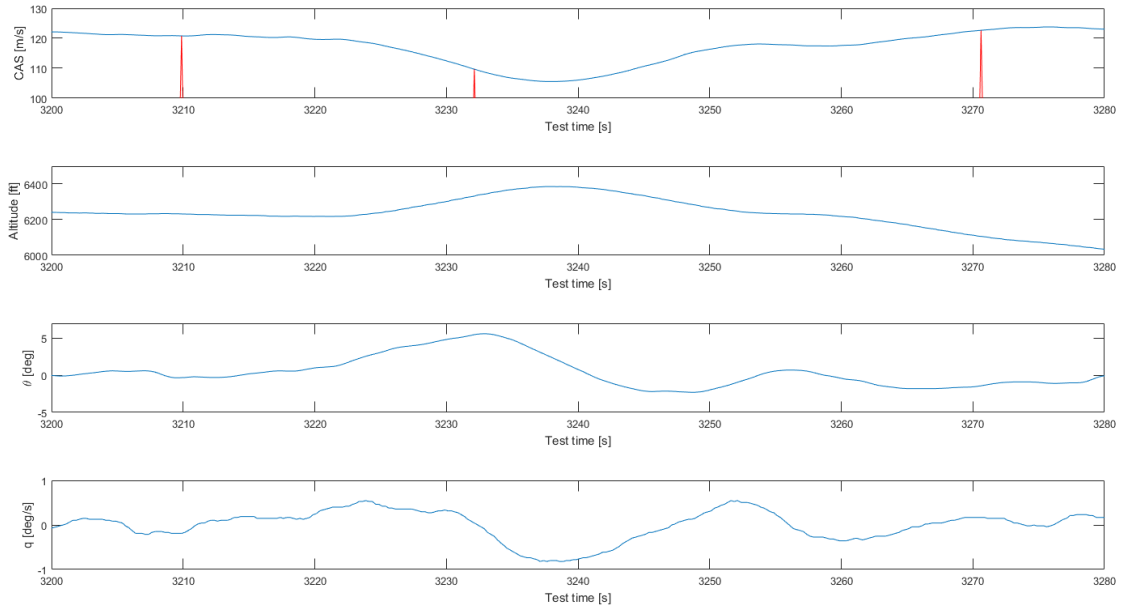


Figure 5.9: Phugoid Oscillation - Test Point 1 - 120 kts

### 5.2.2. PHUGOID MOTION AT TEST POINT 2

For the second test point, the calibrated airspeed can be used to evaluate the motion. CAS is plotted together with altitude, pitch angle and pitch rate in Figure 5.10. Again, pilot markers are displayed in the top plot.

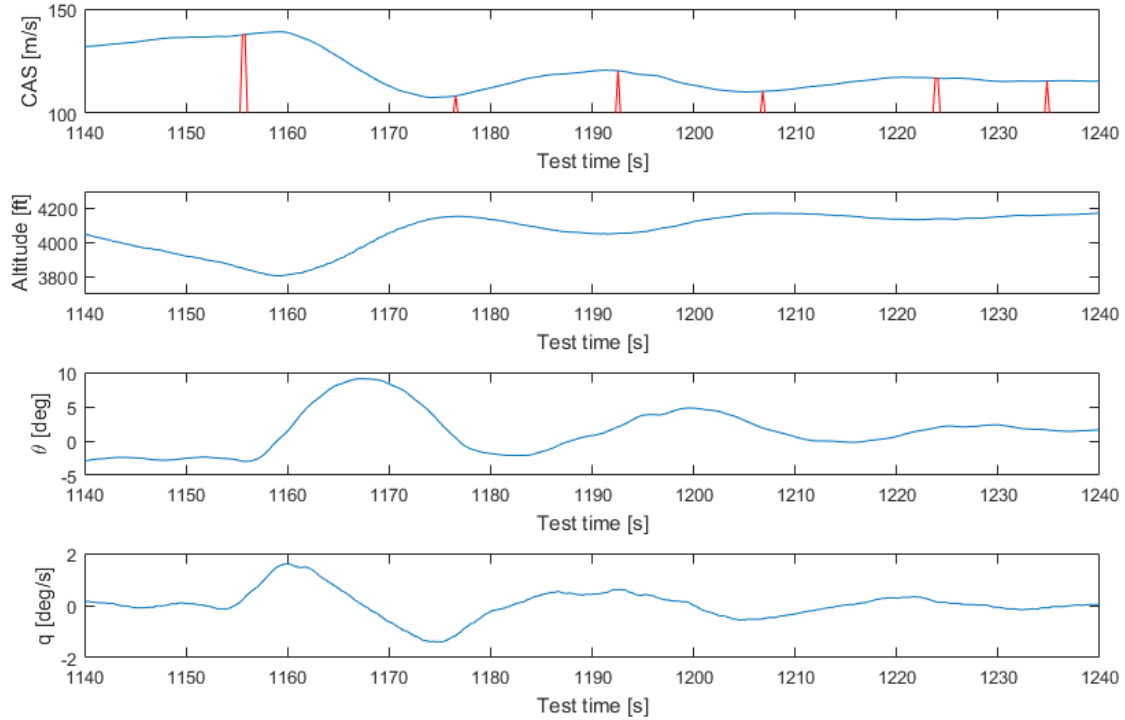


Figure 5.10: Phugoid Oscillation - Test Point 2 - 120 kts

In a similar way as for test point 1, with a steady state system response equal to 115.4 *kts*, the following characteristics are found for test point 2:

- $T_p = 31$  [s]
- $\omega_d = 0.196$  [rad/s]
- $TPR = 0.59$  [-]
- $\zeta_p = 0.168$  [-]
- $\omega_n = 0.202$  [rad/s]

### 5.2.3. PHUGOID MOTION - SUMMARY OF RESULTS

In a similar way as for the above worked out test results, the phugoid motion is examined at several other speeds for the aft CG. The results are summarized in Table 5.3. The accompanying motion plots are given in Appendix F.

Test Point	Speed [kts]	T [s]	$\omega_d$ [rad/s]	TPR [-]	$\zeta$ [rad/s]	$\omega_n$ [rad/s]
2 A	85	29.2	0.215	0.449	0.247	0.229
2 B	90	27.3	0.239	0.421	0.266	0.257
2 C	120	31.0	0.203	0.609	0.156	0.208
2 D	140	39.7	0.158	0.489	0.222	0.166

Table 5.3: Phugoid Motion - Test point 2 - Complete Results

To better understand the accuracy of the obtained results, the 90% confidence interval is plotted in Figure 5.11. As can be seen, there is a relatively large spread in the obtained results with an outlier at measurement point 3. However, since this outlier is towards the critical boundary regarding the training effectiveness evaluation criteria, it will not be disregarded.

The spread in flight test measurements can have several causes. First of all, the test equipment may not be sensitive enough to pick up the precise motion characteristics. This is most evident at test point 1 where it was difficult to use the airspeed recordings to analyse the phugoid, resulting in the pitch angle to be used. Additionally, it is possible that the pilot has not properly executed the manoeuvres in all cases, causing the results to vary. A final contributor to the varying results can be the meteorological conditions at the flight altitude. Even though the test flights were executed during calm weather, local variations might have an influence on the flight test result.

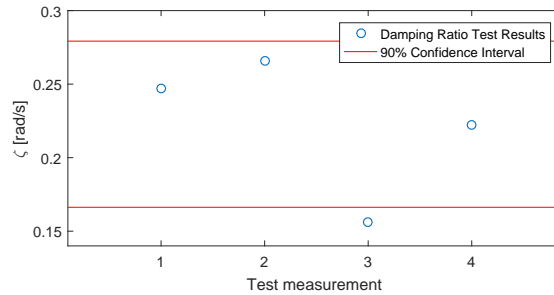


Figure 5.11: Phugoid Confidence Interval (90%) - CG Aft

A final check on the results is made by comparing the obtained damping coefficient with the one obtained from a DATCOM model of the BS115 and some reference aircraft. This is shown in Table 5.4:

	BS115 - Flight test	BS115 - DATCOM	Cessna 172	DA-20
$\zeta_p$ [rad/s]	0.156	0.115	0.104	0.056

Table 5.4: Damping Coefficient Comparison for Various Aircraft

Table 5.4 shows that a higher damping coefficient is achieved in flight testing than the model predicted. According to Ward and Strganoc [37, p. 194] and Crawford [39, p. 7.4], the phugoid damping ratio is significantly affected by the aircraft drag. This might indicate that the actual aircraft drag of the BS115 is higher than predicted by the model. The Da-20 shows significantly less damping than the Cessna and BS115, which is explained by its high L/D ratio compared to the other two aircraft.

As stated in subsection 2.2.2, the phugoid motion should have a damping coefficient  $\zeta_p$  of at least 0.04 to achieve level 1 flight conditions. Based on the results presented above, a minimum damping coefficient of 0.156 is found in flight testing, which satisfies the criteria. The damping coefficient calculated using the BS115 model meets the criteria as well. Therefore the BS115 is shown to have level 1 handling qualities with respect to the phugoid motion.

### 5.3. SHORT PERIOD

To evaluate the short period characteristics of the BS115, test flights are performed at test point 1 and 2. Just as for the phugoid motion, the criteria for the short period are related to the damping coefficient. In this case:

$$0.35 < \zeta_{sp} < 1.30 \quad (5.6)$$

### 5.3.1. SHORT PERIOD MOTION AT TEST POINT 1

For the first test point (CG at mid-range), the manoeuvre has been executed twice at a speed of 108 *kts*. The results are shown in Figures 5.12 and 5.13.

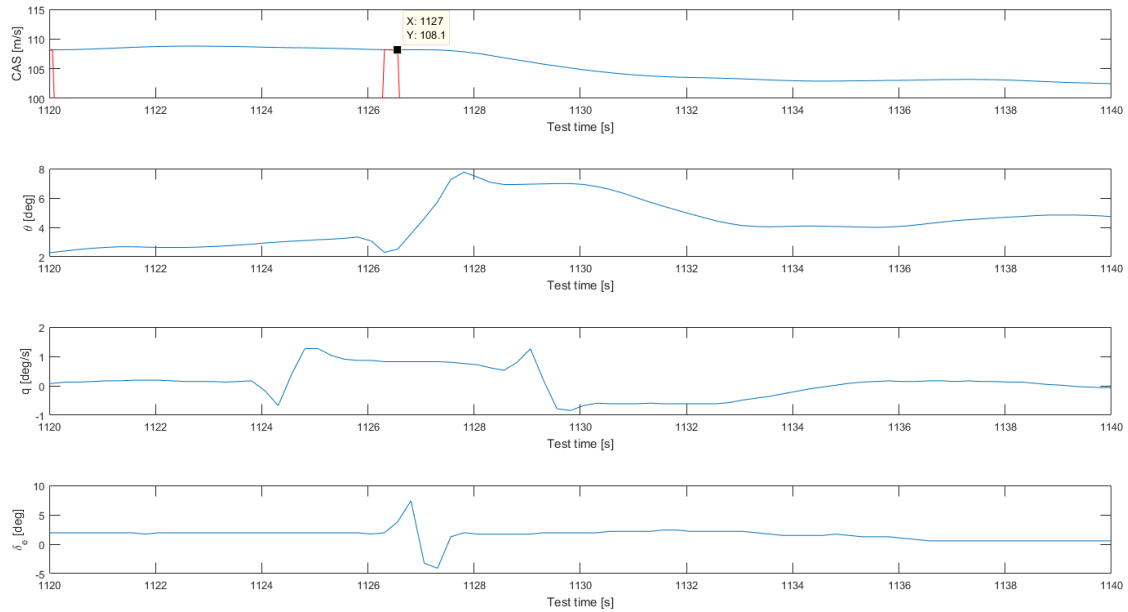


Figure 5.12: Short Period - Test Point 1 - 108 kts

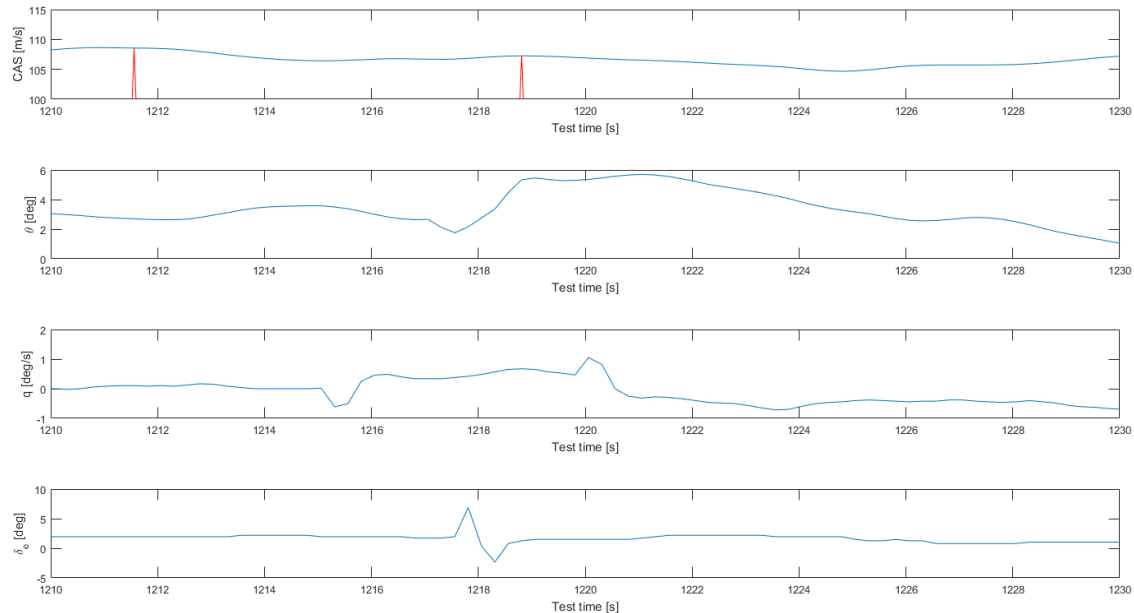


Figure 5.13: Short Period - Test Point 1 - 108 kts

### 5.3.2. SHORT PERIOD MOTION AT TEST POINT 2

The second test point results are shown in Figure 5.14 for a speed of 110 *kts*. As can be seen in this case not only an elevator doublet is used as input, but a series of sinusoidal inputs was made as well. This was done by the pilot in order to try to excite the short period mode before the real doublet was applied at the last peak.

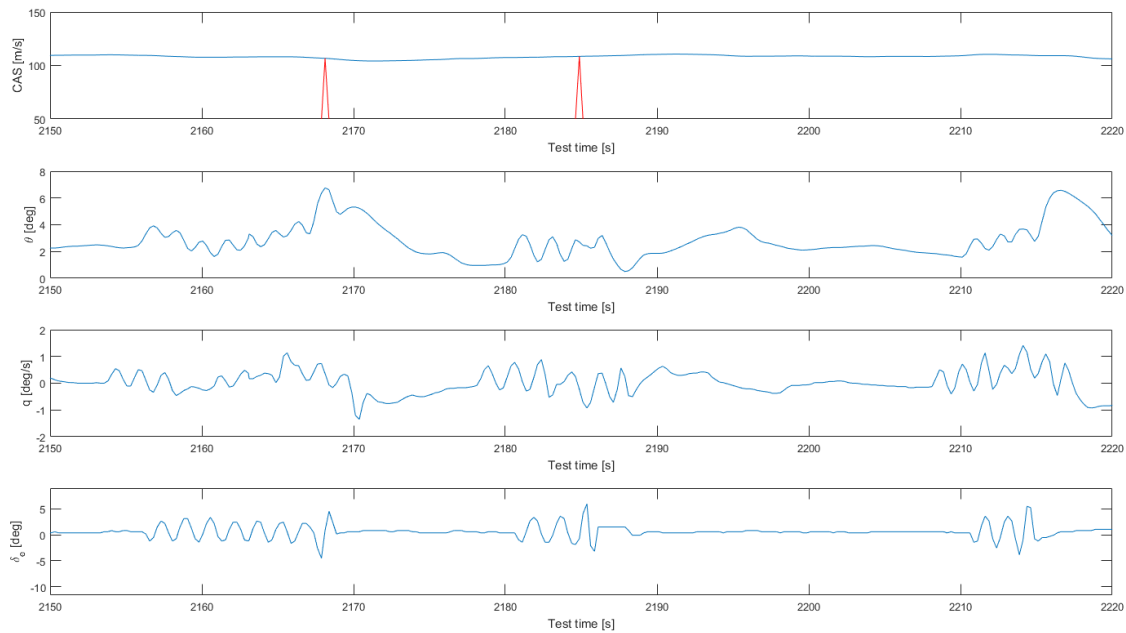


Figure 5.14: Short Period - Test Point 2 - 110 kts

#### SHORT PERIOD MOTION - RESULTS SUMMARY

Although the input as specified in the flight test procedure has been applied to the aircraft, there is no recognizable clear motion resulting from this input. Some response can be identified, but the flight test data provides insufficient detail and accuracy to determine the short period damping. As a consequence, the short period characteristics of the BS115 can only be quantified using the DATCOM model established in Chapter 4.

Using the procedure explained in Section E.4 of the Appendix for both the BS115 and the reference aircraft, the following damping coefficients for the short period motion are found:

	$\zeta_{sp}$ [rad/s]
BS115 - DATCOM	0.574
Cessna 172	0.685
Diamond DA-20	0.559

Table 5.5: Short Period Damping Coefficients for Various Aircraft

As seen in the above results, all aircraft show comparable short period characteristics. Since the BS115 short period damping coefficient lies between the limits posed in the introduction of this section, the BS115 shows level 1 handling qualities in this respect.

## 5.4. BS115 LONGITUDINAL CONTROL CHARACTERISTICS

In order to evaluate the control forces on the BS115, the flight test manoeuvre described in subsection 3.2.5 is executed for all test points. As is done for the previous criteria, one of the test points is worked out completely. The other graphs and plots can be found in Appendix F.

### 5.4.1. CONTROL FORCES AT TEST POINT 3

Shown in Figure 5.15 is the flight test manoeuvre executed for the CG position in accordance with test point 3. After levelling and trimming the aircraft at an airspeed of 120 kts, the elevator is moved to increase the load factor during a turning manoeuvre. Flight speed, load factor, stick force and elevator

deflection are recorded during this process. The maximum values of load factor, stick force and elevator deflection are indicated in the plot.

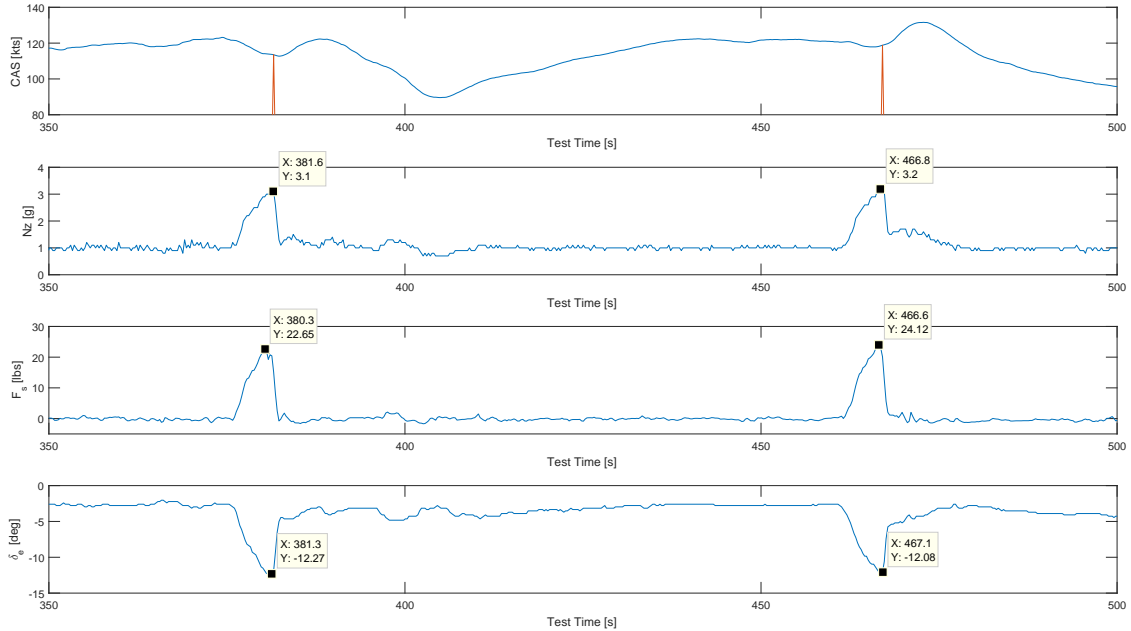


Figure 5.15: Manoeuvring Control Forces - Test point 3 - 120 kts

The next step is to create a stick force per g plot. All tests performed at test point 3 are analysed in the same manner as described above. The resulting stick force vs g points are gathered in Figure 5.16, using steady conditions ( $F_s = 0$ ,  $n_z = 1$ ) as initial point. As can be seen, one of the measurement points at  $V = 100$  kts is disregarded since it lies too far away from the other measurements. Combining the results and taking an average of the measurement points, a value for the stick force per g is found. In the case of test point 3 (CG forward),  $\frac{dF_s}{dn}$  is found to be equal to 4.954 [kg/g]. Additionally, the 90% confidence interval of the flight test measurements is determined. This interval is determined with all test points included, as well as with excluding measurement point 3. The resulting boundaries are shown in Figure 5.17.

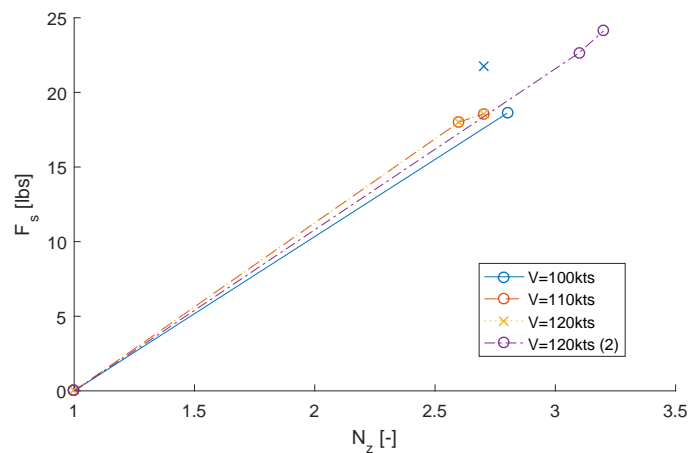


Figure 5.16: Stick Force per G - Test Point 3

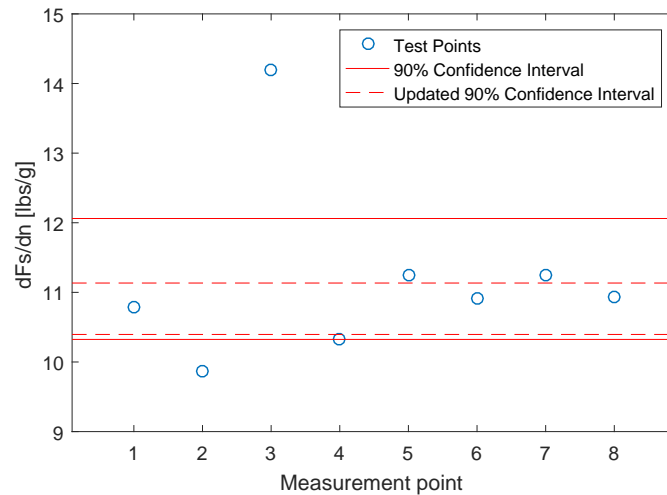


Figure 5.17: 90% Confidence Interval - Test Point 3

The flight test evaluation of the elevator control forces is done using two techniques. As seen in Figure 5.15 the maximum load factor is reached for just a small period of time, resulting in a peak stick force per g measurement. This method is used for both test point 1 and test point 3. The main benefit of this kind of test is that an estimate of the real life stick force per g in a normal manoeuvre is obtained [40]. However, the method also has its drawbacks. Due to the dynamic nature of such a motion, factors like the aircraft pitch inertia influence the final result. In manoeuvring flight this pitch damping increases the stick force required to displace the aircraft from its equilibrium position, causing the measured stick force not to represent the minimum stick force required to apply a certain g to the aircraft.

#### 5.4.2. CONTROL FORCES AT TEST POINT 2

The critical flight configuration for longitudinal control force evaluation is the one with the centre of gravity at the most aft position (test point 2), since the control forces are lowest here. Too low control forces can potentially be dangerous in controlling the aircraft, since the aircraft becomes too sensitive to unintentional variations in control force. Moreover, there also exists a risk of overstressing the aircraft. For this reason CS-VLA requirements dictate a minimum stick force required to achieve the positive limit manoeuvring load. These effects are of even larger importance in pilot training since the pilot is inexperienced in dealing with these situations.

Due to the requirements on minimum stick forces to reach the limit load factor, the method used to determine the stick forces for test point 1 and 3 cannot be used for test point 2. To better identify the minimum stick forces per g at test point 2, a different test manoeuvre is performed. In this case the load factor is increased in a turning manoeuvre and held constant over a prolonged period of time, reducing the dynamic effects. Figure 5.18 shows how the stick force per g varies for different load factors up to  $n_z = 3.9$ . The resulting stick force per g plot is shown in Figure 5.19.

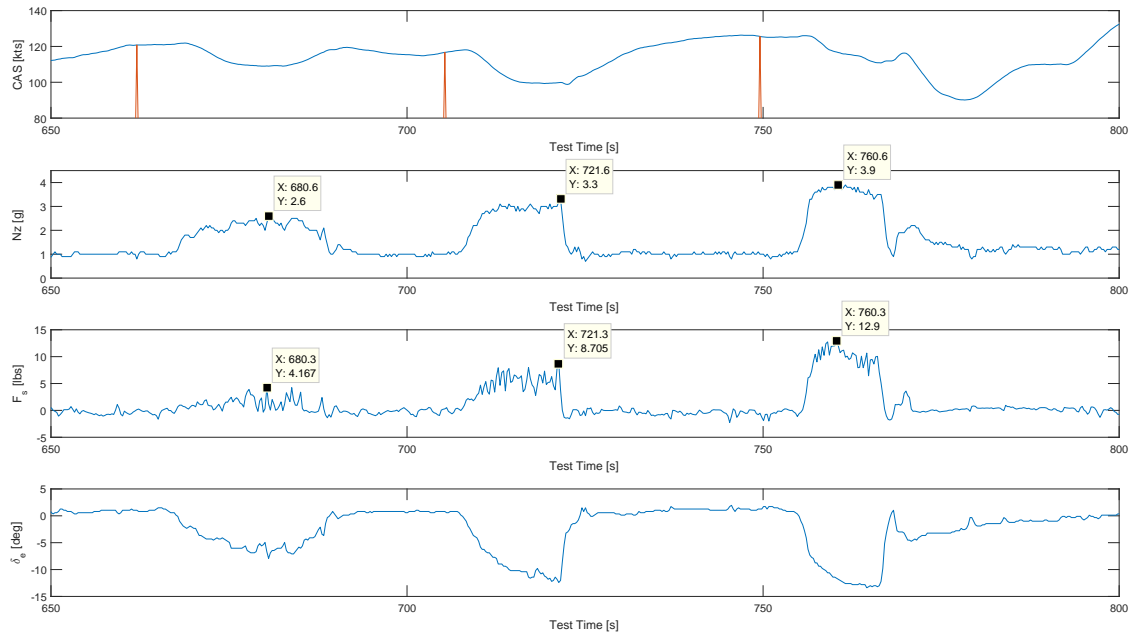


Figure 5.18: Manoeuvring Control Forces - Test point 2 - 120 kts

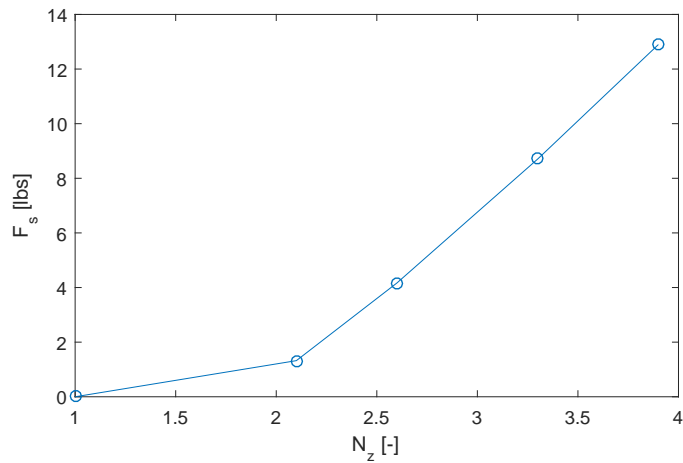


Figure 5.19: Stick force per g - Test point 2 - 120 kts

### 5.4.3. CONTROL FORCES - SUMMARY OF RESULTS

The resulting stick force gradients and their confidence intervals are given in Table 5.6.

	Test Point 1	Test Point 2	Test Point 3
$\frac{dF_s}{dn}$ [lbs/g]	5.106	4.116	10.92
Lower confidence boundary	4.478	2.026	10.40
Upper confidence boundary	5.736	6.206	11.13

Table 5.6: Stick Force per g - Summary

Additionally, a comparison is made with reference data. Using the procedure described in Section E.5 of the Appendix, stick force gradients are obtained for the BS115 model representation as well as for

the reference aircraft used in the previous analyses. For a mid-range reference CG location and similar flight conditions, the following values are found:

	$dFs/dn$ [lbs/g]
BS115 - Flight Test	5.106
BS115 - Model	8.957
Cessna 172	25.68
Redbird	6.063

Table 5.7: Stick Force per g - Comparison with Reference Aircraft

As can be seen in Table 5.7 there exists quite some variation between the results. First of all the difference between the BS115 test flights and the model has to be explained. In order to calculate the stick force gradient, it is necessary to make simplifications to the actual system. For example, the control system is assumed to behave according to a simple model [11, p.341] and the pull-up manoeuvre is a perfect q-motion [11, p.413]. These simplifications introduce uncertainties in the final calculations. Moreover, the necessary hinge moment coefficients and stability derivatives have been estimated using the procedures described in Appendix E. As a result, the stick force per g calculations using the BS115 model are an approximation of the actual situation and therefore introduce uncertainty. Secondly, the test equipment introduces errors as well. Although the test equipment has been calibrated, there is still the possibility of measurement errors. Based on the above comparison the flight test results cannot be guaranteed to be correct. However, no more accurate results are available and therefore the current outcome will be accepted.

Considering the criteria determined in Section 2.2, there are limits posed on the maximum and minimum stick force gradient. As seen in Table 5.6, the maximum stick force gradient is found at the most forward CG (test point 3), while the minimum stick force gradient is found at the most aft CG (test point 2) as expected. The BS115 stick force results in test point 2 give:

- $\left(\frac{dFs}{dn}\right)_{max} = 10.92$  [lbs/g]
- $\left(\frac{dFs}{dn}\right)_{min} = 4.12$  [lbs/g]

For the maximum and minimum stick force gradients of the BS115, Level 3 handling qualities are found for test point 2. Even though the maximum stick force gradient is on the low side already, the main problem with the stick force gradient is the minimum stick force for pitch control. To achieve better handling qualities, ideally a stick force gradient of 5.25 [lbs/g] should be reached for this most aft CG position. Since the maximum stick force gradient is also on the low side, the most obvious way to reach better handling qualities is to increase the stick force gradient.

## 5.5. BS115 DUTCH ROLL CHARACTERISTICS

The first lateral-directional motion to be investigated is the Dutch Roll. Test flights are performed for both test points 1 and 2. As stated in subsection 3.2.6, the damped frequency of the Dutch Roll motion is determined using a rudder frequency sweep. Additionally, the Dutch Roll damping coefficient is determined from the time history traces of the performed manoeuvres. As indicated by the pilot the Dutch Roll tests show more than two overshoots and hence the transient peak ratio method can best be used, similar to the phugoid calculations of Section 5.2.

### 5.5.1. DUTCH ROLL AT TEST POINT 2

To analyse the Dutch Roll motion, a plot is made displaying the calibrated airspeed (CAS), rudder deflection ( $\delta_r$ ), roll angle ( $\phi$ ) and heading angle ( $\xi$ ). This is done in Figure 5.20 for the second test point, at a test speed of 120 *kts*. First of all, the damped frequency  $\omega_d$  is determined using the following formula [9, p.8.35]:

$$\omega_d = \frac{2\pi [\#cycles]}{[totaltime]} \quad (5.7)$$

As is best seen in the heading angle plot of Figure 5.20, a total of 6 cycles are identified in a time span of 13.5 seconds resulting in a damped frequency  $\omega_d$  of 2.793 Hz.

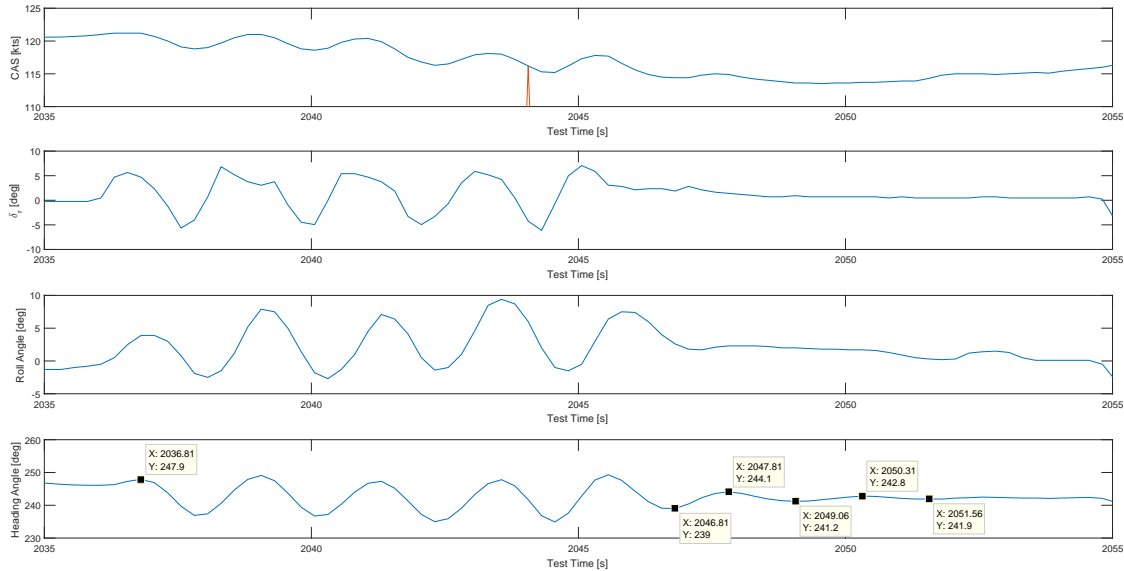


Figure 5.20: Dutch Roll - Test Point 2 - 120 kts

Secondly, the damping coefficient is determined using the transient peak ratio method discussed earlier. For the flight test results of Figure 5.20, a TPR of 0.555 is found using the heading angle. The corresponding Dutch Roll damping ratio  $\zeta_d$  equals 0.184.

### 5.5.2. DUTCH ROLL MOTION - SUMMARY OF RESULTS

As is done for the other criteria investigated, a summary of the flight test results is given in this subsection. The corresponding motion plots can be found in Appendix F. In total five measurement points are available, of which two are taken at test point 1 and three are taken at test point 2. The results are given in Table 5.8.

Test Point	Measurement	Configuration	Speed [kts]	$\omega_d$ [rad/s]	$\zeta_d$ [-]	$\omega_n$ [rad/s]
1	1a	take-off	90	2.578	0.198	2.683
1	1b	clean	130	3.142	0.154	3.218
2	2a	clean	120	2.793	0.184	2.891
2	2b	clean	120	2.957	0.197	3.076
2	2c	clean	140	3.491	0.125	3.546

Table 5.8: Dutch Roll Motion - Complete Results

In a similar way as for the other stability criteria, the Dutch roll characteristics of the BS115 are also obtained using the equations of motion and the stability derivatives determined using DATCOM. Following the method described in Appendix E.4, the Dutch roll damping coefficient is found to be equal to 0.29. The corresponding natural frequency,  $\omega_n$ , is equal to 1.74 [rad/s]. When comparing this value to the flight test results it seems the Dutch roll damping is overestimated by the model, which is most likely a result of the inaccuracy in the stability derivatives estimation from DATCOM as seen in Section 4.4. Another possible cause for the differences between the flight test results and the DATCOM model is the influence of the propeller slipstream. This effect may be considerable, but is not accounted for in

the DATCOM calculations.

Besides the BS115, Dutch roll characteristics are determined for the Diamond Da-20 and Cessna 172. The resulting damping coefficients are 0.149 and 0.175 for the Da-20 and Cessna 172 respectively. The Da-20 has a natural frequency of 2.17 rad/s, while the Cessna 172 has a natural frequency of 2.66 rad/s. Compared to the BS115, the Da-20 has a lower Dutch roll damping, while the Dutch roll damping of the Cessna 172 is comparable. When looking at the lateral stability diagram (Figure 5.21), it is seen the Dutch roll damping is heavily influenced by  $C_{l_\beta}$ . Table 4.6 showed  $C_{l_\beta}$  was found to be -0.00054 for the BS115, -0.0014 for the Da-20 and -0.0015 for the Cessna 172. These variations in  $C_{l_\beta}$  mainly result from differences in aircraft geometry. The most prominent difference is that the Cessna 172 has a high wing configuration as opposed to the Da-20 and BS115, contributing to a more negative  $C_{l_\beta}$ .

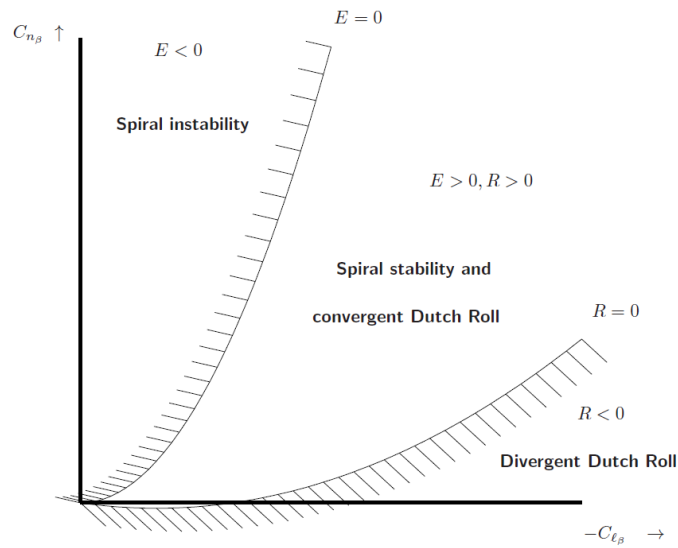


Figure 5.21: Lateral Stability Diagram [11, p.156]

### 5.5.3. DUTCH ROLL EVALUATION CRITERIA

The evaluation criteria for the Dutch Roll properties are given previously in subsection 2.2.3 but are repeated here:

- $\zeta_d$  should be larger than 0.08
- The product of  $\zeta_d$  and  $\omega_n$  should be larger than 0.15
- $\omega_n$  should be larger than 1.0 rad/s

Based on the results in subsection 5.5.2, the following values are found for the flight test measurements:

Measurement	$\zeta_d$ [-]	$\zeta_d \omega_n$ [rad/s]	$\omega_n$ [rad/s]
1a	0.198	0.531	2.683
1b	0.154	0.496	3.218
2a	0.184	0.532	2.891
2b	0.197	0.606	3.076
2c	0.125	0.443	3.546

Table 5.9: Dutch Roll Criteria - Flight Test Comparison

The comparison with reference aircraft shows the following results:

	$\zeta_d$ [-]	$\zeta_d \omega_n$ [rad/s]	$\omega_n$ [rad/s]
BS115 - DATCOM	0.29	0.50	1.74
Diamond Da-20	0.149	0.32	2.17
Cessna 172	0.1749	0.47	2.66

Table 5.10: Dutch Roll Criteria - Model Comparison

As seen in Table 5.9 and 5.10 the criteria for the Dutch Roll motion are met in all measurement points evaluated, as well as for the BS115 DATCOM model. Hence the BS115 shows level 1 handling qualities for the Dutch Roll motion.

## 5.6. BS115 ROLL MODE

The next aircraft mode to be considered in the training effectiveness evaluation is the roll mode. For this mode three evaluation criteria are to be considered, which are restated below:

- The roll-mode time constant,  $\tau_r$ , shall be no greater than 1.0 s.
- A bank angle of 30° should be achieved within 1.3 seconds, while a 60° bank angle should be reached within 1.7 seconds.
- The stick force required to obtain the roll performance should be smaller than 20 lbs and larger than the breakout force plus 5 lbs.

The roll mode evaluation criteria are tested for test point 1 and 3.

### 5.6.1. ROLL-MODE TIME CONSTANT

The roll mode time constant is defined as the time needed to reach 63% of the maximum roll rate, as was seen in Section 3.2. To test this criteria, an aileron input is given such that the roll rate of the aircraft increases to a maximum, after which the aileron controls are returned to the neutral position. Figure 5.22 shows the time history of such an input for test point 1 at a speed of 130 kts. The roll rate is not measured directly in flight but is determined from the roll angle derivative. The other time history plots for the roll mode are given in Appendix F.

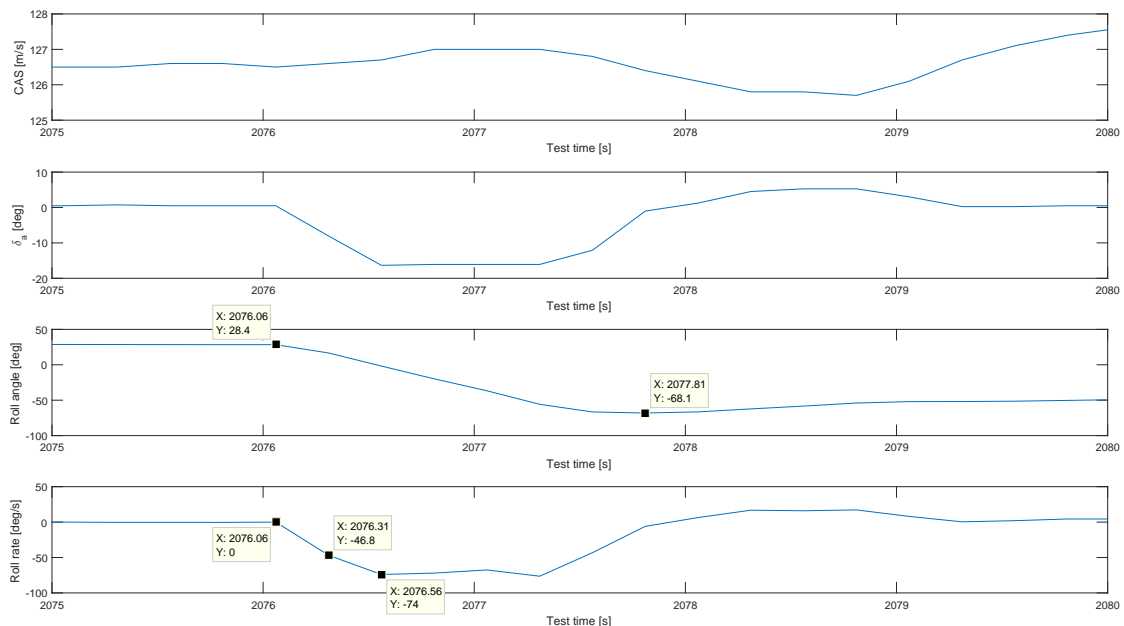


Figure 5.22: Roll Mode - Test Point 1 - 130 kts

As can be seen the time required to reach the maximum roll rate is 0.5 seconds. Additionally, the 63% value of the maximum roll rate is indicated, which is reached after 0.25 seconds. This value falls well within the required 1.0 seconds. Since the other test points are evaluated in the same manner, the test results are summarized by giving the obtained roll mode time constant  $\tau$  for these test points in Tables 5.11 and 5.12. The accompanying time plots are given in Appendix F.

Configuration	V [kts]	$\tau$
Take-off	65	0.5
Take-off	65	0.6
Landing	70	0.5
Landing	70	0.5
Clean	90	0.3
Clean	90	0.4
Clean	95	0.4
Clean	120	0.3
Clean	120	0.4
Clean	130	0.3
Clean	140	0.5

Table 5.11: Roll Mode Time Constant - Test Point 1 Summary

Configuration	V [kts]	$\tau$
Take-off	70	0.3
Landing	70	0.3
Landing	70	0.4
Clean	80	0.3
Clean	100	0.3

Table 5.12: Roll Mode Time Constant - Test Point 3 Summary

Tables 5.11 and 5.12 show the roll mode time constant is never larger than 0.6 s. As a result, the BS115 meets the roll mode criteria and shows level 1 handling qualities in this respect.

### 5.6.2. ROLL PERFORMANCE

To check whether or not the BS115 meets the roll performance criteria, the same flight tests as for the determination of the roll-mode time constant are used. This allows the same example as in subsection 5.6.1 (Test Point 1 - 130 kts) to be used here.

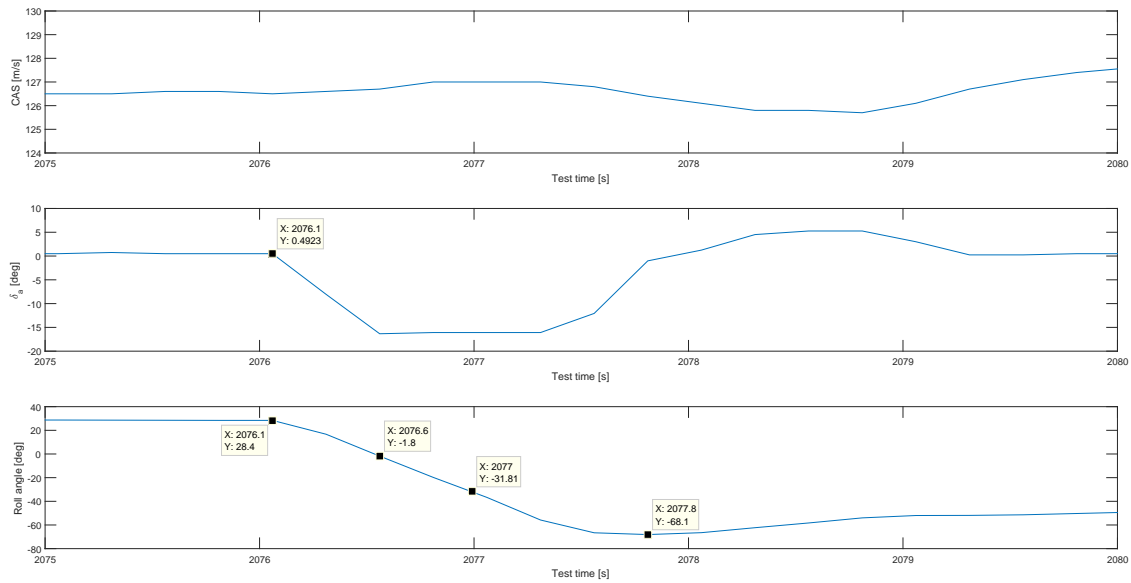


Figure 5.23: Roll Performance - Test Point 1 - 130 kts

As can be seen in Figure 5.23, datapoints are given at the start of the manoeuvre, as well as the points where a 30° and 60° change in bank angle has been achieved. It follows that a 30° bank angle change is achieved within 0.5 seconds, while a 60° bank angle change is achieved within 0.9 seconds. Given the performance criteria established before, the roll performance of the BS115 is more than adequate in this test point.

The roll performance for the other test points evaluated is summarized in Tables 5.13 and 5.14. These tables show the aircraft configuration, the airspeed at which the manoeuvre is performed, the total bank angle change and the time required for that change, the time required for a 30° bank angle change and the time required for a 60° bank angle change. The corresponding graphs can be found in Appendix F.

Configuration	V [kts]	$\Delta\Phi$ [deg]	$\Delta t$ [s]	30°Performance [s]	60°Performance [s]
Take-off	65	133.6	2.8	0.6	1.3
Take-off	65	150.7	2.7	0.6	1.1
Landing	70	133.4	3.0	0.7	1.3
Landing	70	139	3.0	0.7	1.3
Clean	90	135.4	2.5	0.6	1.1
Clean	90	129.6	2.8	0.6	1.3
Clean	95	128.6	2.3	0.5	1.0
Clean	120	95.9	1.8	0.6	1.1
Clean	120	93.4	1.5	0.5	1.0
Clean	130	95.0	1.5	0.5	0.9
Clean	140	87.5	1.5	0.5	1.0

Table 5.13: Roll Performance - Test Point 1 Summary

Configuration	V [kts]	$\Delta\Phi$ [deg]	$\Delta t$ [s]	30°Performance [s]	60°Performance [s]
Take-off	70	79.8	2.0	0.9	1.5
Landing	70	77.6	2.3	0.9	1.7
Landing	70	76.8	2.3	0.8	1.5
Clean	80	65.3	2.0	0.9	1.8
Clean	100	74.5	1.7	0.7	1.4

Table 5.14: Roll Performance - Test Point 3 Summary

The roll performance of the BS115 shown in Tables 5.13 and 5.14 indicates that a 30° bank angle change is achieved in all cases within 0.9 seconds, which is within the 1.3 second requirement. For the 60° bank angle change, all measurements performed at test point 1 fall within the 1.7 seconds criteria, with a maximum time required of 1.3 seconds. For test point 3, the measurement performed at 80 kts in clean configuration shows a required time of 1.8 seconds. However, this is the only test point above the limit. To check whether or not the measurement might be off, the 90% confidence interval for test point 3 is plotted in Figure 5.24. The corresponding 90% confidence interval lower boundary is 1.42 s, while the upper boundary is 1.74 s.

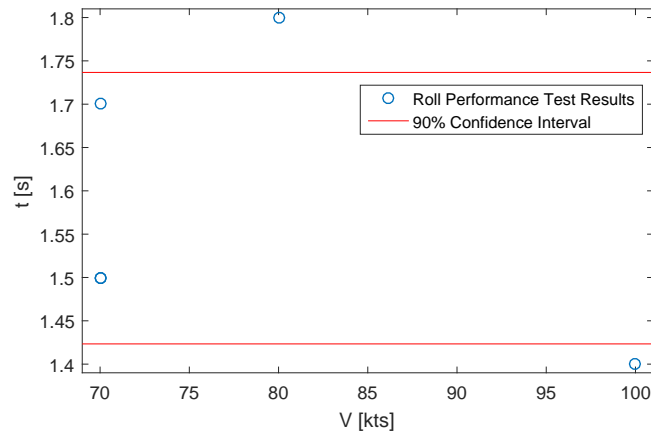


Figure 5.24: Roll Performance - Test Point 3 - Confidence Interval

Based on the test points available and the confidence interval plot shown above, it is suspected the measurement at 80 kts in clean configuration is slightly off. One possible cause of this is that the maximum aileron deflection is not reached instantly, as would be the case with a step input, but that the pilot took a bit longer to reach the maximum aileron deflection. This is for example also seen in Figure 5.23 where it took 0.5 s to reach maximum aileron deflection. If the mean value of all measurements is taken as representative for the roll performance at test point 3, a bank angle change of 60° can be reached within 1.58 s. Therefore the BS115 shows level 1 handling qualities when considering the roll performance.

### 5.6.3. ROLL CONTROL FORCE

The final criteria related to the roll mode of the BS115 is the control force required to reach the roll performance evaluated in subsections 5.6.1 and 5.6.2. Unfortunately no strain gauges were attached to the aileron controls during the test flights, so the aileron control forces have not been measured during flight. As a result, these forces need to be calculated.

The force required to move the ailerons can be determined using equation 5.8 [11, p.449]:

$$F_a = - \left( \frac{d\delta_{ar}}{dS_a} C_{h_{ar}} + \frac{d\delta_{al}}{dS_a} C_{h_{al}} \right) \frac{1}{2} \rho V^2 S_a \bar{c}_a \quad (5.8)$$

With  $C_{h_a}$  the aileron hinge moment coefficient:

$$C_{h_a} = C_{h_0} + C_{h_\alpha} \alpha + C_{h_\delta} \delta \quad (5.9)$$

In equation 5.9,  $C_{h_0}$  represents the breakout force component. Both  $C_{h_\alpha}$  and  $C_{h_\delta}$  are determined using ESDU [41]. During the flight test manoeuvre the ailerons are at their maximum deflection angle,  $15^\circ$  for the upwards moving aileron and  $11^\circ$  for the downwards moving aileron. Assuming the hinge moment coefficients and altitude are constant for all test points, the required force is only dependent on airspeed. Using the BS115 data provided in Appendix A, Figure 5.25 is created:

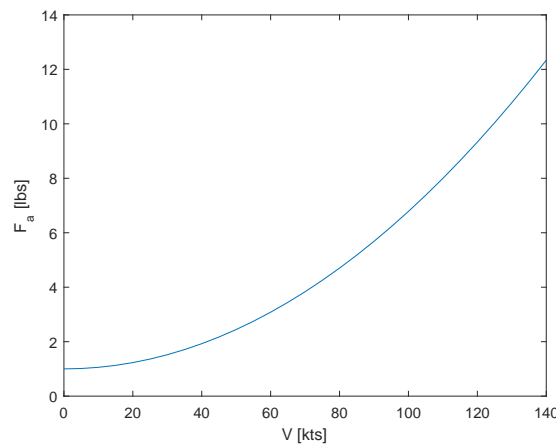


Figure 5.25: Aileron Control Forces - BS115

With a minimum speed of  $65 \text{ kts}$  and a maximum speed of  $140 \text{ kts}$ , the corresponding minimum and maximum aileron control forces are  $3.4 \text{ lbs}$  and  $12.3 \text{ lbs}$  respectively. The corresponding training effectiveness evaluation criteria states that the roll control force should be smaller than  $20 \text{ lbs}$ , but larger than  $5 \text{ lbs}$  plus the breakout force if one wants to achieve level 1 handling qualities. With the breakout force at  $1 \text{ lbs}$ , it can be seen that for low airspeeds the aileron control force does not meet these requirements. Using the definitions of Section 2.2, it is seen the BS115 shows level 3 handling qualities for airspeeds up to  $65 \text{ kts}$  and level 2 handling qualities for airspeeds between  $70$  and  $95 \text{ kts}$ . In this low-speed region the aircraft may become over-sensitive to roll control. This is potentially dangerous, as it makes it easy for student pilots to unintentionally apply a rolling motion to the aircraft. At all speeds above  $95 \text{ kts}$  level 1 handling qualities are found.

A final check on the aileron force results is made by making a comparison with the Cessna 172 and Diamond Da-20. The aileron control forces are determined without considering the breakout force. Calculating the control forces using equation 5.8 and assuming the gearing ratio of the control system is comparable, Figure 5.26 is created. The Cessna 172 shows much higher control forces than the other two aircraft, which is caused by the larger hinge moments found in the control system. The Da-20 has lower control forces than the BS115 due to the lower hinge moment coefficients, which can be seen in Table 5.15.

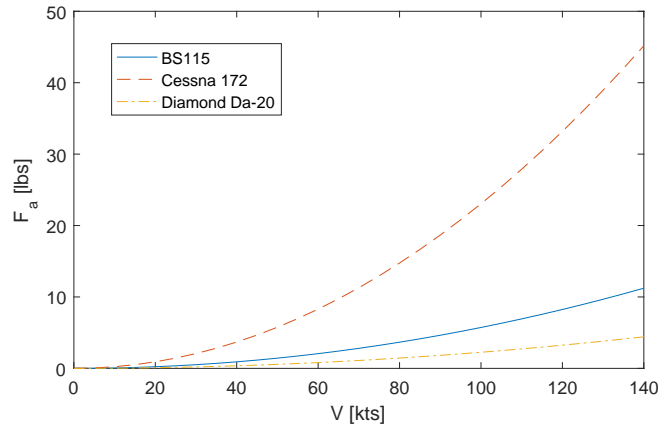


Figure 5.26: Aileron Control Forces - Reference Aircraft Comparison

	$S_a [m^2]$	$\bar{c}_a [m]$	$C_{h_\alpha} [1/rad]$	$C_{h_\delta} [1/rad]$
BS115	0.315	0.225	-0.309	-0.706
Cessna 172	1.55	0.285	-0.164	-0.548
Da-20	0.55	0.168	-0.015	-0.483

Table 5.15: Aileron Control Surface Comparison

## 5.7. SPIRAL MODE

Since no test flights have been performed on quantifying the spiral mode characteristics of the BS115 aircraft, these characteristics can only be determined from the DATCOM model retrieved earlier in Chapter 4. Using the asymmetric equations of motion [11, p.143] and the procedure described in Appendix E, Figure 5.27 is created. In this plot the eigenvalues for the asymmetric motions are shown for the BS115. Three eigenmotions may be distinguished:

- A highly damped aperiodic motion which is most apparent in the rate of roll.
- A lightly damped aperiodic motion in which the aircraft sideslips, yaws and rolls. This eigenmotion is called the spiral motion.
- A periodic mode in which the aircraft sideslips, yaws and rolls, better known as the Dutch roll motion.

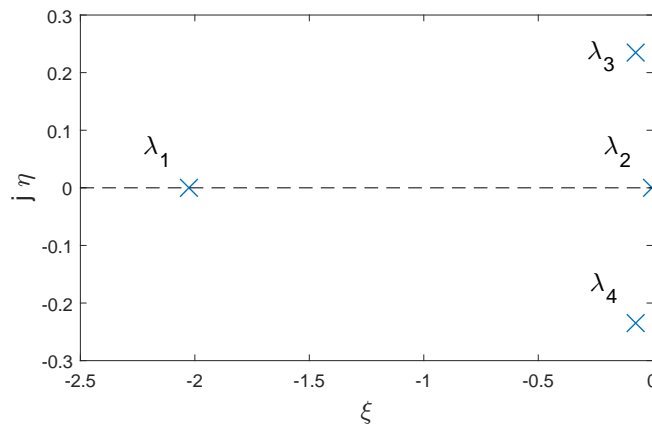


Figure 5.27: Eigenvalue location for the asymmetric motions - BS115

Corresponding to the spiral motion of the aircraft is  $\lambda_2$ , which is found to be equal to -0.0034 for the BS115. The time to damp to half the amplitude is then equal to 27.3 seconds. Additionally, a comparison is made with the Cessna 172 and Diamond Da-20. Using the same procedure, the following values are found:

	$\lambda_2$	$T_{1/2}$
BS115	-0.0034	27.3
Cessna 172	-0.0033	34.3
Da-20	-0.0008	140

Table 5.16: Spiral Mode - Comparison with Reference Aircraft

As can be seen, the Cessna 172 performs very similar to the BS115. When looking again at the lateral stability diagram (Figure 5.21 of subsection 5.5.2, it can be seen spiral stability is improved either by decreasing  $C_{n_\beta}$  or increasing  $-C_{l_\beta}$ . However, the difference between the BS115 and the Da-20 cannot be explained by comparing only  $C_{n_\beta}$  and  $C_{l_\beta}$  since both are more favourable for the Da-20. In this case also the yaw rate derivatives  $C_{n_r}$  and  $C_{l_r}$  play a role, as can be seen from the definition of E (Equation 5.10).

$$E = C_{l_\beta} C_{n_r} - C_{n_\beta} C_{l_r} \quad (5.10)$$

The accompanying training effectiveness evaluation criteria was determined in subsection 2.2.3 and stated that the time for the bank angle to double should be greater than 12 seconds to achieve level 1 handling qualities. Since the BS115 is found to have spiral stability and the bank angle actually decreases over time, the criteria for spiral stability is met.

## 5.8. BS115 PILOT FEEDBACK

As stated in Section 2.3.1, four training manoeuvres have been chosen to be evaluated using the modified Cooper-Harper scale by the test pilot. The obtained results are discussed below.

### NORMAL APPROACH AND LANDING

The pilot has evaluated a normal approach and landing manoeuvre using the criteria in Figure 5.28. It is found that for such a manoeuvre, the closed loop handling qualities fall between a rating of 2 and 3. A rating of 3 applies mainly when attempting the task with mechanical or thermal turbulence or crosswind.

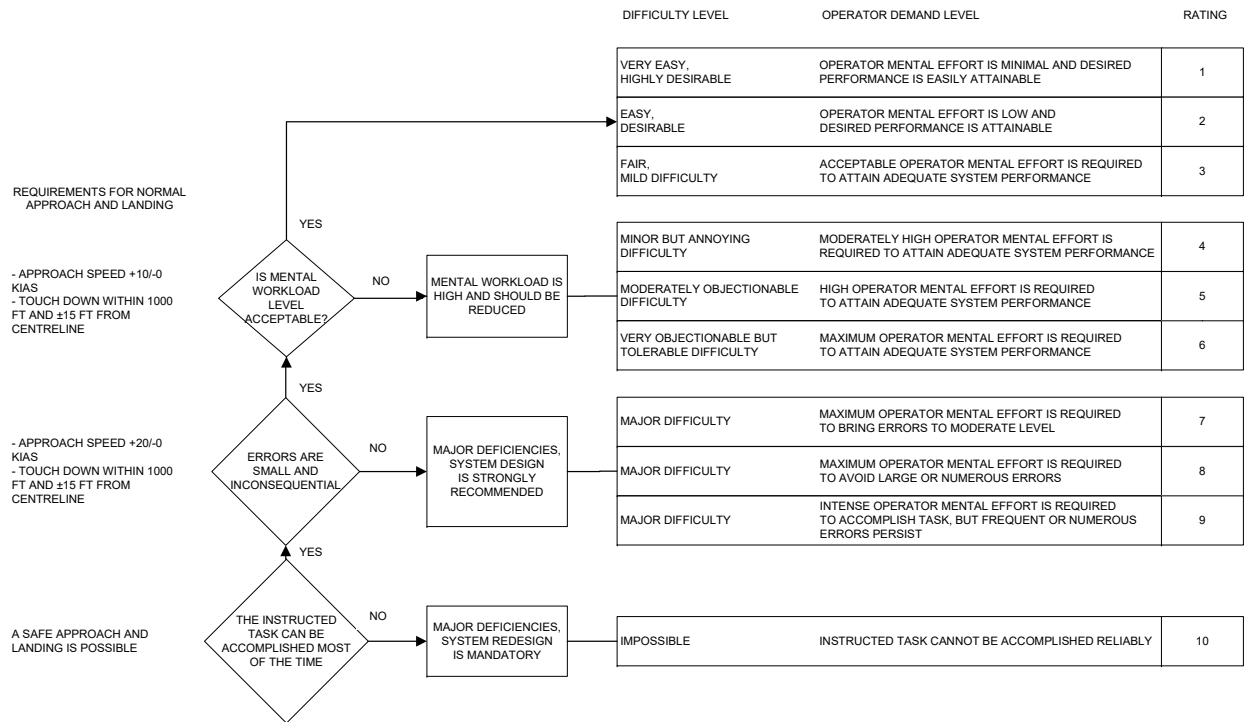


Figure 5.28: Normal Approach and Landing - Cooper Harper Evaluation

### S-TURN GROUND REFERENCE MANOEUVRE

The S-turn ground reference manoeuvre is given a rating between 4 and 5, when Figure 5.29 is used. The execution of S-turn manoeuvres requires accurate and constant cross-checking of airspeed, altitude, vertical speed and bank angle. The avionics system of the BS115 presents a lot of data on small displays and additionally has split the VSI. Therefore it lacks intuitivity in capturing immediately the trend, which makes the S turn manoeuvre cumbersome. This is especially the case for student pilots.

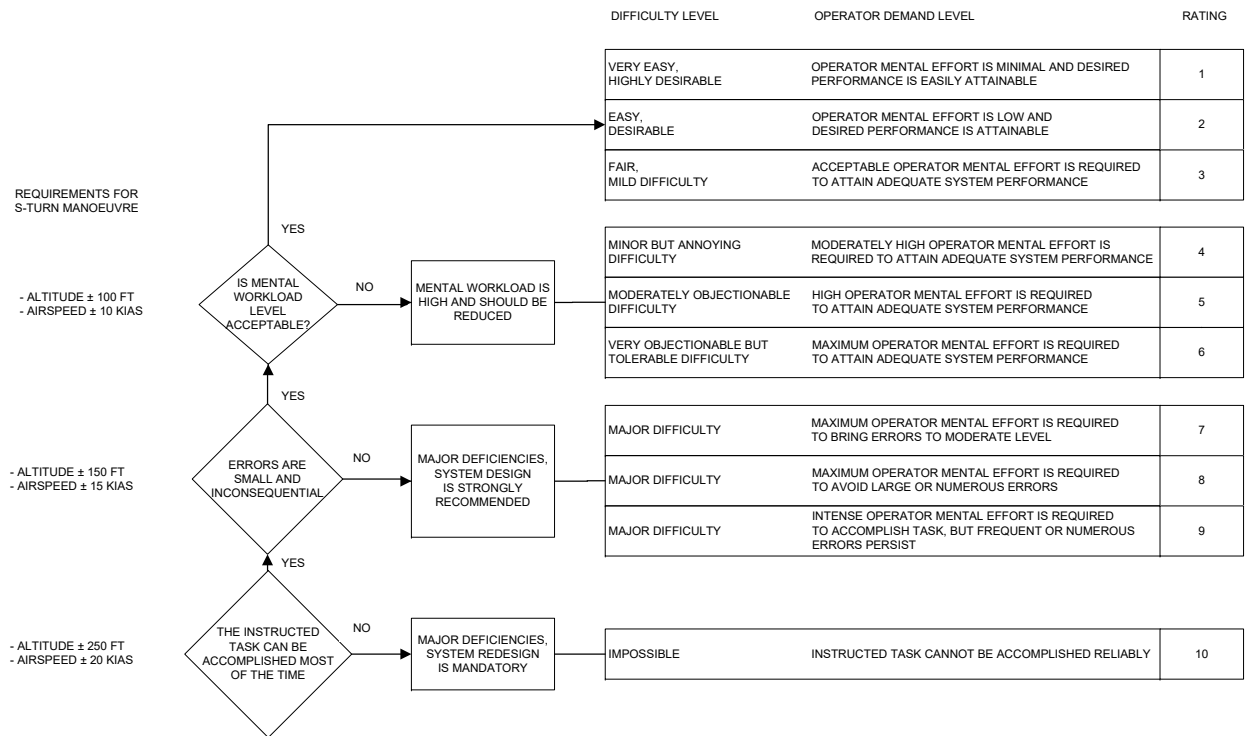


Figure 5.29: S-turn ground reference Manoeuvre - Cooper Harper Evaluation

STEEP TURN PERFORMANCE MANOEUVRE

The steep turn manoeuvre is evaluated using the rating system of Figure 5.30. Depending on the level of turbulence, the rating varies between 2 and 4. Level 4 occurs mainly when working in turbulent air, due to the low wing loading and hence turbulence sensitivity of the BS115.

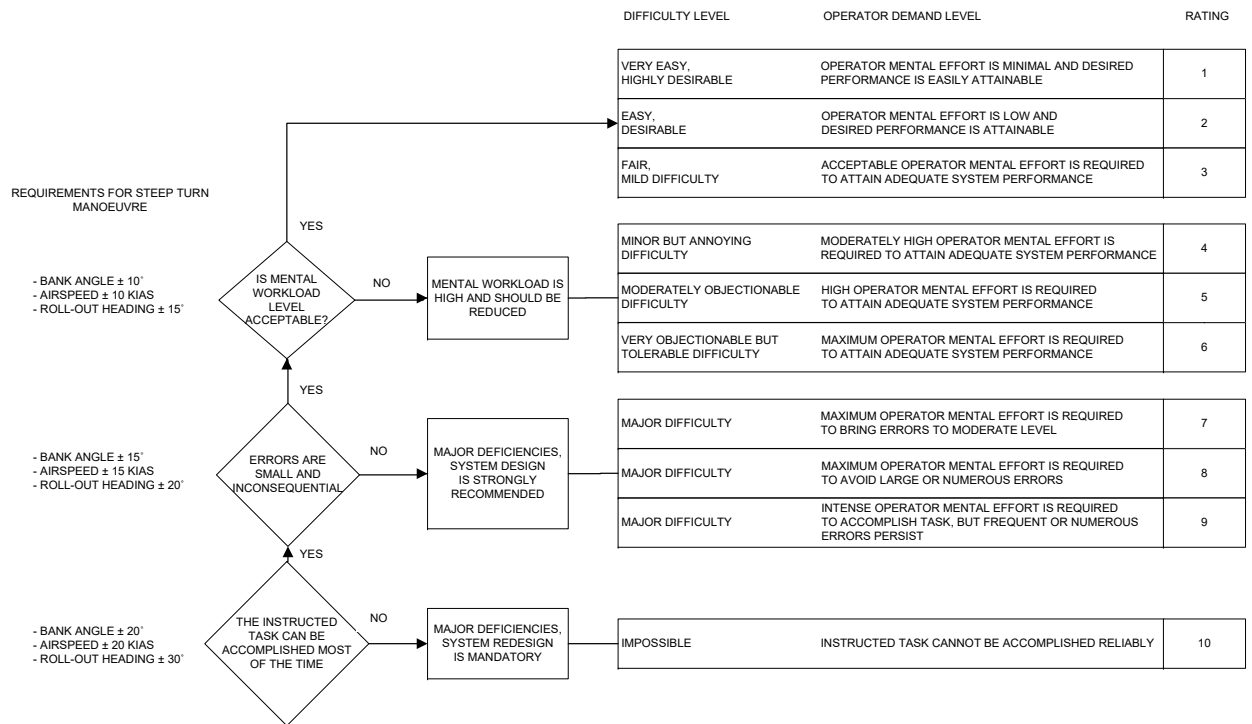


Figure 5.30: Steep Turn Performance Manoeuvre - Cooper Harper Evaluation

UNUSUAL ATTITUDE RECOVERY

Figure 5.31 shows the rating system for unusual attitude recovery. It is found by the test pilot that the BS115 achieves a rating of 2 or 3. Unusual attitude recovery characteristics are very well adapted for the role of a basic trainer. Stalls are very benign and recovery from intentional or inadvertent departure is intuitive.



such as CFD have to be implemented.

Even though the other criteria could be evaluated using flight testing, these have some shortcomings as well. Although the BS115 has been tested at three different CG positions, not all manoeuvres have been flown at all test points. Additionally, the number of test points for each criteria are limited as well. For example, the phugoid motion is only evaluated once at four measurement points at test point 2, all at different speeds. Moreover, at test point 1 only one measurement is performed. If the manoeuvre is not executed accurately at each of these measurement points, a large data scatter in the results will be obtained. As was seen in Figure 5.11, this is the case with 90% confidence bounds for the damping coefficient at 0.166 and 0.279. The most efficient way to increase confidence in the obtained results, and thereby accuracy, is by increasing the sampling size in the flight test data. Not only the phugoid, but most other evaluation criteria suffer from the same lack of sampling size. This is most critical for the longitudinal control, Dutch roll and aforementioned phugoid evaluation.

Due to these limitations, the current evaluation of handling quality criteria has some drawbacks. While all aircraft properties have been determined using either flight test data or the DATCOM model, there exists a high degree of uncertainty in the obtained results. Even though statements from the test pilots support the conclusions drawn in this chapter, the results should be considered as indicative only. Subsequently, the goal of the handling quality evaluation in this chapter has not been entirely completed. Although the handling quality characteristics that need improvement have been identified, it has not been possible to obtain accurate data on these characteristics. The only way to improve these results is by improving the BS115 model or by performing more extensive flight testing on this topic.



# 6

## CONCLUSIONS

As discussed in the introduction of this report, the objective of this thesis was to assess the effect of handling qualities on the training effectiveness of the BS115 aircraft. The research question for this project was defined as follows:

*Which handling qualities of the BS115 should be improved such that the training effectiveness of the aircraft is maximized for the development of flying skills?*

To answer this question, training effectiveness evaluation criteria have been determined and tested. After conducting a literature review, several criteria were established and a grading system was adapted from the MIL-STD. These criteria were evaluated using flight testing and a computational model based on Digital DATCOM.

Using the flight test results and the BS115 model, the following conclusions can be drawn related to the BS115 training effectiveness:

- The BS115 showed level 1 flying qualities for all longitudinal and lateral-directional stability criteria. The phugoid, short period, Dutch roll and spiral mode all show the required stability.
- Roll performance of the BS115 has been shown to be adequate in all test points and hence demonstrates level 1 flying qualities.
- Both longitudinal control forces and roll control forces are too low to meet level 1 flying qualities. Longitudinal control meets only level 3 flying qualities, while roll control achieves level 2 flying qualities at speeds above 70 kts. At lower speeds, level 3 flying qualities are demonstrated for roll control.
- When performing an S-turn ground reference manoeuvre, level 2 flying qualities are achieved. This is mainly caused by the BS115 avionics system, which presents a lot of data on small displays. Avionics of the BS115 are therefore not best adapted for IFR training. Steep turn performance reduces to level 2 flying qualities in turbulent air, while in calm conditions level 1 flying qualities are demonstrated. Normal approach and landing, as well as unusual attitude recovery are possible with level 1 flying qualities.

Therefore, longitudinal manoeuvrability and lateral-directional control should be improved to maximize the BS115 training effectiveness.



# 7

## RECOMMENDATIONS

Based on the research performed and the results that have been obtained, a number of recommendations for future research and improvements on the current work can be given.

Evaluating the training effectiveness criteria was done using both a DATCOM model of the BS115 aircraft and a series of flight tests available. Although the DATCOM model provides a relatively quick way to evaluate the aircraft characteristics, its accuracy is limited and hence its applicability should be mostly limited to the initial design stages. To obtain better results ideally a complete training effectiveness evaluation is performed during the flight test campaign. Unfortunately the training effectiveness assessment was performed only towards the end of the flight test campaign, meaning the test flights were not optimized for training effectiveness evaluation. If the evaluation of training effectiveness is taken into account early in the flight test planning of future projects, accuracy could be increased greatly leading to a better design evaluation.

The training effectiveness evaluation performed in this thesis only focuses on the handling qualities of an aircraft and hence does not cover the entire spectrum of skills relevant in pilot training. A next step that should be taken is to integrate the handling quality evaluation into the general training effectiveness method presented in the introduction. To this purpose a weighting value should be assigned to each of the handling quality evaluation criteria, based on the input of expert pilots. Using the steps mentioned in Section 1.3, a complete training effectiveness evaluation method can then be obtained.



# A

## BS115 AIRCRAFT DATA

### A.1. BS115 3-VIEW

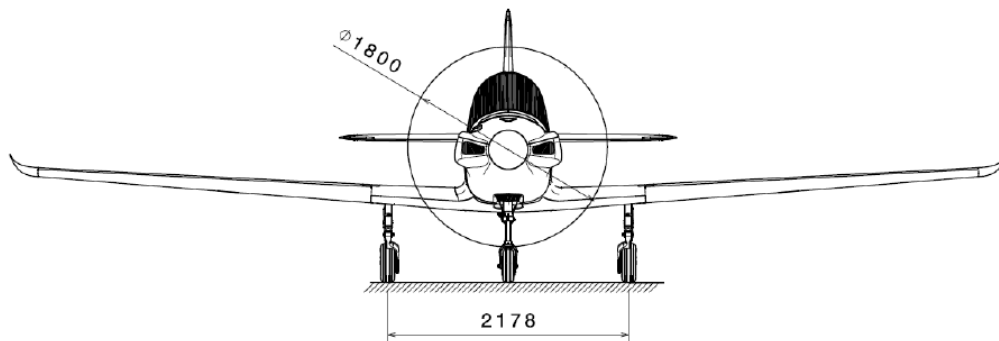


Figure A.1: BS115 - Front View

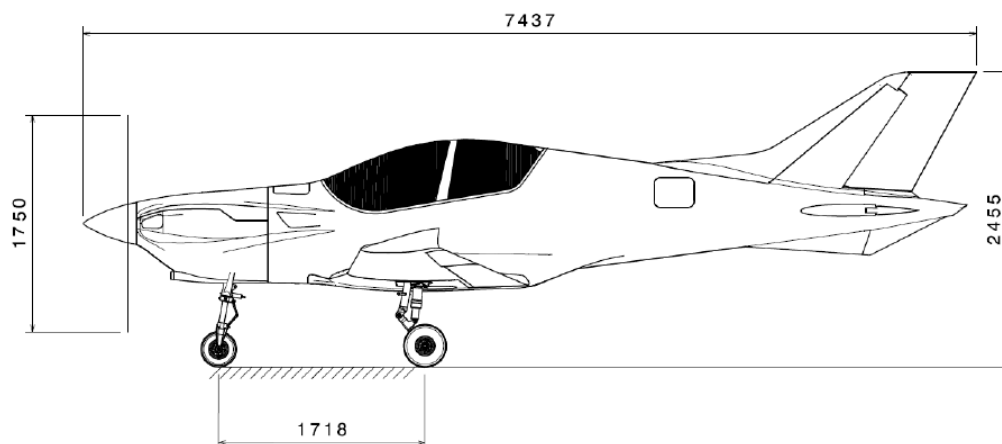


Figure A.2: BS115 - Side View

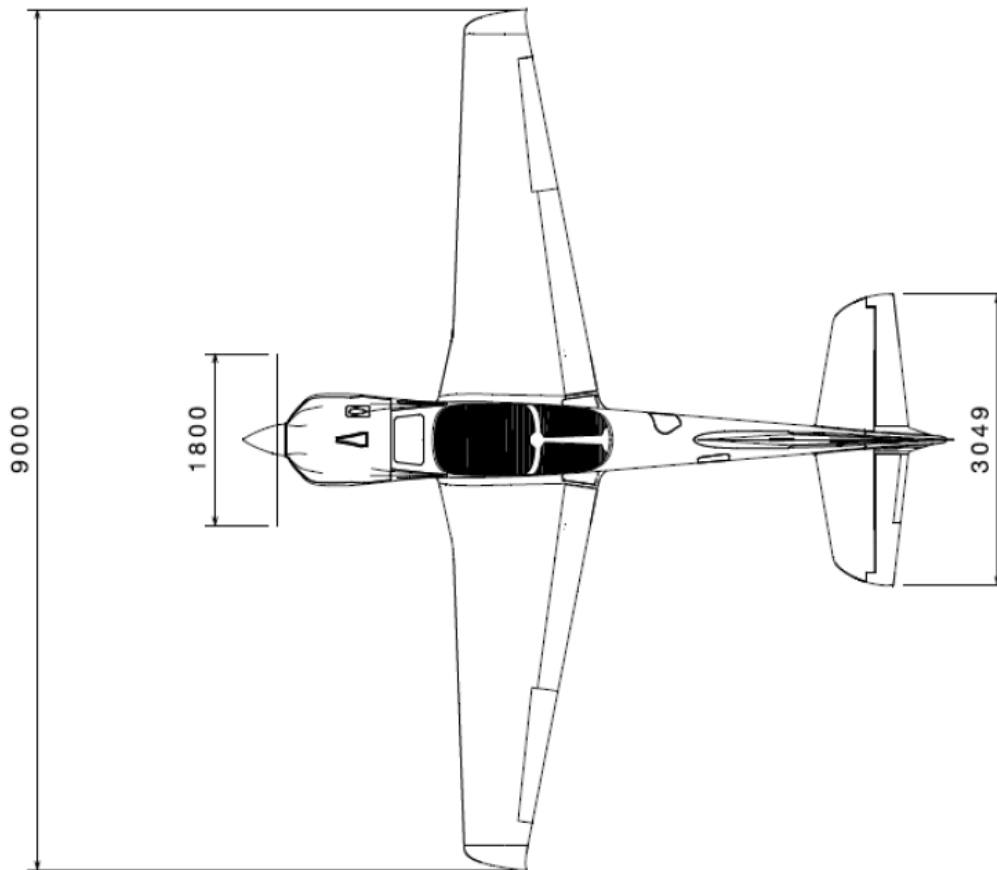


Figure A.3: BS115 - Top View

## A.2. GENERAL CHARACTERISTICS

	<i>Symbol</i>	<i>Value</i>	<i>Unit</i>
Total Length	$L_{tot}$	7.44	[m]
Total Height	$H_{tot}$	2.46	[m]
Empty Weight	$EW$	519.5	[kg]
Maximum Take-Off Weight	$MTOW$	750	[kg]
Maximum Engine Power	$P_{max}$	160	[hp]
Propeller Radius	$r_{prop}$	1.75	[m]

Table A.1: BS115 General Characteristics

### A.3. WING CHARACTERISTICS

	<i>Symbol</i>	<i>Value</i>	<i>Unit</i>
Wing Surface Area	$S$	10.31	$[m^2]$
Wing Span	$b$	9.00	$[m]$
Mean Aerodynamic Chord	$\bar{c}_w$	1.261	$[m]$
Aspect Ratio	$A$	6.98	$[-]$
Wing Incidence Angle	$i_w$	2.0	$[\circ]$
Wing Dihedral Angle	$\tau_w$	4.6	$[\circ]$
Taper Ratio	$\lambda_w$	0.34	$[-]$
Root Chord	$c_{rw}$	1.845	$[m]$
Tip Chord	$c_{tw}$	0.660	$[m]$

Table A.2: BS115 Wing Characteristics

### A.4. EMPENNAGE CHARACTERISTICS

	<i>Symbol</i>	<i>Value</i>	<i>Unit</i>
HT Surface Area	$S_h$	2.43	$[m^2]$
HT Span	$b_h$	3.02	$[m]$
Mean Aerodynamic Chord	$\bar{c}_h$	0.833	$[m]$
Aspect Ratio	$A_h$	3.75	$[-]$
HT setting	$i_t$	-2.0	$[\circ]$
HT Taper Ratio	$\lambda_h$	0.60	$[-]$
Root Chord	$c_{rh}$	1.02	$[m]$
Tip Chord	$c_{th}$	0.61	$[m]$
Tail Distance	$l_h$	3.75	$[m]$
Tail Volume	$\bar{V}_h = \frac{l_h S_h}{S \bar{c}}$	0.701	$[-]$

Table A.3: BS115 Horizontal Tail Characteristics

	<i>Symbol</i>	<i>Value</i>	<i>Unit</i>
Elevator Surface Area	$S_e$	0.70	$[m^2]$
Elevator Span	$b_e$	1.51	$[m]$
Mean Aerodynamic Chord	$\bar{c}_e$	0.27	$[m]$
Root Chord	$c_{re}$	0.372	$[m]$
Tip Chord	$c_{te}$	0.217	$[m]$

Table A.4: BS115 Elevator Characteristics



# B

## BS115 WEIGHT AND BALANCE

The BS115 aircraft weight can be divided into several components. Each of these components has an influence on the total aircraft weight considered in the flight tests, as well as on the centre of gravity position.

First of all, a reference location has to be defined. For the BS115, this is the datum indicated in Figure B.1. It is located 800 mm behind the bulkhead in X-direction, 165 mm above the BS115 body centreline, and coincides with the aircraft line of symmetry.

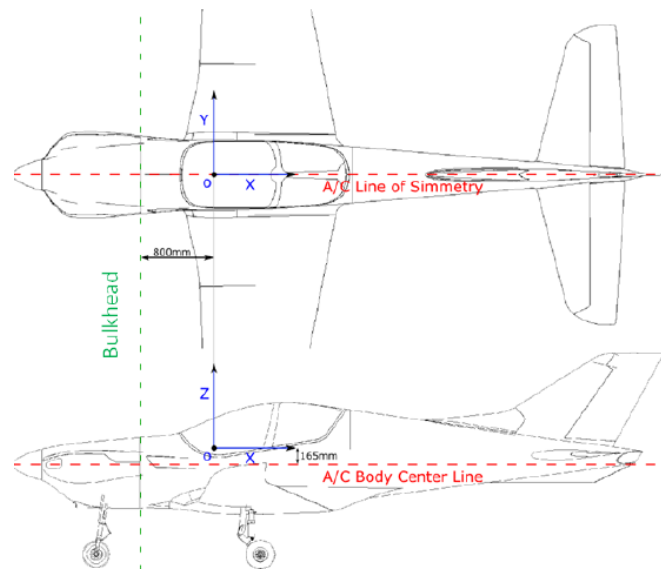


Figure B.1: BS115 reference point definition

For the three test points used in the flight test analysis, the weight breakdowns are provided in Tables B.1 to B.3. The empty weight condition is the same for all test points and is given in Table B.4. Provided are the weight contributions, the location of their centre of gravity with respect to the datum, and the centre of gravity location specified in percentage of the mean aerodynamic chord for the complete layout. The extra weight is provided by slabs of lead, placed on the passenger seat.

	Weight [kg]	$X_{CG}$ [mm]	$X_{CG}$ [%MAC]
Empty Weight	520	19	
Pilot	86	280	
Fuel (full)	100	45	
Baggage	33	1681	
Extra Weight	5	1282	
Total	745		23.6%

Table B.1: Weight Breakdown for Test Point 1

	Weight [kg]	$X_{CG}$ [mm]	$X_{CG}$ [%MAC]
Empty Weight	520	19	
Pilot	86	280	
Fuel (allowable)	38	45	
Baggage	20	1681	
Extra Weight	86	1282	
Total	750		31.0%

Table B.2: Weight Breakdown for Test Point 2

	Weight [kg]	$X_{CG}$ [mm]	$X_{CG}$ [%MAC]
Empty Weight	520	19	
Pilot	86	280	
Fuel (full)	100	45	
Total	706		17.3%

Table B.3: Weight Breakdown for Test Point 3

	Weight [kg]	$X_{CG}$ [mm]
Fuel Tank	10.8	45
Fuselage	75.5	1003
Tail Cover	2.5	4460
Horizontal Stabilizer	8.6	4030
Elevators	6.9	4313
Rudder	3.1	4528
Wing	47.8	553
Main Landing Gear	31.5	432
Nose Landing Gear	12.5	-752
Aileron Control	3.0	295
Rudder Control	11.9	417
Control Column	4.7	365
Elevator Control	2.0	2419
Flaps Control	2.9	743
Engine Mount	10.4	-1046
Propeller	24.1	-1920
Firewall	3.2	-1001
Engine	145.5	-1430
Oil Cooler	1.3	-909
Avionics	33.3	2122
Engine Cowling	5.0	-1300
Exhaust	4.2	-1350
Instrument Panel	12.7	-260
Fuel System	7.5	-450
Landing Gear Doors	1.3	150
Seat Upholstery Forward	2.5	507
Seat Upholstery Rearward	2.5	1282
Canopy	13.5	534
Miscellaneous	18.5	273
Unusable Fuel	11.0	45
Total	520.0	19.0 %

Table B.4: Weight Breakdown for Empty Weight



# C

## DYNON FLIGHT TEST LOGGING PARAMETERS

- Time,  $t$  [s]
- Pitch angle,  $\theta$  [deg]
- Roll angle,  $\phi$  [deg]
- Heading angle,  $\psi$  [deg]
- Calibrated Airspeed,  $CAS$  [kts]
- Altitude,  $h$  [ft]
- Turn rate,  $r$  [deg/s]
- Lateral acceleration,  $a_y$  [ $m/s^2$ ]
- Vertical acceleration,  $a_z$  [ $m/s^2$ ]
- Vertical speed,  $w$  [ft/min]
- Density altitude,  $h_{dens}$  [ft]
- Elevator bar force,  $F_{elev}$  [kg]
- Elevator Stick force,  $F_S$  [kg]
- Left hand pedal force,  $F_{PLH}$  [kg]
- Right hand pedal force,  $F_{PRH}$  [kg]
- Aileron deflection,  $\delta_a$  [deg]
- Rudder deflection,  $\delta_r$  [deg]
- Elevator deflection,  $\delta_e$  [deg]
- Trim tab deflection,  $\delta_t$  [deg]
- Angle of attack,  $\alpha$  [deg]
- Angle of sideslip,  $\beta$  [deg]

Several other parameters are recorded in the EDM logfile, which are listed below:

- Engine speed,  $RPM$  [rev/min]
- Absolute manifold pressure,  $MAP$  [Hg]
- Outside air temperature,  $T_{out}$  [°C]

Finally, weight and balance parameters are recorded manually pre-flight:

- Aircraft weight,  $W$  [kg]
- Centre of gravity location,  $cg$  [%MAC]

# D

## DATCOM FILES

```
$FLTCON NMACH=1.0,MACH(1)=0.201$
$FLTCON NALT=1.0,ALT(1)=1981.2$
$FLTCON NALPHA=9.0,
  ALSCHD(1)=2.0,4.0,6.0,8.0,10.0,12.0,14.0,16.0,18.0,
  LOOP=1.0$
$OPTINS SREF=10.31,CBARR=1.261,BLREF=9.0$
$SYNTHS XCG=2.569,ZCG=-0.165,XW=1.943,ZW=-0.627,ALIW=2.0,
  XH=5.956,ZH=-0.056,ALIH=-2.0,
  XV=5.158,XVF=5.8425,ZV=-0.105,ZVF=-0.358,VERTUP=.TRUE.$
$BODY NX=12.0,
X(1)=0.0,0.425,0.525,0.840,1.281,1.521,1.961,2.921,3.887,
  6.483,7.203,7.337,
S(1)=0.0,0.096,0.210,0.464,0.526,0.542,0.590,0.905,0.578,
  0.054,0.007,0.0,
ZU(1)=-0.157,0.009,0.032,0.080,0.119,0.140,0.195,0.546,
  0.452,0.124,0.010,0.009,
ZL(1)=-0.157,-0.339,-0.400,-0.634,-0.650,-0.660,-0.670,-0.725,
  -0.622,-0.228,-0.102,-0.009$
$WGPLNF CHRDTP=0.6603,SSPNOP=3.0359,SSPNE=4.107,SSPN=4.50,CHRDBP=1.3624,
  CHRDR=1.845,SAVSI=5.6,SAVSO=-1.2,CHSTAT=0.25,TWISTA=-3.0,SSPND=3.0359,
  DHDADI=4.6,DHDADO=4.6,TYPE=1.0$
$WGSCHR TOVC=0.0844,DELTAY=3.688,XOVC=0.3417,CLI=0.2414,ALPHAI=1.175,
  CLALPA=0.1084,CLMAX=1.6086,CMO=-0.0510,LERI=0.013,LERO=0.0155,
  CAMBER=.TRUE.,TOVCO=0.0788,XOVCO=0.4102,CMOT=-0.0738,YCM=0.0218$
$HTPLNF CHRDTP=0.613,SSPNE=1.424,SSPN=1.525,
  CHRDR=1.023,SAVSI=9.6,CHSTAT=0.0,TWISTA=0.0,
  DHDADI=0.0,TYPE=1.0$
NACA-H-6-63A010
$VTPLNF CHRDTP=0.694,SSPNE=0.995,SSPN=0.995,
  CHRDR=1.745,SAVSI=58.0,CHSTAT=0.0,TYPE=1.0$
NACA-V-6-63A010
$VFPLNF CHRDTP=1.2424,SSPNE=0.112,SSPN=0.224,
  CHRDR=1.2424,SAVSI=-26.0,CHSTAT=0.5,TYPE=1.0$
NACA-VF-6-63A010
$EXPR01 DEODA(1)=0.3,0.3,0.3,0.3,0.3,0.3,0.3,0.3,0.3,
  EPSLON(1)=0.35,0.95,1.55,2.15,2.75,3.35,3.95,4.55,5.15,
  QOQINF(1)=0.903,0.903,0.903,0.903,0.903,0.903,0.903,0.903,0.903$
$PROPWR AIETLP=0.0,NENGS=1.0,THSTCP=0.0620,PHALOC=0.364,PHVLOC=0.0,
  PRPRAD=0.877,BWAPR3=0.113,BWAPR6=0.167,BWAPR9=0.127,NOPBPE=3.0,
  BAPR75=20.84,YP=0.0,CROT=.FALSE.$
CASEID BS115 COMPLETE MODE
DAMP
DIM M
TRIM
NEXT CASE
```

Figure D.1: Digital DATCOM Input File for the BS115

AUTOMATED STABILITY AND CONTROL METHODS PER APRIL 1976 VERSION OF DATCOM  
 CHARACTERISTICS AT ANGLE OF ATTACK AND IN SIDESLIP  
 WING-BODY-HORIZONTAL TAIL-VERTICAL TAIL-VENTRAL FIN CONFIGURATION  
 PROPELLER POWER EFFECTS INCLUDED IN THE LONGITUDINAL STABILITY RESULTS  
 BS115 COMPLETE MODE

FLIGHT CONDITIONS							REFERENCE DIMENSIONS				
MACH NUMBER	ALTITUDE	VELOCITY	PRESSURE	TEMPERATURE	REYNOLDS NUMBER	REF. AREA	REFERENCE LONG.	LENGTH LAT.	MOMENT HORIZ	REF. CENTER VERT	
	M	M/SEC	N/ M**2	DEG K	1/ M	M**2	M	M	M	M	
0.201	1981.20	66.85	7.9687E+04	275.276	3.8868E+06	10.310	1.261	9.000	2.569	-0.165	
-----DERIVATIVE (PER DEGREE)-----											
ALPHA	CD	CL	CM	CN	CA	XCP	CLA	CMA	CYB	CNB	CLB
2.0	0.024	0.346	-0.0295	0.347	0.012	-0.085	1.084E-01	-1.645E-02	-8.250E-03	4.376E-04	-5.368E-04
4.0	0.034	0.572	-0.0623	0.573	-0.006	-0.109	1.121E-01	-1.983E-02			-5.595E-04
6.0	0.048	0.806	-0.0924	0.807	-0.036	-0.114	1.153E-01	-2.002E-02			-5.847E-04
8.0	0.069	1.040	-0.1033	1.039	-0.076	-0.099	1.177E-01	-2.072E-02			-6.121E-04
10.0	0.096	1.280	-0.1263	1.277	-0.127	-0.099	1.088E-01	-2.193E-02			-6.408E-04
12.0	0.125	1.481	-0.1508	1.474	-0.186	-0.102	9.156E-02	-2.258E-02			-6.619E-04
14.0	0.154	1.651	-0.1741	1.639	-0.250	-0.106	7.541E-02	-2.337E-02			-6.772E-04
16.0	0.184	1.786	-0.1995	1.767	-0.315	-0.113	4.831E-02	-2.503E-02			-6.814E-04
18.0	0.208	1.846	0.1613	1.820	-0.373	0.089	1.129E-02	NA			-6.648E-04
-----											
			ALPHA	Q/QINF	EPSLON	D(EPSLON)/D(ALPHA)					
			2.0	0.903	0.350	0.300					
			4.0	0.903	0.950	0.300					
			6.0	0.903	1.550	0.300					
			8.0	0.903	2.150	0.300					
			10.0	0.903	2.750	0.300					
			12.0	0.903	3.350	0.300					
			14.0	0.903	3.950	0.300					
			16.0	0.903	4.550	0.300					
			18.0	0.903	5.150	0.300					

AUTOMATED STABILITY AND CONTROL METHODS PER APRIL 1976 VERSION OF DATCOM  
 DYNAMIC DERIVATIVES  
 WING-BODY-HORIZONTAL TAIL-VERTICAL TAIL-VENTRAL FIN CONFIGURATION  
 BS115 COMPLETE MODE

FLIGHT CONDITIONS						REFERENCE DIMENSIONS				
MACH NUMBER	ALTITUDE	VELOCITY	PRESSURE	TEMPERATURE	REYNOLDS NUMBER	REF. AREA	REFERENCE LONG.	LENGTH LAT.	MOMENT HORIZ	REF. CENTER VERT
	M	M/SEC	N/ M**2	DEG K	1/ M	M**2	M	M	M	M
0.201	1981.20	66.85	7.9687E+04	275.276	3.8868E+06	10.310	1.261	9.000	2.569	-0.165
-----DYNAMIC DERIVATIVES (PER DEGREE)-----										
ALPHA	-----PITCHING-----		-----ACCELERATION-----			-----ROLLING-----			-----YAWING-----	
	CLQ	CMQ	CLAD	CMAD	CLP	CYP	CNP	CNR	CLR	
2.00	1.209E-01	-2.428E-01	2.479E-02	-7.331E-02	-8.398E-03	-2.303E-03	-4.852E-04	-1.972E-03	1.183E-03	
4.00			2.479E-02	-7.331E-02	-8.571E-03	-2.422E-03	-7.534E-04	-2.010E-03	1.841E-03	
6.00			2.479E-02	-7.331E-02	-8.714E-03	-2.545E-03	-1.026E-03	-2.057E-03	2.512E-03	
8.00			2.479E-02	-7.331E-02	-8.760E-03	-2.670E-03	-1.304E-03	-2.113E-03	3.190E-03	
10.00			2.479E-02	-7.331E-02	-7.774E-03	-2.808E-03	-1.642E-03	-2.177E-03	3.863E-03	
12.00			2.479E-02	-7.331E-02	-6.150E-03	-2.914E-03	-1.969E-03	-2.229E-03	4.373E-03	

Figure D.2: Digital DATCOM Output File for the BS115

# E

## CHARACTERISTICS OF REFERENCE AIRCRAFT

In order to better understand the results obtained of the BS115, a comparison is made with several reference aircraft as well as a model of the BS115. For these reference aircraft, the same calculations are made as for the BS115. Sections E.1 to E.3 discuss the relevant stability and control derivatives and how they have been obtained.

### E.1. BS115 MODEL

As discussed in Chapter 4, the stability and control characteristics for the BS115 model are obtained using DATCOM. However, this is not the only data needed to make a complete analysis. Several other characteristics had to be calculated, such as the hinge moment coefficients. These calculations have been reported in the BS115 aerodynamic data collection [34]. All final values used in the calculations are reported in Appendix A. Sections E.4 and E.5 give the formulas used to compute the relevant aircraft characteristics.

### E.2. CESSNA 172 SKYHAWK

#### E.2.1. LONGITUDINAL STABILITY AND CONTROL DERIVATIVES

The longitudinal stability and control derivatives of the Cessna 172 are readily obtained from Mulder *et al.* [11, p. 544]:

$C_{X_0}$	=	0	$C_{Z_0}$	=	-0.310			
$C_{X_u}$	=	-0.093	$C_{Z_u}$	=	-0.620	$C_{m_u}$	=	0
$C_{X_\alpha}$	=	0.18	$C_{Z_\alpha}$	=	-4.631	$C_{m_\alpha}$	=	-0.890
$C_{X_{\dot{\alpha}}}$	=	0	$C_{Z_{\dot{\alpha}}}$	=	-0.850	$C_{m_{\dot{\alpha}}}$	=	-2.600
$C_{X_q}$	=	0	$C_{Z_q}$	=	-1.95	$C_{m_q}$	=	-6.200
$C_{X_{\delta_e}}$	=	0	$C_{Z_{\delta_e}}$	=	-0.430	$C_{m_{\delta_e}}$	=	-1.28

Table E.1: Longitudinal Stability and Control Derivatives - Cessna 172

#### E.2.2. LATERAL-DIRECTIONAL STABILITY AND CONTROL DERIVATIVES

The lateral-directional stability and control derivatives of the Cessna 172 are readily obtained from Roskam [43, p. 482]:

$C_{l_\beta}$	=	-0.0923	$C_{l_p}$	=	-0.484	$C_{l_r}$	=	0.0798
$C_{y_\beta}$	=	-0.393	$C_{y_p}$	=	-0.075	$C_{y_r}$	=	0.214
$C_{n_\beta}$	=	0.0587	$C_{n_p}$	=	-0.0278	$C_{n_r}$	=	-0.0937

Table E.2: Lateral-directional Stability and Control Derivatives - Cessna 172

### E.2.3. HINGE MOMENT COEFFICIENTS

To obtain the hinge moment coefficients necessary for stick force evaluation, the ESDU series on aerodynamics are used [41]. The resulting hinge moment coefficients for elevator control are as follows:

- $C_{h_\alpha} = 0.0283$  [1/rad]
- $C_{h_\delta} = -0.274$  [1/rad]

## E.3. DIAMOND DA-20

Just as for the BS115 model, the DA-20 stability and control derivatives have been determined using DATCOM.

	DA-20 Derivatives
$C_{L_\alpha}$ [1/deg]	0.0842
$C_{m_\alpha}$ [1/deg]	-0.0223
$C_{L_q}$ [1/deg]	0.060
$C_{m_q}$ [1/deg]	-0.116
$C_{L_{\dot{\alpha}}}$ [1/deg]	0.0141
$C_{m_{\dot{\alpha}}}$ [1/deg]	-0.0516

Table E.3: DA-20 Longitudinal Stability Derivatives

	DA-20 Derivatives
$C_{l_\beta}$ [1/deg]	-0.00138
$C_{Y_\beta}$ [1/deg]	-0.00354
$C_{n_\beta}$ [1/deg]	-0.000505
$C_{l_p}$ [1/deg]	0.00928
$C_{Y_p}$ [1/deg]	-0.00091
$C_{n_p}$ [1/deg]	0.000847
$C_{l_r}$ [1/deg]	0.00442
$C_{n_r}$ [1/deg]	-0.00105

Table E.4: DA-20 Lateral-Directional Stability Derivatives

## E.4. STABILITY CHARACTERISTICS

In this section, the equations used to obtain the stability characteristics are given.

### E.4.1. LONGITUDINAL STABILITY CHARACTERISTICS

To obtain the longitudinal stability characteristics from the derivatives determined in the previous sections, the characteristic equation (Equation E.1, [11, p.122]) is used:

$$A\lambda_c^4 + B\lambda_c^3 + C\lambda_c^2 + D\lambda_c + E = 0 \quad (\text{E.1})$$

In which:

$$A = 4\mu_c^2 K_Y^2 (C_{Z_{\dot{\alpha}}} - 2\mu_c) \quad (\text{E.2})$$

$$B = C_{m\dot{\alpha}} 2\mu_c (C_{Z_q} + 2\mu_c) - C_{m_q} 2\mu_c (C_{Z\dot{\alpha}} - 2\mu_c) - 2\mu_c K_Y^2 (C_{X_u} (C_{Z\dot{\alpha}} - 2\mu_c) - 2\mu_c C_{Z\alpha}) \quad (\text{E.3})$$

$$C = C_{m\alpha} 2\mu_c (C_{Z_q} + 2\mu_c) - C_{m\dot{\alpha}} (2\mu_c C_{X_0} + C_{X_u} (C_{Z_q} + 2\mu_c)) + C_{m_q} (C_{X_u} (C_{Z\dot{\alpha}} - 2\mu_c) - 2\mu_c C_{Z\alpha}) + 2\mu_c K_Y^2 (C_{X\alpha} C_{Z_u} - C_{Z\alpha} C_{X_u}) \quad (\text{E.4})$$

$$D = C_{m_u} (C_{X\alpha} (C_{Z_q} + 2\mu_c) - C_{Z_0} (C_{Z\dot{\alpha}} - 2\mu_c)) - C_{m\alpha} (2\mu_c C_{X_0} + C_{X_u} (C_{Z_q} + 2\mu_c)) + C_{m\dot{\alpha}} (C_{X_0} C_{X_u} - C_{Z_0} C_{Z_u}) + C_{m_q} (C_{X_u} C_{Z\alpha} - C_{Z_u} C_{X\alpha}) \quad (\text{E.5})$$

$$E = -C_{m_u} (C_{X_0} C_{X\alpha} + C_{Z_0} C_{Z\alpha}) + C_{m\alpha} (C_{X_0} C_{X_u} + C_{Z_0} C_{Z_u}) \quad (\text{E.6})$$

As can be seen, these stability coefficients refer to  $C_X$  and  $C_Z$  instead of  $C_L$  and  $C_D$ . Therefore some conversions have to be made. For this the assumption is made that the aircraft is in steady horizontal flight with constant thrust setting. Using the definitions of Mulder *et al.* [11, p.164], the final stability derivative conversions are listed in Equations E.7 to E.12.

$$C_{X_u} = -3C_{D_0} \quad (\text{E.7})$$

$$C_{X\alpha} = C_{L_0} \left( 1 - 2 \frac{C_{L\alpha}}{\pi A e} \right) \quad (\text{E.8})$$

$$C_{Z_u} = -2C_{L_0} \quad (\text{E.9})$$

$$C_{Z\alpha} = -C_{L\alpha} - C_{D_0} \quad (\text{E.10})$$

$$C_{Z\dot{\alpha}} = -C_{L\dot{\alpha}} \quad (\text{E.11})$$

$$C_{Z_q} = -C_{L_q} \quad (\text{E.12})$$

With the above input, calculating the roots of Equation E.1 results in two pairs of complex conjugate eigenvalues resembling the phugoid and short period modes.

#### E.4.2. LATERAL-DIRECTIONAL STABILITY CHARACTERISTICS

Just as for the longitudinal stability characteristics, a quartic characteristic equation can be constructed for the lateral-directional aircraft motions:

$$A\lambda_b^4 + B\lambda_b^3 + C\lambda_b^2 + D\lambda_b + E = 0 \quad (\text{E.13})$$

In Equation E.13, the coefficients  $A$  to  $E$  are defined as follows:

$$A = 16\mu_b^3 (K_X^2 K_Z^2 - K_{XZ}^2) \quad (\text{E.14})$$

$$B = -4\mu_b^2 \left( 2C_{Y\beta} (K_X^2 K_Z^2 - K_{XZ}^2) + C_{n_r} K_X^2 + C_{l_p} K_Z^2 + (C_{l_r} + C_{n_p}) K_{XZ} \right) \quad (\text{E.15})$$

$$\begin{aligned}
C = & 2\mu_b \left[ \left( C_{Y\beta} C_{n_r} - C_{Y_r} C_{n\beta} \right) K_X^2 + \left( C_{Y\beta} C_{l_p} - C_{l\beta} C_{Y_p} \right) K_Z^2 \right. \\
& + \left. \left\{ \left( C_{Y\beta} C_{n_p} - C_{n\beta} C_{Y_p} \right) + \left( C_{Y\beta} C_{l_r} - C_{l\beta} C_{Y_r} \right) \right\} K_{XZ} + \right. \\
& \left. 4\mu_b C_{n\beta} K_X^2 + 4\mu_b C_{l\beta} K_{XZ} + \frac{1}{2} \left( C_{l_p} C_{n_r} - C_{n_p} C_{l_r} \right) \right] \quad (E.16)
\end{aligned}$$

$$\begin{aligned}
D = & -4\mu_b C_L \left( C_{l\beta} K_Z^2 + C_{n\beta} K_{XZ} \right) + 2\mu_b \left( C_{l\beta} C_{n_p} - C_{n\beta} C_{l_p} \right) + \\
& \frac{1}{2} C_{Y\beta} \left( C_{l_r} C_{n_p} - C_{n_r} C_{l_p} \right) + \frac{1}{2} C_{Y_p} \left( C_{l\beta} C_{n_r} - C_{n\beta} C_{l_r} \right) + \\
& \frac{1}{2} C_{Y_r} \left( C_{l_p} C_{n\beta} - C_{n_p} C_{l\beta} \right) \quad (E.17)
\end{aligned}$$

$$E = C_L \left( C_{l\beta} C_{n_r} - C_{n\beta} C_{l_r} \right) \quad (E.18)$$

### E.5. CONTROL FORCES IN MANOEUVRING FLIGHT

The stick force gradient for longitudinal control is approximated by the following formula [11, p.415]:

$$\frac{dF_e}{dn} = \frac{d\delta_e}{ds_e} \frac{W}{S} \left( \frac{V_h}{V} \right)^2 S_e \bar{c}_e \frac{C_{h\delta}}{C_{m\delta_e}} \left( \frac{C_{m_{a_{free}}}}{C_{N\alpha}} + \frac{C_{m_{q_{free}}}}{2\mu_c} \right) \quad (E.19)$$

# F

## FLIGHT TEST RESULTS - ADDITIONAL PLOTS

### F.1. PHUGOID OSCILLATION

#### F.1.1. TEST POINT 1 ADDITIONAL RESULTS

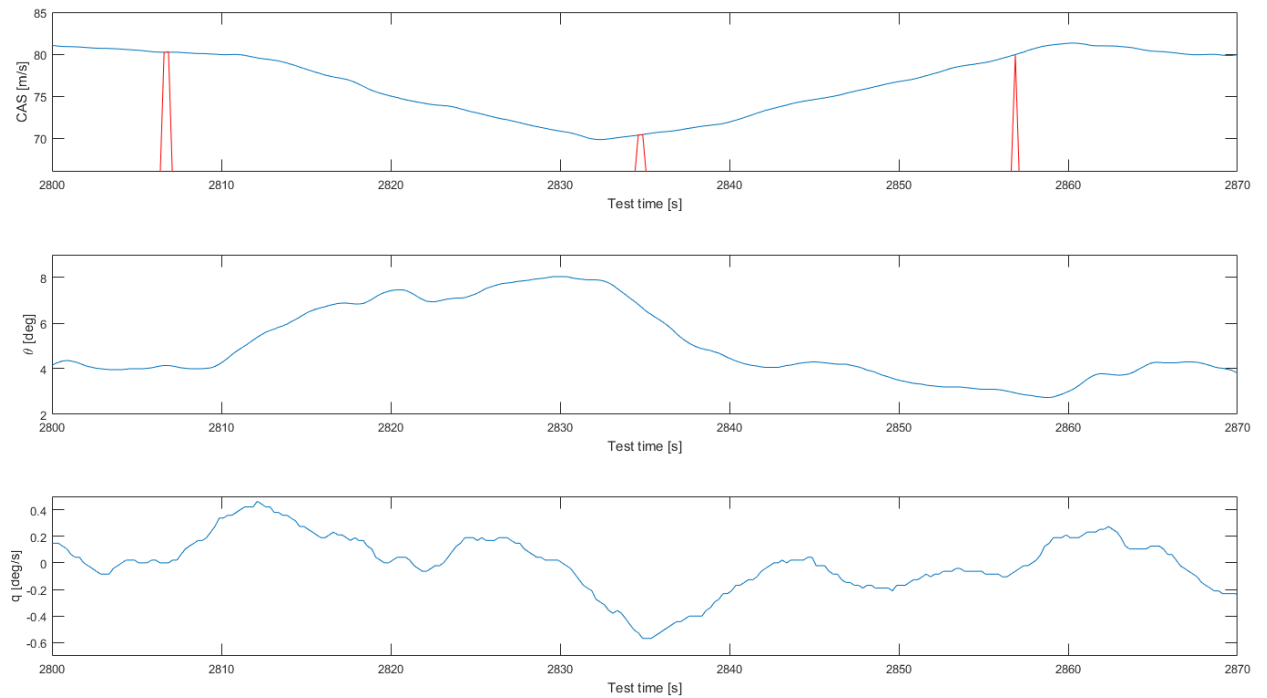


Figure F.1: Phugoid Oscillation - Test Point 1 - 80 kts

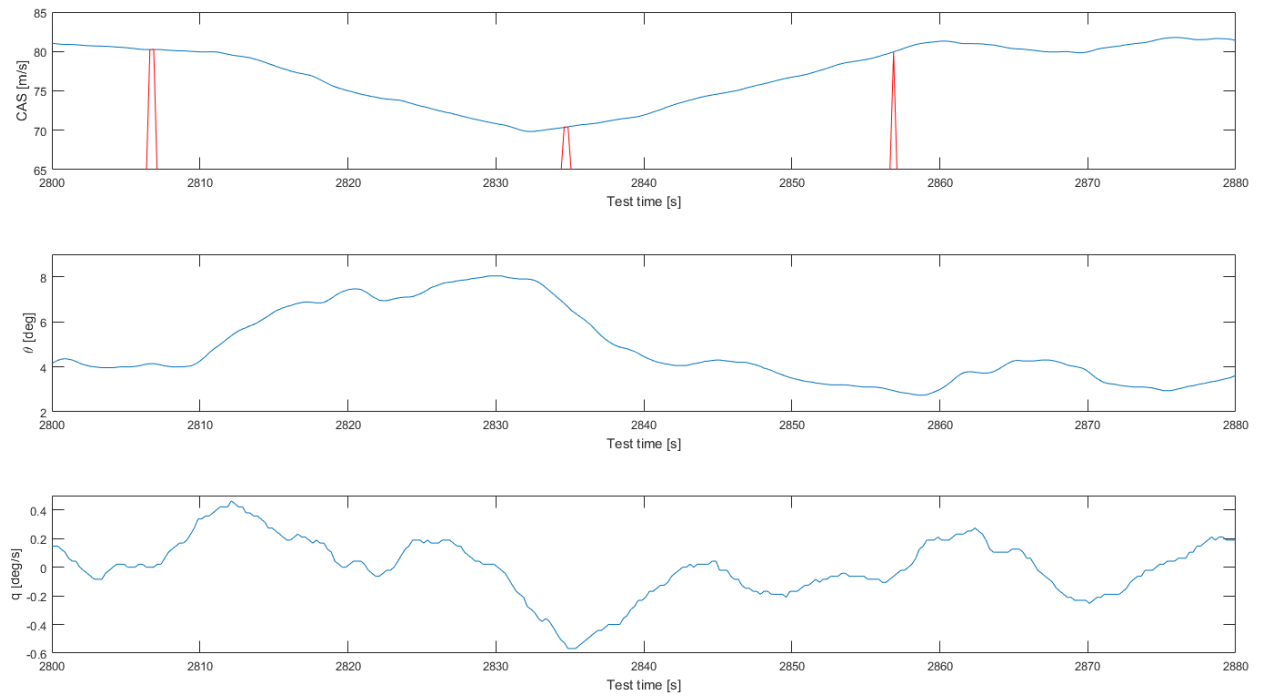


Figure F2: Phugoid Oscillation - Test Point 1 - 85 kts

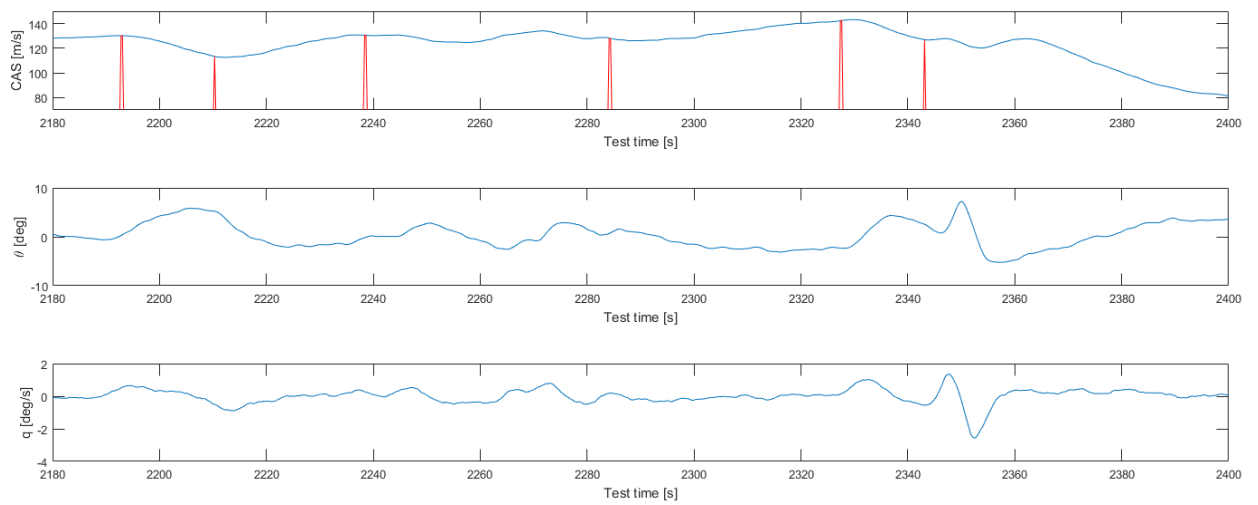


Figure F3: Phugoid Oscillation - Test Point 1 - 130 kts

F.1.2. TEST POINT 2 ADDITIONAL RESULTS

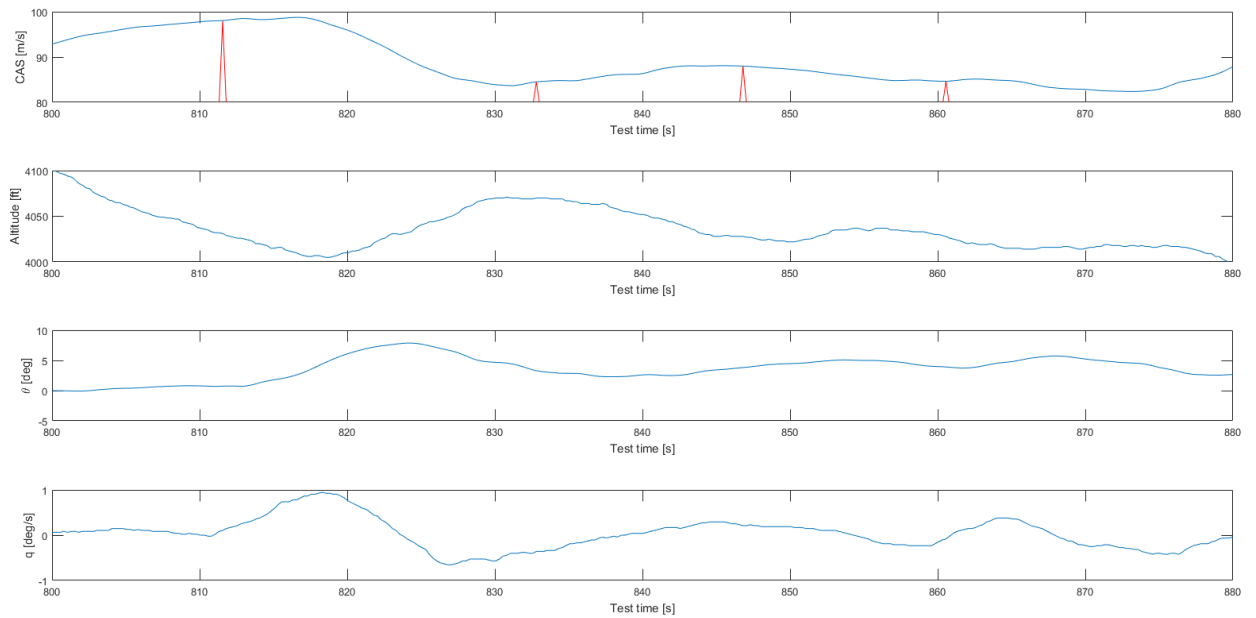


Figure E4: Phugoid Oscillation - Test Point 2 - 85 kts

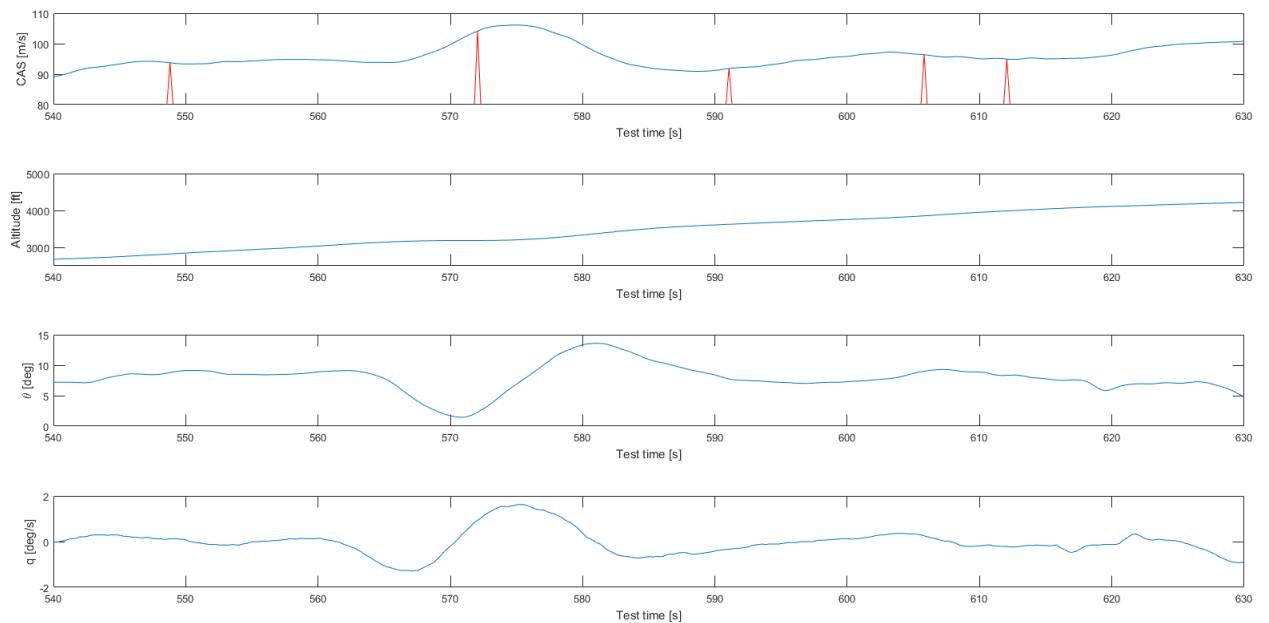


Figure E5: Phugoid Oscillation - Test Point 2 - 90 kts climb

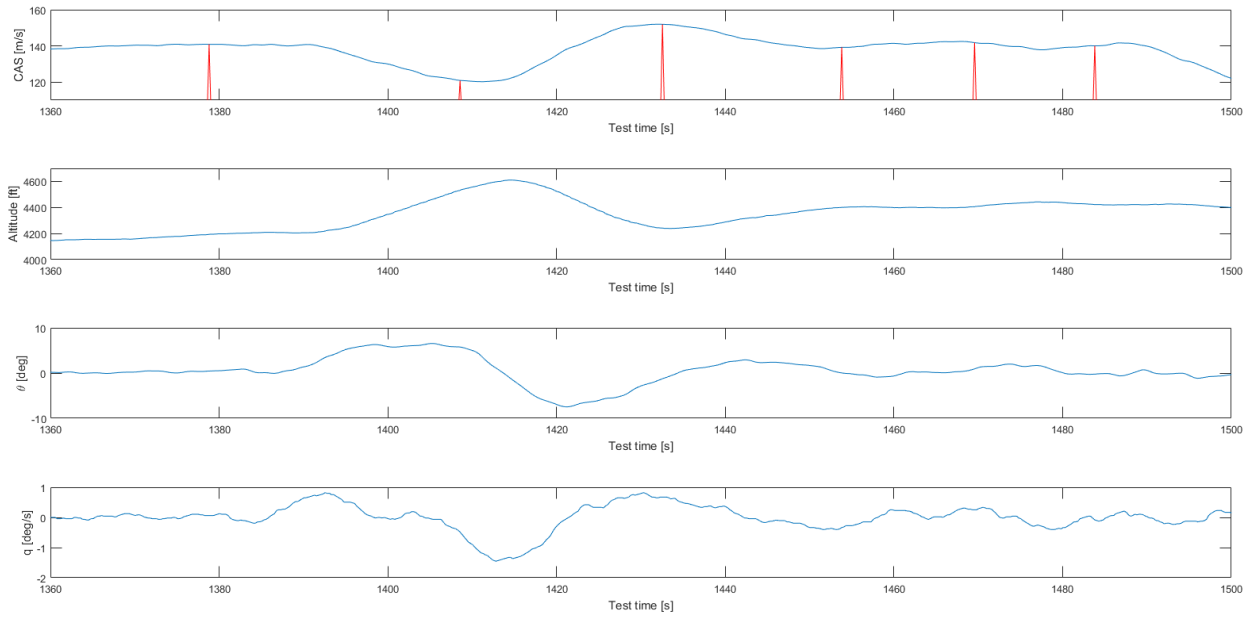


Figure F6: Phugoid Oscillation - Test Point 2 - 140 kts

## F.2. LONGITUDINAL CONTROL FORCES

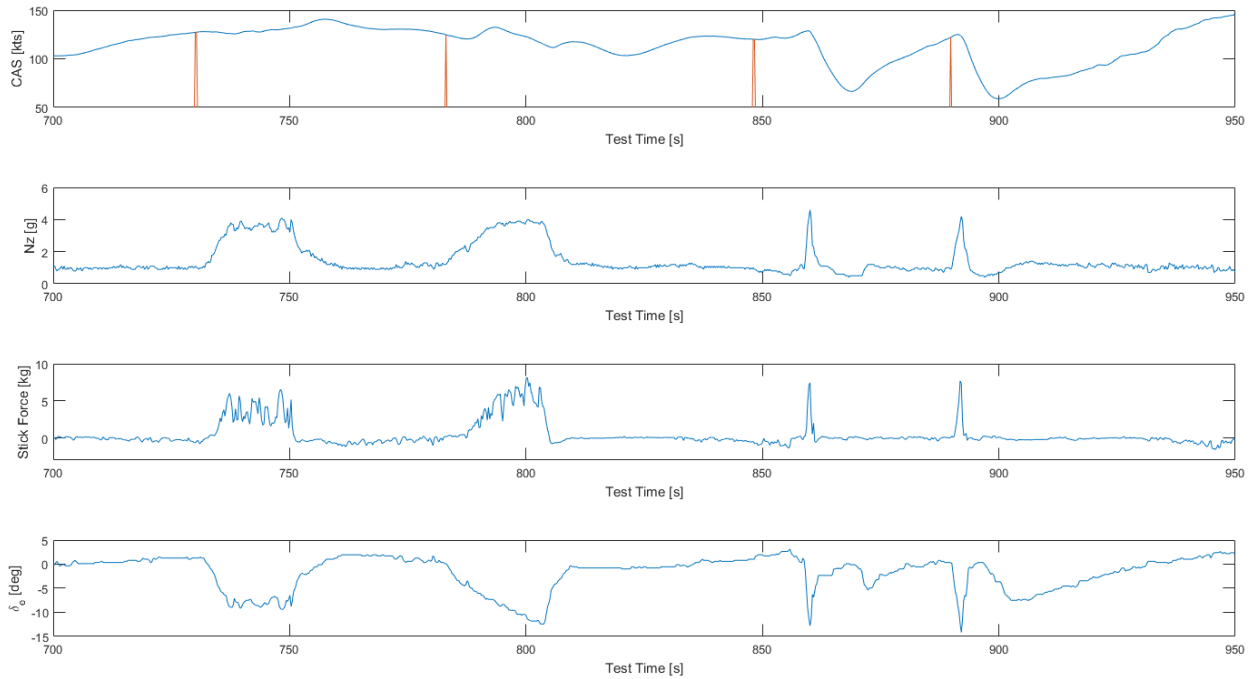


Figure F7: Manoeuvring Control Forces - Test Point 1

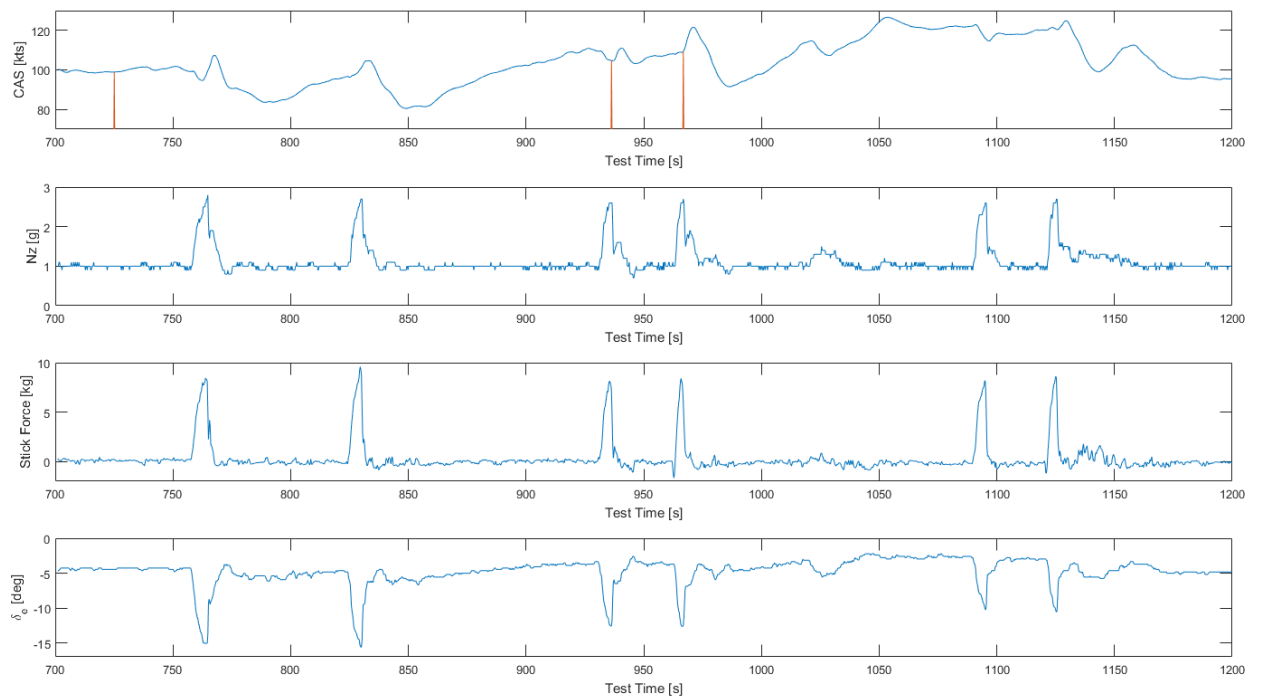


Figure F8: Manoeuvring Control Forces - Test Point 3 - Other Speeds

### F.3. DUTCH ROLL

#### F.3.1. TEST POINT 1 ADDITIONAL RESULTS

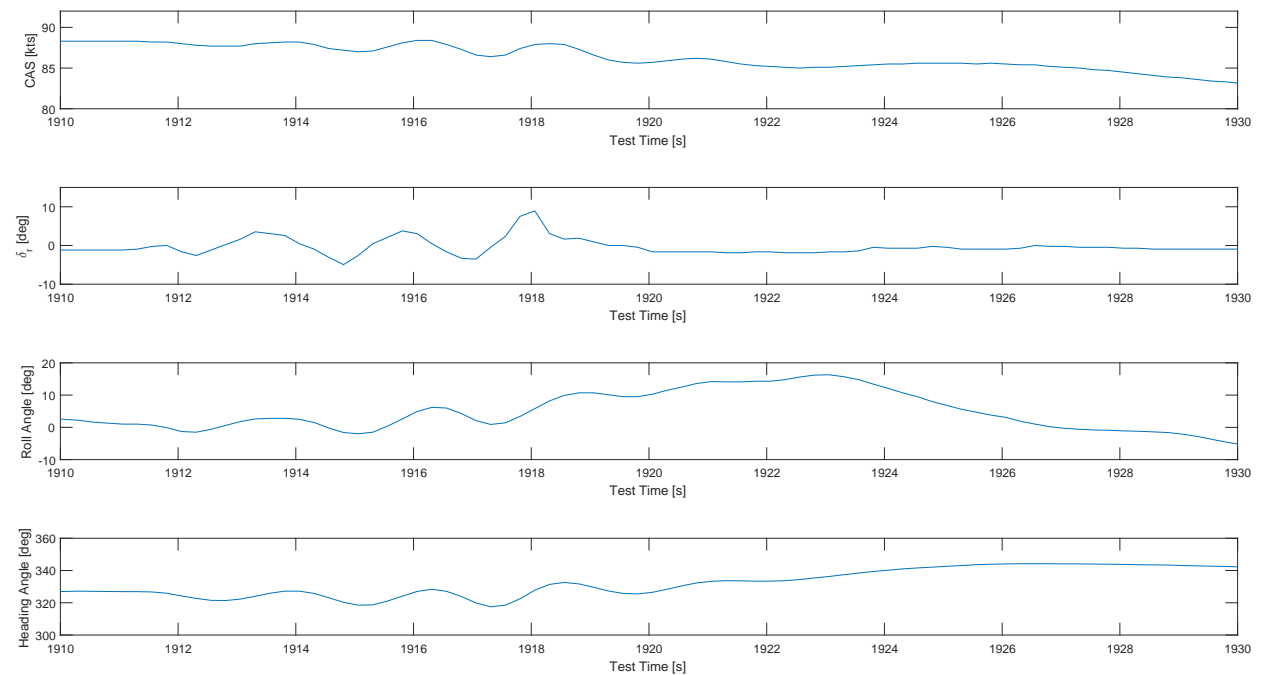


Figure F9: Dutch Roll - Test Point 1 - 90 kts

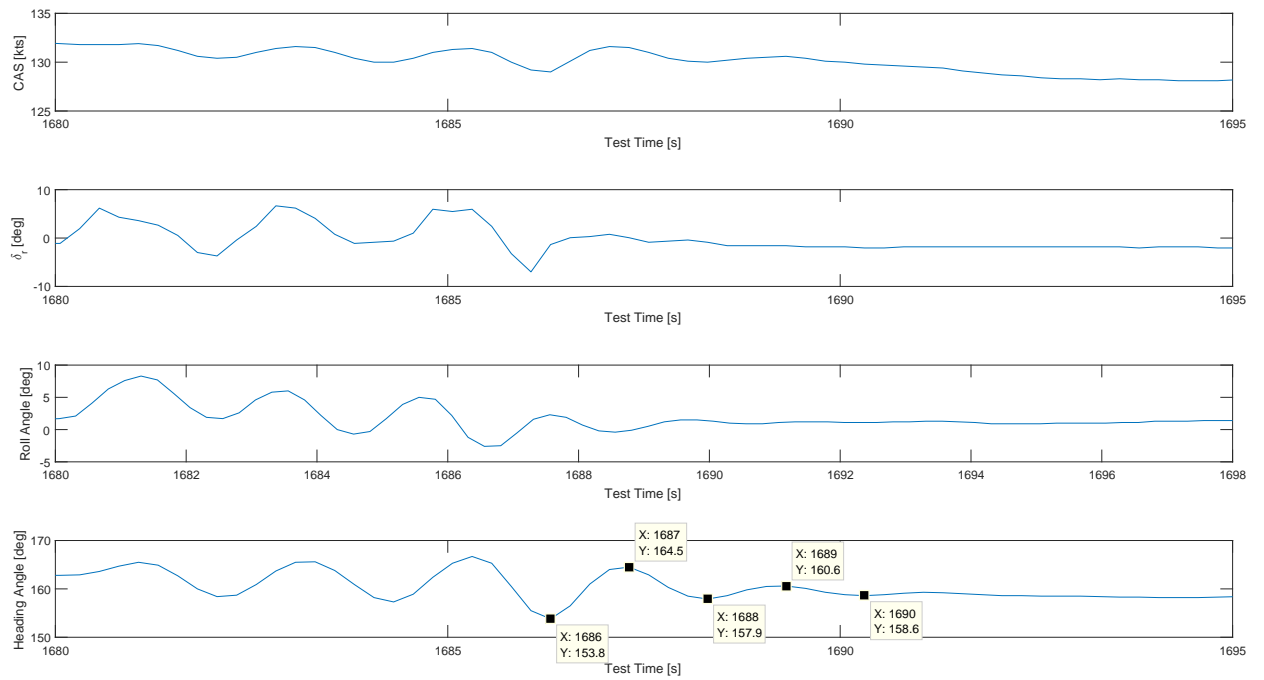


Figure F.10: Dutch Roll - Test Point 1 - 130 kts

### F.3.2. TEST POINT 2 ADDITIONAL RESULTS

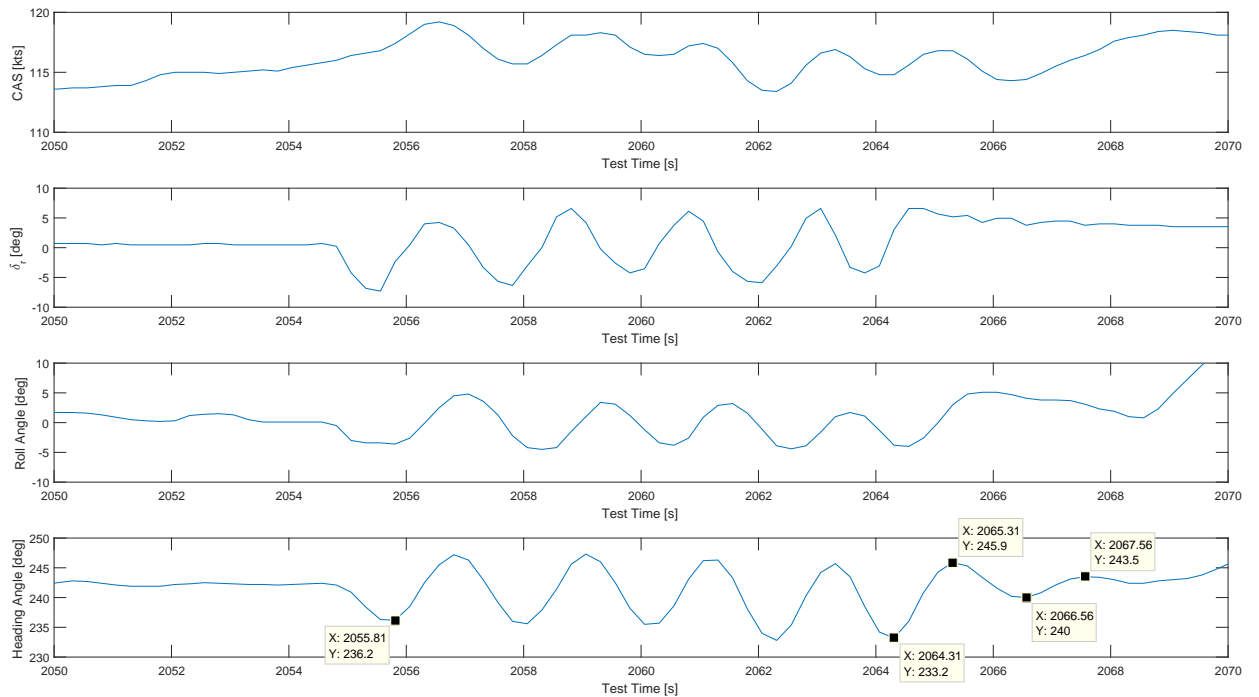


Figure F.11: Dutch Roll - Test Point 2 - 120 kts - run 2

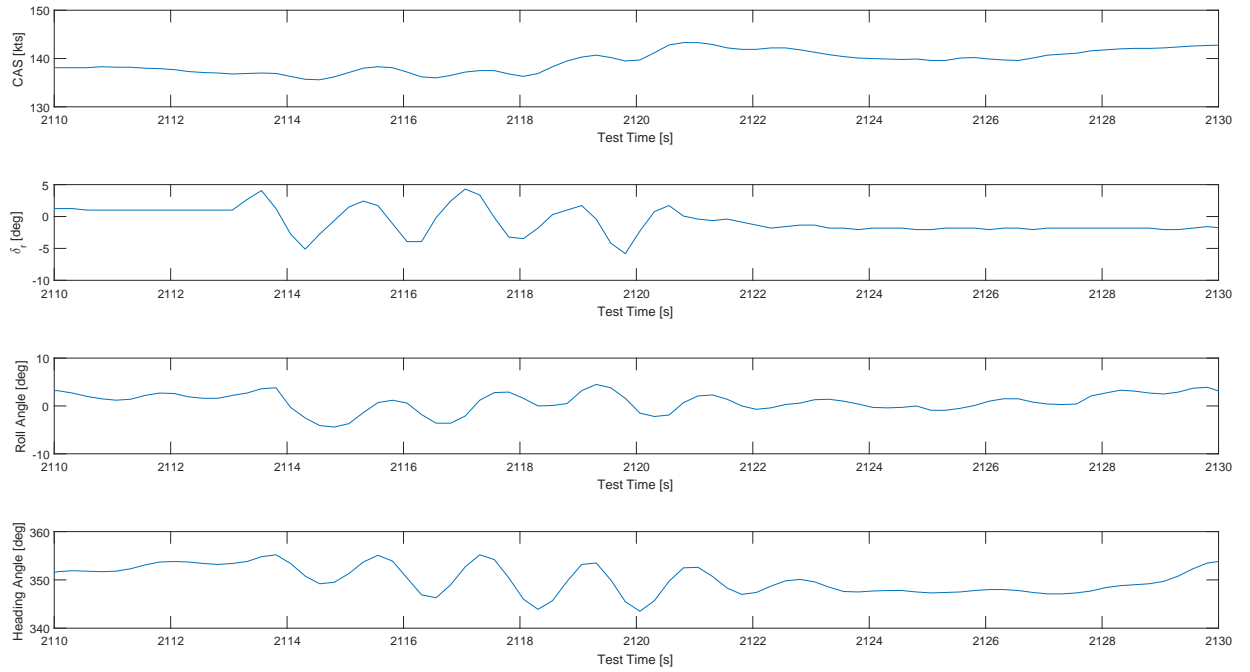


Figure F.12: Dutch Roll - Test Point 2 - 140 kts

## F.4. ROLL MODE

### F.4.1. TEST POINT 1 ADDITIONAL RESULTS

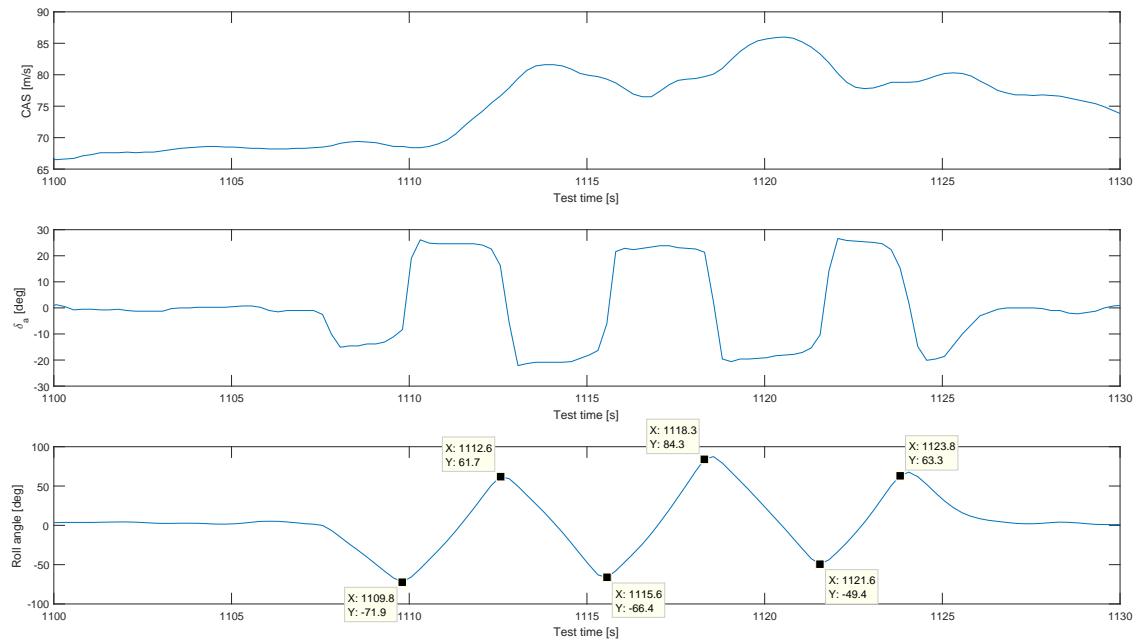


Figure F.13: Roll Mode - Test Point 1 - 65 kts (Take-off)

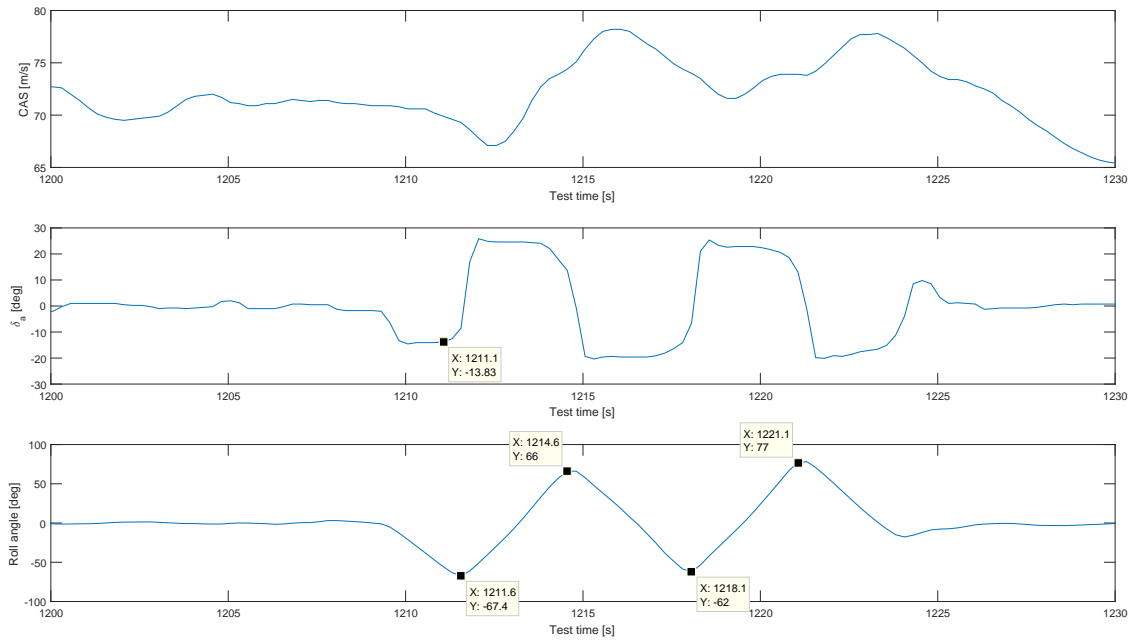


Figure F.14: Roll Mode - Test Point 1 - 70 kts (Landing)

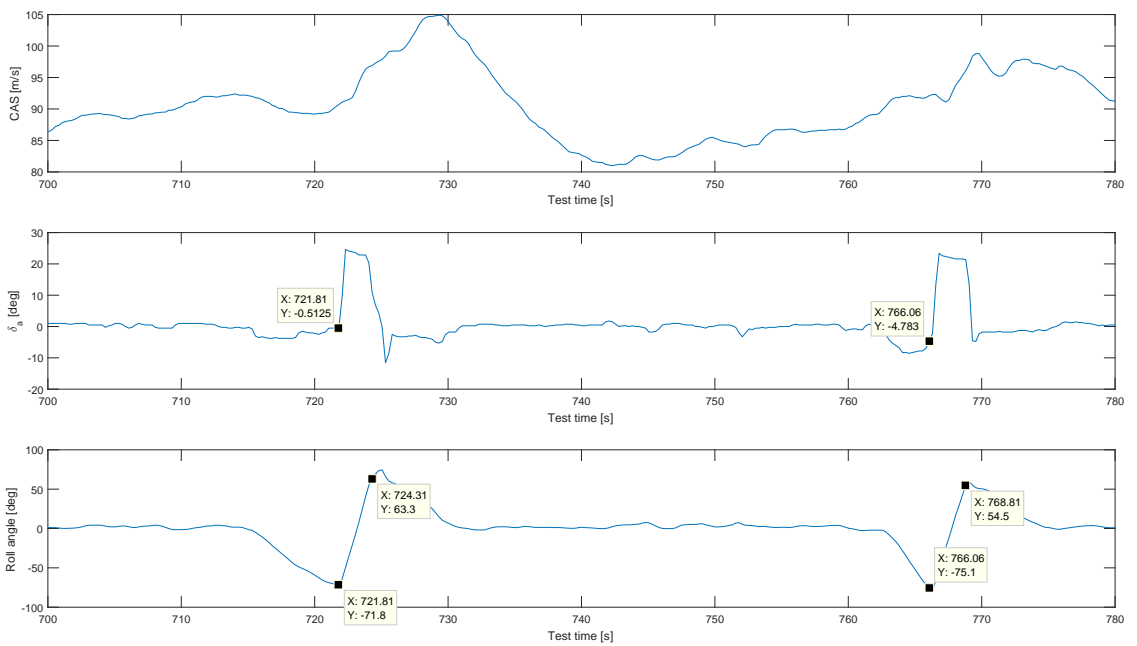


Figure F.15: Roll Mode - Test Point 1 - 90 kts

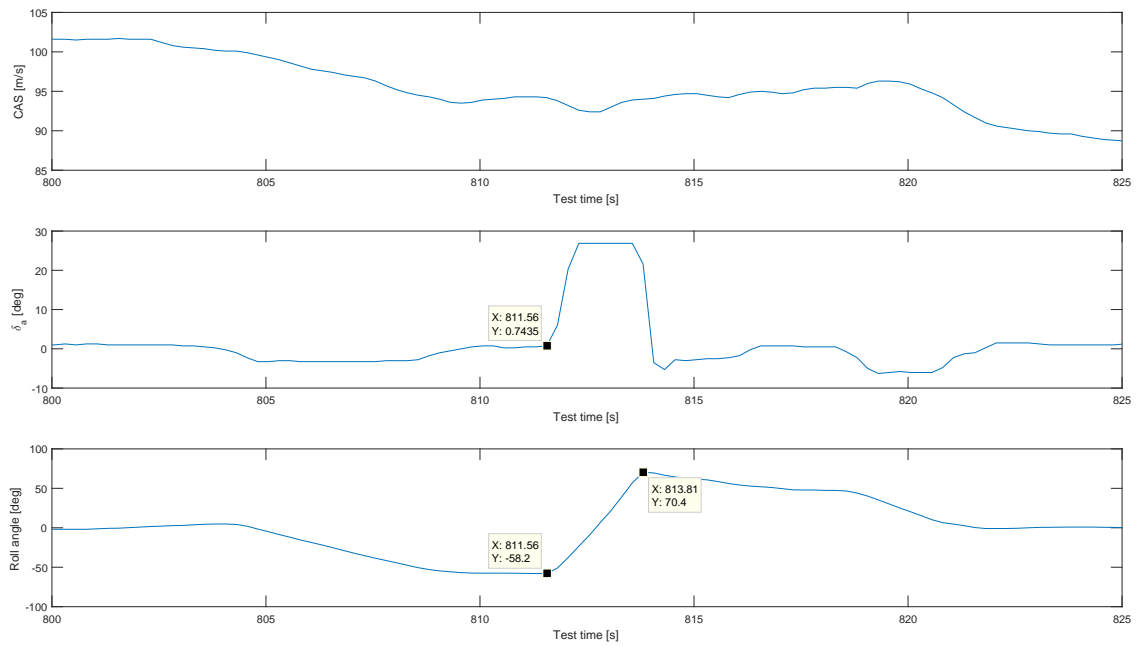


Figure F.16: Roll Mode - Test Point 1 - 95 kts

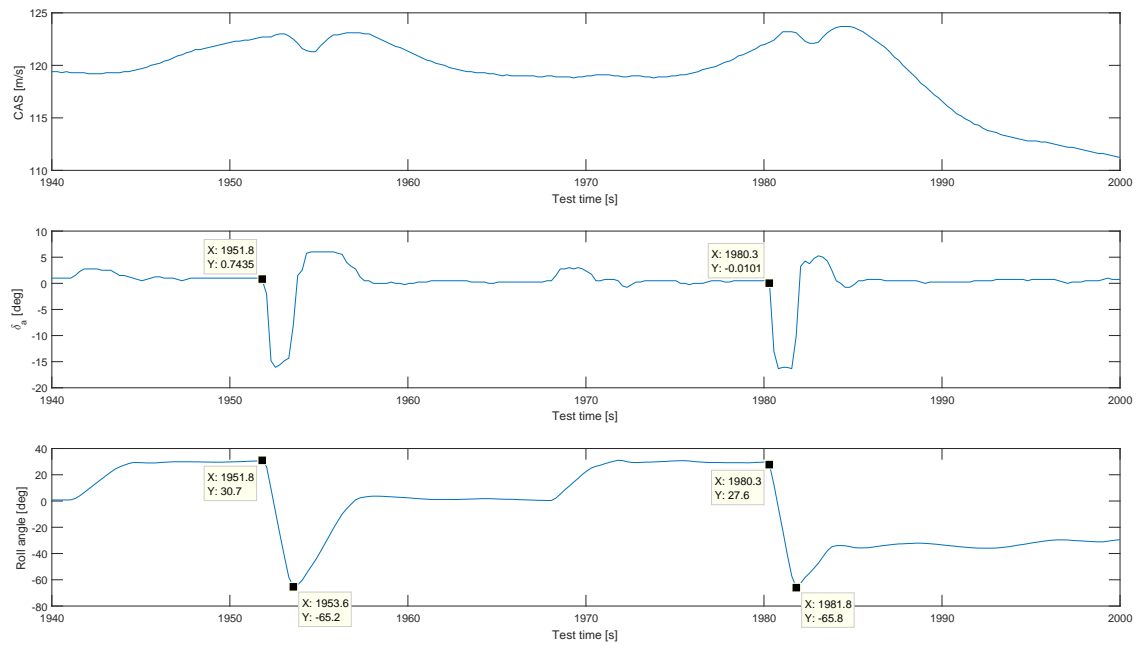


Figure F.17: Roll Mode - Test Point 1 - 120 kts

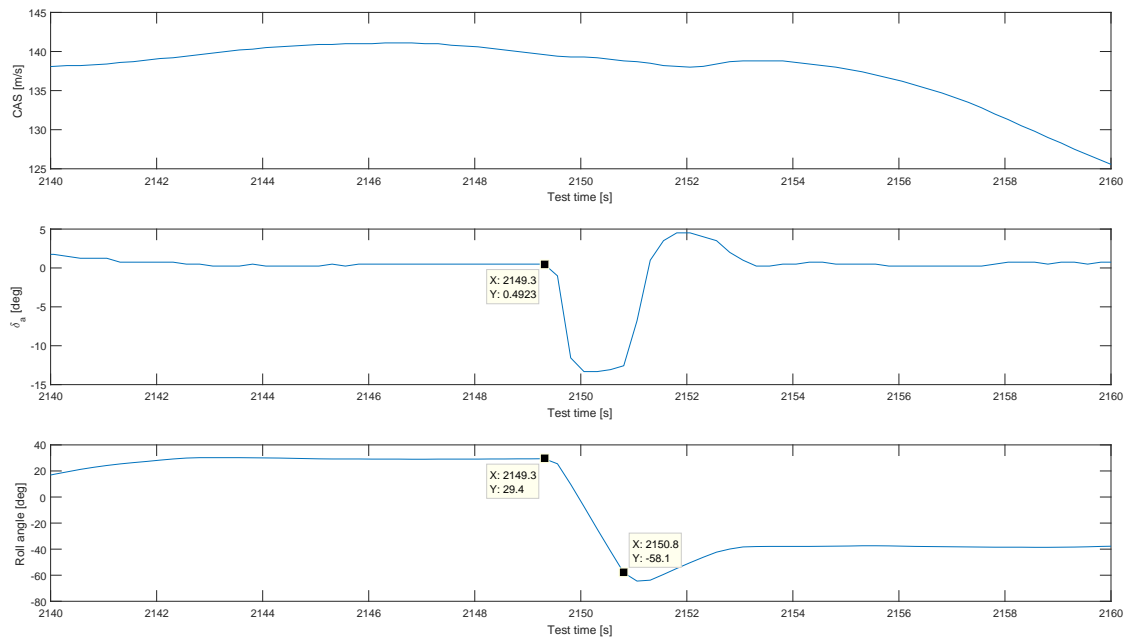


Figure F.18: Roll Mode - Test Point 1 - 140 kts

### F.4.2. TEST POINT 3 ADDITIONAL RESULTS

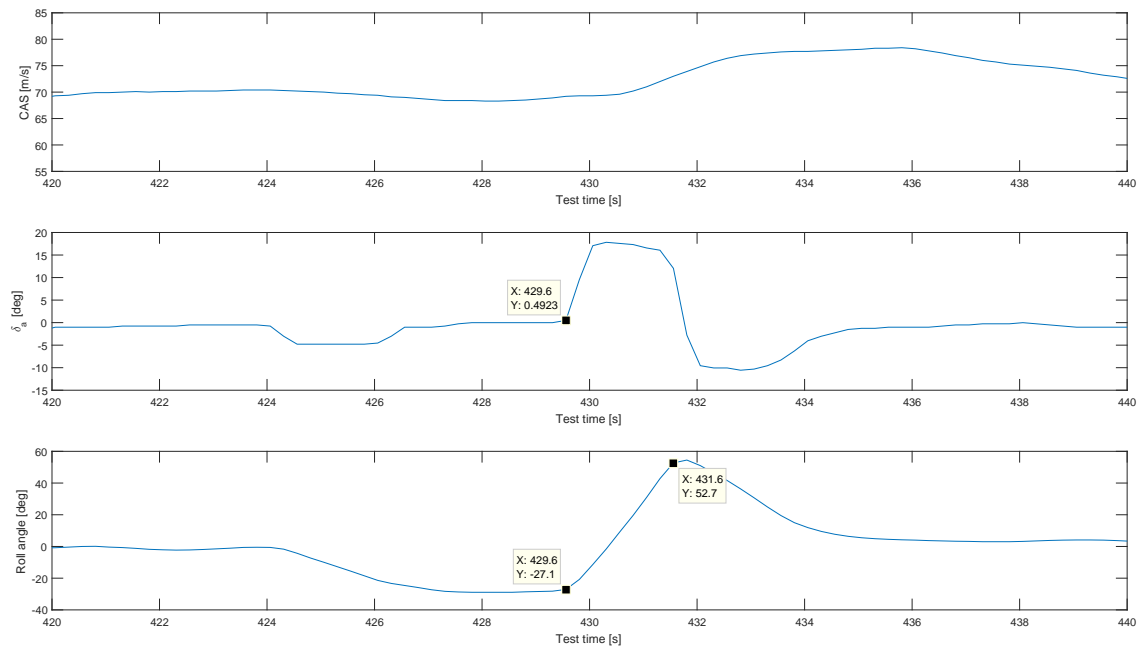


Figure F.19: Roll Mode - Test Point 3 - 70 kts (Take-off)

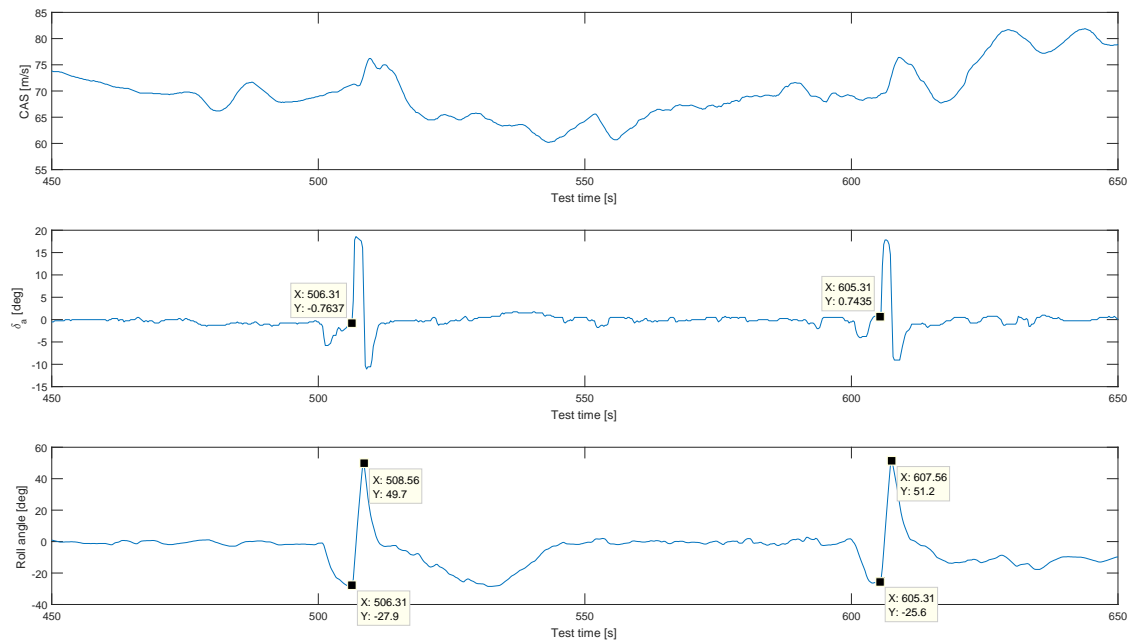


Figure F20: Roll Mode - Test Point 3 - 70 kts (Landing)

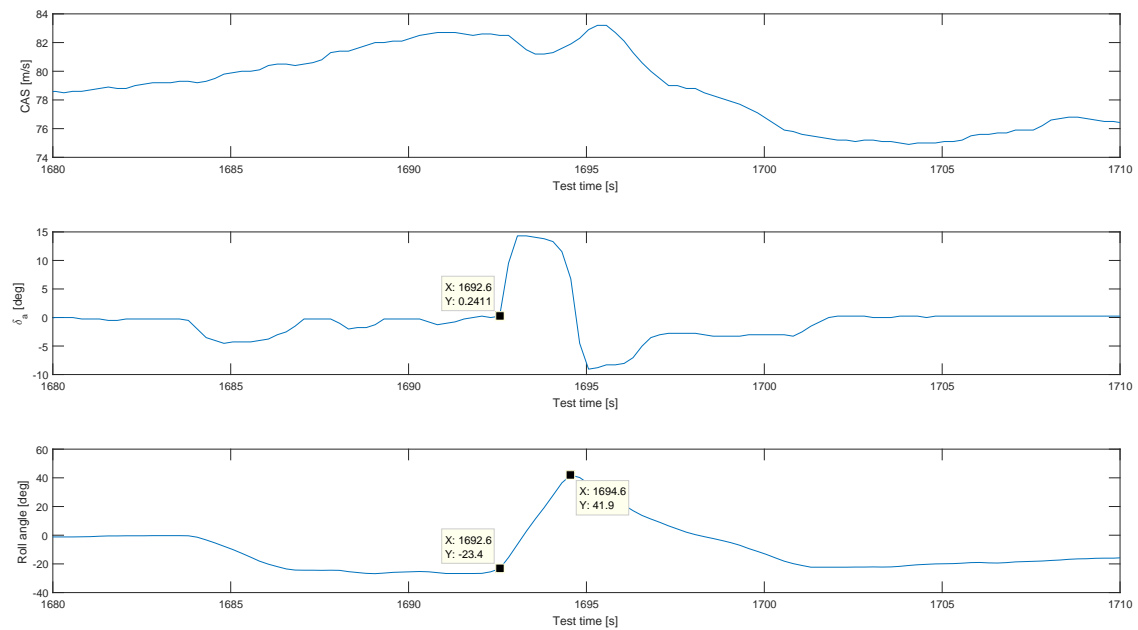


Figure F21: Roll Mode - Test Point 3 - 80 kts

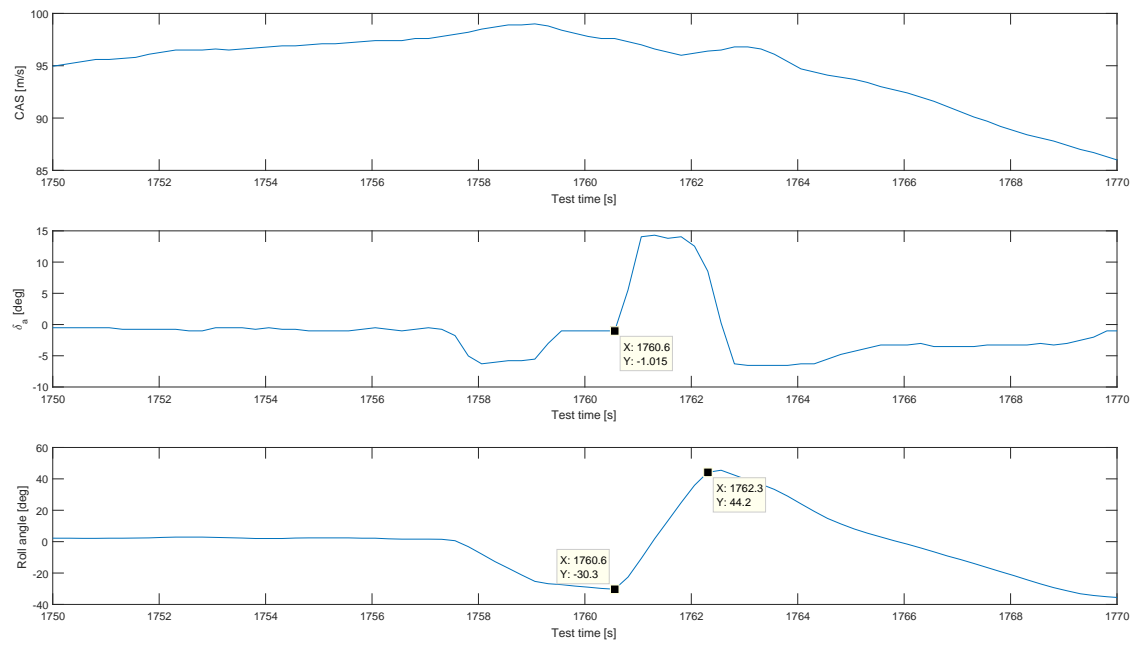


Figure E22: Roll Mode - Test Point 3 - 100 kts

# BIBLIOGRAPHY

- [1] E. Bazzocchi, *Military Pilots Training and its Equipment*, Lecture (Aeronautica Macchi, 1978) lecture held at the Federal Institute of Technology in Zürich.
- [2] Cattaneo, D., *Dino Cattaneo's Aermachi MB.326 Liveries*, Available at: <http://www.flightsimulatorpilot.com/fspmain/?p=13488> (2016), accessed on 7 December 2016.
- [3] Dunaway, A., *A T-37 Tweet aircraft from the 85th Fighter Training Squadron, Laughlin AFB, Texas, flies over Lake Amistad during a training mission*, Available at: [https://commons.wikimedia.org/wiki/File:T-37\\_021203-0-9999G-003.jpg](https://commons.wikimedia.org/wiki/File:T-37_021203-0-9999G-003.jpg) (2016), accessed on 7 December 2016.
- [4] G. E. Cooper and R. P. Harper, *The Use of Pilot Rating in the Evaluation of Aircraft Handling Qualities*, PDF (Washington D.C., National Aeronautics and Space Administration, 1969).
- [5] M. V. Cook, *Flight Dynamics Principles: A Linear Systems Approach to Aircraft Stability and Control*, 3rd ed. (Elsevier Butterworth-Heinemann, Burlington, UK, 2013).
- [6] Aircraft Wiki, *Diamond DA20*, Available at: [http://aircraft.wikia.com/wiki/Diamond\\_DA20?file=DA\\_20.jpg](http://aircraft.wikia.com/wiki/Diamond_DA20?file=DA_20.jpg) (2017), accessed on 19 January 2017.
- [7] Naval Air Training Command, , *T-6B Texan*, Available at: <https://www.flickr.com/photos/cnatrapao/5238353462> (2009), accessed on 19 January 2017.
- [8] YSFHQ, *T-38C Talon*, Available at: <https://forum.ysfhq.com/viewtopic.php?t=7745> (2015), accessed on 19 January 2017.
- [9] S. C. Roberts, N. Roberts, A. Lawless, G. Lewis, S. Cherry, L. Davis, J. Hagen, P. Reukauf, F. Watts, and E. Arnold, *Introduction to Performance and Flying Qualities Flight Testing*, 2nd ed. (National Test Pilot School, Mojave (CA), 1995).
- [10] A. De Giuseppe, *Flight Test Technique*, PDF (Monopoli, Italy: Blackshape SpA, 2015).
- [11] J. Mulder, W. van Staveren, J. van der Vaart, E. de Weerd, C. de Visser, A. in 't Veld, and E. Mooij, *Flight Dynamics: Lecture Notes AE3202* (Delft University of Technology, Delft, The Netherlands, 2013).
- [12] Marketwired, *High-Performance Blackshape CF300 Prime Sport Two-Seater Plane Now in Canada*, Available at: <http://www.marketwired.com/press-release/high-performance-blackshape-cf300-prime-sport-two-seater-plane-now-in-canada-1886851.htm> (2014), accessed on 11 June 2016.
- [13] G. Min, A. Jianliang, L. Zhiwen, D. Juan, and W. Jing, *On Exploring Method and Software for Evaluating Effectiveness of Military Training Aircraft*, Chinese Journal of Aeronautics **22**, pp.607 (2009).
- [14] Pilatus, *Primary Aircraft Training System Study*, PDF (Pilatus, 1988).
- [15] J. Huang, M. I. Mostafa, and Z. Wu, *Conceptual Design Optimization of Fighter Trainer Aircraft with Double-delta Wing Configuration*, Chinese Journal of Aeronautics **16**, 80 (2003).
- [16] J. Sánchez-Lozano, J. Serna, and A. Dolón-Payán, *Evaluating Military Training Aircrafts Through the Combination of Multi-Criteria Decision Making Processes with Fuzzy Logic. A Case Study in the Spanish Air Force Academy*, Aerospace Science and Technology **42**, pp.58 (2014).

- [17] C. L. Hwang and K. Yoon, *Multiple Attribute Decision Making: Methods and Applications* (Springer, Berlin, 1981).
- [18] W. H. Phillips, *Flying Qualities from Early Airplanes to the Space Shuttle*, in *AIAA, 26th Aerospace Sciences Meeting* (Washington D.C.: American Institute of Aeronautics and Astronautics, Reno (NV), 11-14 January 1988, 1988).
- [19] G. G. Piccolomini, *Specialized Air Training Project V/S Multi-Skilled operators*, in *ItAF Air Training Command, European Air Training Symposium* (ItAF Air Training Command, Rome, 27-29 November 2013, 2013).
- [20] Baseops, *USAF Initial Flight Screening Program*, Available at: [http://www.baseops.net/militarypilot/usaf\\_ift.html](http://www.baseops.net/militarypilot/usaf_ift.html) (2016), accessed on 10 May 2016.
- [21] European Aviation Safety Agency, *Acceptable Means of Compliance and Guidance Material to Part-FCL*, PDF (Cologne: European Aviation Safety Agency, 2011) accessed on 10 May 2016.
- [22] C. Korger, *The Road To Wings: How to Become a U.S. Air Force Pilot*, Available at: <https://fightersweep.com/262/how-to-become-a-us-air-force-pilot/> (2014), accessed on 6 October 2016.
- [23] Air Education and Training Command, *Combat Systems Officer (CSO) Initial Flight Screening (IFS) for Civilian Part 61/141 Flight Schools*, PDF (Randolph AFB: Air Education and Training Command, 2009) accessed on 10 May 2016.
- [24] Naval Air Training Command, *T-6B Joint Primary Pilot Training (JPPT)*, Report (Texas, Naval Air Training Command, 2012).
- [25] J. A. Ausink, R. S. Marken, L. Miller, T. Manacapili, W. W. Taylor, and M. R. Thirtle, *Assessing the Impact of Future Operations on Trainer Aircraft Requirements*, PDF (Santa Monica: RAND Corporation, 2005) accessed on 15 April 2016.
- [26] T. J. Lafortune, *Preparing Specialized Undergraduate Pilot Training Graduates for F-35A Training*, Master thesis, United States Air Force Academy (2010), accessed on 7 April 2016.
- [27] Department of Defense, *Military Specification: Flying Qualities of Piloted Airplanes MIL-F-8785C*, PDF (Department of Defense, 1980).
- [28] J. Casali and W. Wierwille, *A Comparison of Rating Scale, Secondary Task, Physiological, and Primary Task Workload Estimation Techniques in a Simulated Flight Task emphasising Communications Load*, *Human Factors* **25**, pp.623 (1983).
- [29] Air Education and Training Command, *Combat Systems Officer (CSO) Initial Flight Screening (IFS) for Civilian Part 61 / 141 Flight Schools*, PDF (Randolph AFB (TX): Air Education and Training Command, 2009) accessed on 19 October 2016.
- [30] Naval Air Training Command, *T-6B Joint Primary Pilot Training (JPPT)*, PDF (NAS Corpus Christi (TX): Naval Air Training Command, 2012) accessed on 10 May 2016.
- [31] McDonnell Douglas Astronautics Company, *The USAF Stability and Control Digital Datcom*, PDF (Missouri: McDonnell Douglas, 1979) accessed on 31 January 2017.
- [32] J. E. Williams and S. R. Vukelich, *The USAF Stability and Control Digital DATCOM. Volume I, Users Manual*, PDF (St. Louis (MO): McDonnell Douglas Astronautics Company, 1979) accessed on 23 August 2016.
- [33] A. De Giuseppe, *BK200 - Horizontal Tail Volume Ratio Analysis*, PDF (Monopoli: Blackshape SpA, 2016).

- [34] B. van Lierop and P. Baratto, *BS115 Aerodynamic Data Collection*, PDF (Monopoli, Italy: Blackshape SpA, 2014).
- [35] R.W. Gilbey, *ESDU 84002 - Estimation of sideforce, yawing moment and rolling moment derivatives due to rate of yaw for complete aircraft at subsonic speeds.*, PDF (London: IHS, 1984) accessed on 19 April 2017.
- [36] A.J. Clarke and R.W. Gilbey and S.F. Wood, *ESDU 85010 - Estimation of sideforce, yawing moment and rolling moment derivatives due to rate of roll for complete aircraft at subsonic speeds*, PDF (London: IHS, 2014) accessed on 19 April 2017.
- [37] D. T. Ward and T. W. Strganoc, *Introduction to Flight Test Engineering*, 2nd ed. (National Test Pilot School, Dubuque (IA), 1998).
- [38] P. A. Vitsas, *Vitsas Modified Transient Peak Ratio Method*, Available at: <https://aeroscience.wordpress.com/2012/09/30/vitsas-modified-transient-peak-ratio-method/> (2012), accessed on 2 November 2016.
- [39] B. Crawford, *Unusual Attitudes and the Aerodynamics of Maneuvering Flight*, PDF (Boston (MA): Flightlab, 2009) accessed on 24 April 2017.
- [40] Lyons, D.J., *An Examination of the Technique of the Measurement of Longitudinal Manoeuvring Characteristics of an Aeroplane, and a Porposal for a Standardised Method*, PDF (London: Ministry of Supply, 1947) accessed on 4 August 2017.
- [41] Gilbey, R.W., *Example of procedure in calculation of control hinge moments*, PDF (London: IHS ESDU, 1989).
- [42] European Aviation Safety Agency, *Certification Specifications for Very Light Aeroplanes*, PDF (Cologne: European Aviation Safety Agency, 2009) accessed on 5 August 2017.
- [43] J. Roskam, *Airplane Flight Dynamics and Automatic Flight Controls*, 3rd ed. (Lawrence (KS), 2001).